Alexander Schenk

Novel metal-xanthates for preparation of metal sulphides for photovoltaic applications

MASTER THESIS

zur Erlangung des akademischen Grades eines Diplom-Ingenieurs
der technischen Wissenschaften

erreicht an der

Technischen Universität Graz

Betreuer:

Assoc. Prof. DI Dr. Gregor Trimmel

Christian Doppler Labor für Nanokomposit-Solarzellen
Institut für Chemische Technologie von Materialien
Technische Universität Graz

2011

STATUTORY DECLARATION

I declare that I have authored this thesis independently, that I have not used other than the declared sources/resources, and that I have explicitly marked all material which has been quoted either literally or by content from the used sources.

…… ……..

date signature

to my parents

ABSTRACT

Within this work novel metal-xanthates, also named dithiocarbonates, for gaining semiconducting metal sulphides as solar absorber materials have been synthesised. Metal dithiocarbonates were chosen to give the desired metal sulphides, due to the fact that they are known to have low decomposition temperatures and a defined decomposition pathway enabled by the Chugaev rearrangement.

Metal dithiocarbonates employing copper, indium, cadmium, zinc, tin and gallium as metal atoms were synthesised with two different alcoholic moieties and were extensively characterised by ^{1}H- and ^{13}C nuclear magnetic resonance spectroscopy, Fourier transform infrared spectroscopy, elemental analysis, mass spectrometry and thermal gravimetric analysis.

Chalcopyrite type semiconductors like copper indium disulphide and kesterite type semiconductors like copper zinc tin sulphide are of strong scientific interest due to their beneficial properties for photovoltaic applications. Therefore investigations to gain these semiconductors by thermal treatment of metal dithiocarbonate mixtures were done. The resulting metal sulphides were studied by X-ray diffraction, energy dispersive X-ray analysis and optical transmittance and reflectance measurements.

The syntheses of copper indium disulphide and copper zinc tin sulphide were achieved by heat treatment of metal dithiocarbonate mixtures, with promising properties for photovoltaic applications. For this reason first attempts to fabricate inorganic solar cells have been carried out in a basic bilayer assembly of $CdS/CuInS_2$ and CdS/Cu_2ZnSnS_4, respectively, on indium tin oxide as transparent conductive electrode.

KURZFASSUNG

Im Rahmen dieser Arbeit wurden neuartige Metall-Xanthate als Precursorverbindungen für Metallsulfidhalbleiter, die als Absorbermaterialien für photovoltaische Anwendungen Einsatz finden, hergestellt. Aufgrund der niedrigen Zersetzungstemperaturen und der rückstandslosen Zersetzung wurden Metalldithiocarbonate, auch Xanthate genannt, herangezogen, um die gewünschten Metallsulfidhalbleiter herzustellen.

Kupfer-, Indium-, Cadmium-, Zink-, Zinn- und Galliumdithiocarbonate wurden mit zwei unterschiedlichen alkoholischen Resten hergestellt und weitreichend mittels ^{1}H-, ^{13}C-Kernspinresonanzspektroskopie, Fourier-Transformations-Infrarotspektroskopie, Elementaranalyse, Massenspektrometrie und Thermogravimetrie untersucht.

Halbleitermaterialien, wie Kupfer-Indiumdisulfid und Kupfer-Zink-Zinnsulfid, haben aufgrund ihrer vorteilhaften Eigenschaften große Bedeutung in der Herstellung von photovoltaischen Systemen. Daher wurden im Rahmen dieser Arbeit Untersuchungen durchgeführt, solche Halbleitermaterialien durch Zersetzung von Metalldithiocarbonaten herzustellen. Die erhaltenen Metallsulfide wurden anschließend mittels Röntgendiffraktometrie, energiedispersiver Röntgenspektroskopie und optischer Transmissions- und Reflexionsmessungen charakterisiert.

Aufgrund der erfolgreichen Herstellung der gewünschten Kupfer-Indiumdisulfid- und Kupfer-Zink-Zinnsulfid-Halbleiter, wurden zusätzlich erste Anstrengungen unternommen anorganische Solarzellen mit einfachem Zweischichtaufbau zu produzieren.

ACKNOWLEDGEMENTS

First of all, I want to thank Assoc. Prof. Dipl.-Ing. Dr. Gregor Trimmel, my supervising tutor and Univ.-Prof. Dipl.-Ing. Dr. Franz Stelzer, head of the Institute for Chemistry and Technology of Materials at Graz University of Technology, for the opportunity to write this master thesis and all the support I got during the course of my thesis.
Special thanks go to Dipl.-Ing. Dr. Thomas Rath and Dipl.-Ing. Achim Fischereder, who were like co-tutors to me, for their help and support.

In addition I thank all my colleagues of the Christian Doppler Laboratory for Nanocomposite Solar Cells for their collaboration, assistance, friendship and the great time we had.

I want to express my gratitude to all who contributed to this work:
Amtsrätin Ing. Josefine Hobisch for thermal gravimetric analysis; Dipl.-Ing. Wernfried Haas for TEM-EDX measurements; Dipl.-Ing. Dorith Meischler, Ing. Karin Bartl and Ao. Univ.-Prof. Dipl.-Ing. Dr. Robert Saf for mass-spectrometric analysis; Ao. Univ.-Prof. Dipl.-Ing. Dr. Franz-Andreas Mautner for X-ray diffraction measurements; Monika Filzwieser for elemental analysis; Stefan Moscher and Dipl.-Ing. Michael Edler for their constant support during my time at this institute.

Financial support by the Christian Doppler Forschungsgesellschaft, the federal ministry of Economy, Family and Youth of Austria (BMWFJ) and the Isovoltaic AG is gratefully acknowledged.

Furthermore, I would like to thank my friends for their support and all the fun beginning with the first day of our studies.

I'm very grateful to my family, because they made everything possible and provided me with all the support and help I needed.

Last, and most of all, I wish to express my deepest gratitude to Dorith for motivating me in difficult times and her understanding.

This would not have been possible without any of you.

TABLE OF CONTENTS

INTRODUCTION

THE WORLD ENERGY DEMAND – CURRENT STATUS AND FUTURE PROSPECTS

Since the industrial revolution the world energy demand has grown tremendously. The world today's energy consumption is accounted to 10 terawatts per year. [1] Figure 1 depicts the world energy supply within the period of the last 37 years.

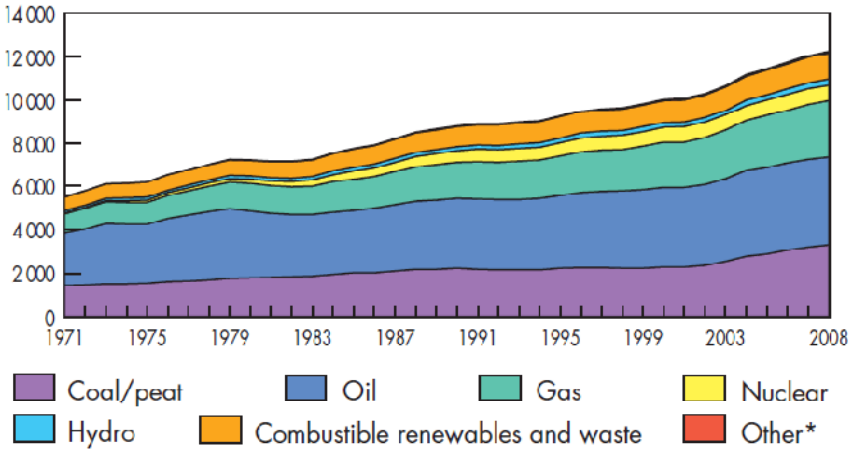

FIGURE 1: WORLD TOTAL PRIMARY ENERGY SUPPLY IN MTOE IN THE YEARS FROM 1971 TO 2008 [2]

It is outstanding that more than 80 % of the consumed energy derives from utilising fossil fuels like oil, natural gas and coal. [3]

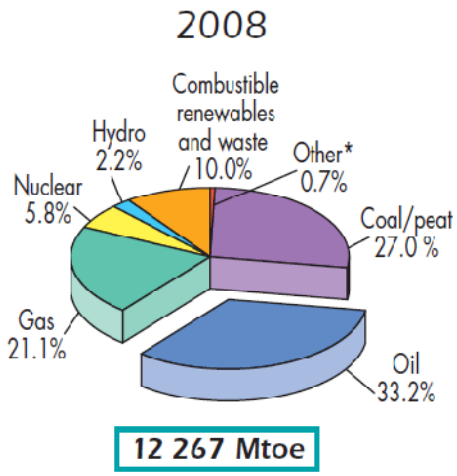

FIGURE 2: FUEL SHARE IN WORLD TOTAL PRIMARY ENERGY SUPPLY IN 2008 [2]

As the world's primary energy demand is projected to grow by 1.6 % per year on average within the period of 2006 to 2030 the depletion of fossil energy reserves is only a matter of time.

According to all scenarios of future's energy resources, fossil fuels will still account for 80 % of the worldwide primary energy mix in 2030. Oil will remain the dominant fuel, though demand for coal will rise more than demand for any other fuel (see Figure 3). [4]

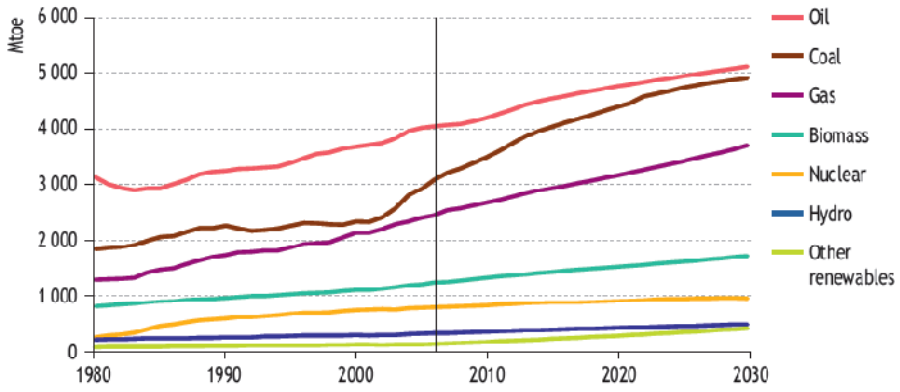

FIGURE 3: WORLD PRIMARY ENERGY DEMAND BY FUEL [4]

Due to the harmful effects of utilising fossil fuels on the environment, the world will need a major change in its energy supply chain to achieve a stabilisation of carbon dioxide in the atmosphere, to slow down the global warming caused by the greenhouse effect. [1] Within the recent decades new technologies based on renewable and hence carbon dioxide-free resources have been developed. Mainly wind, water, tides, geothermal heat, biomass and sunlight are of interest for world's future energy supply.

RENEWABLE ENERGY RESOURCES - SOLAR PHOTOVOLTAICS

Due to the energy and oil crises in the early and late 1970s, research for alternative energies has been initiated. Benefiting from high fossil fuel prices and an increasing public awareness the share of renewable energy resources has been extended in recent years and is set to follow this trend over the next years of time.

Photovoltaics are expected to be significant and important for electricity generation based on renewables over the coming decades. [1], [4]

Since the discovery of the photoelectric effect by *A. E Becquerel* the concept of converting freely available sunlight energy into electrical energy engaged scientists and engineers all over the world. [5] Not only the free availability of sunlight energy has increased the interest in photovoltaics, but also the fact that the annual supply of sunlight energy is estimated to be $3*10^{24}$ Joules, which exceeds the current world's energy consumption 10,000 times fold. [6]

Within the last 20 years the photovoltaic market has developed progressively and the worldwide photovoltaic production has exceeded 10 GW per year in 2009 as shown in Figure 4. [1]

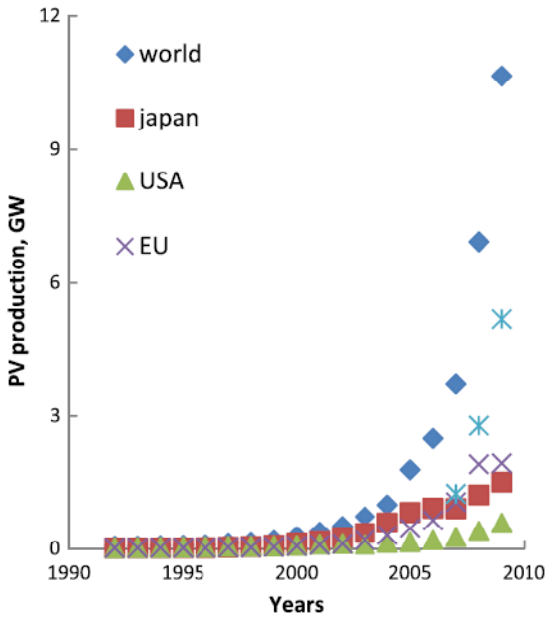

FIGURE 4: EVOLUTION OF WORLD PHOTOVOLTAIC CELL AND MODULE PRODUCTION THROUGH 2009 [1]

MATERIALS AND PRODUCTION METHODS FOR PHOTOVOLTAICS

Today's photovoltaic industry is based on silicon wafer technologies, but technologies employing other materials are growing fast, due to the expected shortcut of semiconductor-pure silicon. To avoid this shortcut of silicon semiconductor production, thin film technologies are in focus of the industry, nowadays.

Cadmium telluride is a promising direct band gap material for thin film photovoltaics production with a favourable optical band gap of 1.45 eV for the conversion of the solar spectrum into electricity. The highest to-date efficiency of CdTe photovoltaics is reported to be 16.5 % [7] Though cadmium telluride is a non toxic compound, it suffers from the hazardous cadmium containing chemicals, which are involved in production processes. Therefore other materials having a direct band gap have been investigated. I-III-VI_2 semiconducting compounds, like copper indium diselenide, copper gallium diselenide and their mixed alloys copper indium gallium diselenide exhibit desired properties for photovoltaic applications. Depending on gallium to indium ratios the band gap of copper indium gallium diselenide solar cells can be varied continuously from 1.04 to 1.68 eV and cell efficiencies of almost 20 % [8], [9] were reached. [1] To avoid the use of the toxic element selenium, copper indium disulphide and copper indium gallium disulphide have been investigated and recent activities yielded 11.4 % efficiency. [1] Although constant progress in research activities and expanding production of copper indium gallium diselenide/disulphide and copper indium diselenide/disulphide solar cells, respectively, this technology is reliant on metals that are scarce in the earth's crust. In addition much of the annual production of indium is required for the flat panel display industry. Hence the future's supply of this rare and expensive metal is problematic and new solar absorber materials have gained interest. [10], [11] The kesterite type and I_2-II-IV-VI_6 quaternary compound semiconductor copper zinc tin sulphide is formed by substituting the rare metal indium in the ternary compound copper indium disulphide with zinc and tin. [11] Each component of copper zinc tin sulphide is abundant in the earth's crust and therefore cheap. In recent years the efficiencies of copper zinc tin sulphide devices have progressed and achieved the 10 % mark in 2010. [12]

Several production processes have been established and are part of the thin film photovoltaics industry. The most common techniques are based on vacuum processes, due to its high uniformity and controllable element deposition. Multi-source evaporation has yielded the highest performance materials and can be cost effective as a result of its high deposition rate, but is very difficult to scale up to large area production while retaining the composition and microstructure. Sputtering processes have been investigated because of their easier industrial scale up, but have been less effective due to their slow deposition rates. [13]

To overcome the high production costs of vacuum based processes, non-vacuum deposition approaches have been explored and offer the potential of unprecedented growth in photovoltaic manufacturing. [10] Spray pyrolysis, in which precursor-containing solutions are deposited on heated substrates, is a possible method for photovoltaics production under ambient conditions. [14] Electrochemical bath deposition methods showed that metal precursor and complete solar absorber

film deposition is possible. Other methods for low-cost solar cell production are ink-based approaches, which have been mainly explored by industrial groups and are therefore not described in detail in literature. Ink-printing is a very attractive solar absorber formation process, because it is well established in industry, it offers enormous deposition rates, as known from newspaper printing and it is roll-to-roll processable. [10], [13] The IBM Research Centre developed a hydrazine-ink based process including a short annealing step at 540 °C and demonstrated its functionality with the to-date record efficiency of 9.7 % for kesterite copper zinc tin sulphide/selenide solar cells. [10], [12] A more industry-friendly aqueous-based ink-printing process of IBM gained initial efficiencies of 8.1 %. [15]

Though this ink-based processes offer new possibilities for solar cell production, they have yet to overcome the employment of toxic solvents. Therefore new and high soluble precursor materials have to be investigated.

SINGLE-SOURCE PRECURSOR MATERIALS FOR METAL SULPHIDES

Literature contains lots of reports for metal dithiocarbamates, thiolates and thiocarboxylates as precursor materials for binary metal sulphides. [16], [17], [18], [19], [20], [21], [22] All of these precursor materials show high solubility depending on their moieties in most common solvents and yield metal sulphides by heat treatment. Metal dithiocarbonates, named xanthates too, have lower decomposition temperatures, than those complexes mentioned above. Several reports can be found in literature, in which attempts were made to gain metal sulphides by heat treatment of metal dithiocarbonates. [23], [24], [25], [26], [27], [28] *D. P. Dutta* and *G. Sharma* showed that mixtures of two metal dithiocarbonates can yield ternary metal sulphides, like copper indium disulphide, which are in photovoltaic industry's focus. [16]

Not only ternary metal sulphides synthesised by thermal treatment of metal dithiocarbonates have gained interest for photovoltaic applications, but also binary chalcogenide phases synthesised the same way are subject to recent research activities. The group of *S. A. Haque* produced hybrid solar cells, in which the nanostructured inorganic cadmium sulphide phase was achieved in an in situ growth process by annealing cadmium dithiocarbonate in a polymer matrix. [29]

METAL DITHIOCARBONATES – WHY?

Metal dithiocarbonates have gained that much interest, due to their favourable properties for photovoltaics production. They are easy to handle due to their appreciable high stability to air and moisture and they exhibit depending on their alcoholic moieties good solubility in common solvents and are therefore non-vacuum processable, but can be, if wanted, vacuum processable [30] too. Furthermore the presence of metal-S bonds and the absence of metal-C bonds enable the clean conversion of metal dithiocarbonates to metal sulphides at temperatures lower than 200 °C. This conversion mechanism was discovered and published by *L. Tschugaeff* in 1899 and is nowadays named the Chuegav rearrangement. [31]

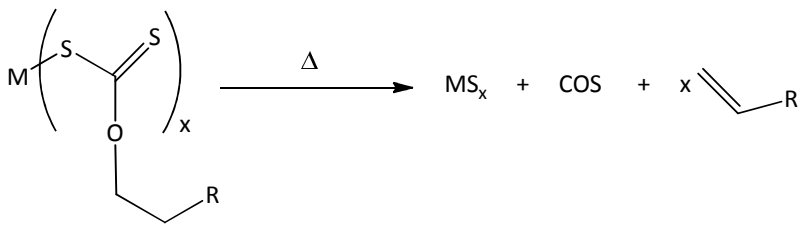

FIGURE 5: THE CHUAGEV REARRANGEMENT

According to the reaction scheme in Figure 5 the heat treatment of metal dithiocarbonates yields remainder-free metal sulphides and volatile side products, as carbon oxide sulphide and the alkenylic residue of the alcoholic moiety.

OBJECTIVES OF THIS WORK

For solution processable solar cells precursor materials with good solubility and low processing temperatures are necessary. In addition, the final absorber material should be of high purity. The aim of this work is to synthesise novel metal xanthates as precursor compounds for metal sulphide based semiconductors with possible applications in photovoltaics.

Two major issues have been targeted: good solubility in organic solvents (chloroform, tetrahydrofuran, benzene, toluene, chlorobenzene, trichlorobenzene, xylene and pyridine) and conversion temperatures below 200 °C.

Therefore two families of metal xanthates, based on 3,3-dimethylbutan-2-yl and 2,2-dimethylpentan-3-yl dithiocarbonates, will be employed to study the influence of differing chain lengths on the above

described properties of the metal dithiocarbonates. All synthesised metal xanthates will be characterised properly by various analysing methods.

In the second part of this work, the thermal conversion of the previously synthesised metal dithiocarbonates to semiconducting metal sulphides, as possible solar absorber materials, will be investigated regarding their crystal phase and their optical properties. Furthermore first attempts to fabricate solution processed inorganic solar cells by deployment of the synthesised metal dithiocarbonates will be carried out.

RESULTS AND DISCUSSION

POTASSIUM DITHIOCARBONATES

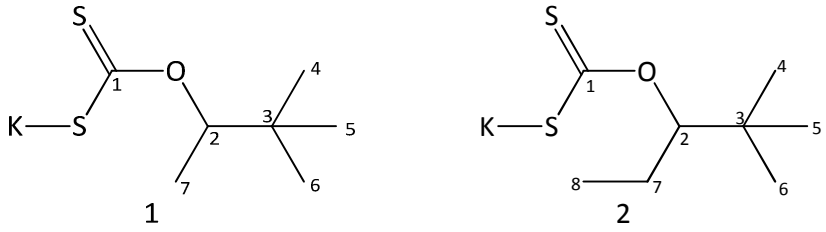

FIGURE 6: POTASSIUM *O*-3,3-DIMETHYLBUTAN-2-YL DITHIOCARBONATE (1) AND POTASSIUM *O*-2,2-DIMETHYLPENTAN-3-YL DITHIOCARBONATE (2)

Potassium *O*-3,3-dimethylbutan-2-yl (**1**) and potassium *O*-2,2-dimethylpentan-3-yl (**2**) dithiocarbonates (Figure 6) were synthesised as educts for further metal xanthates syntheses.

The classical approach to synthesise alkali metal dithiocarbonates is based on the reaction of alkali hydroxides with alcohols and carbon disulphide. [23], [24], [30] Attempts to follow these protocols to obtain **1** and **2** have been carried out, but were not successful, so alternative approaches to gain the desired products were investigated. *Albert González-Roura* and his working group published another way to obtain potassium dithiocarbonates. [32] The described procedure worked very well and gave the products in high yields.

NMR-spectroscopy revealed a good purity of the products and chemical shifts match with literature data. [32] The typical high shift of the proton on C_2 in the ^{1}H-NMR spectra and the typical high shifts of C_1 and of C_2 in the ^{13}C-NMR spectra give proof of a successful reaction, as shown in Table 1.

TABLE 1: TYPICAL CHEMICAL SHIFTS IN NMR-SPECTROSCOPY

1	chemical shift (ppm)	2	chemical shift (ppm)
H-C_2 (^{1}H-NMR)	5.4	**H-C_2 (^{1}H-NMR)**	5.6
C_1 (^{13}C-NMR)	233.7	**C_1 (^{13}C-NMR)**	235.4
C_2 (^{13}C-NMR)	84.4	**C_2 (^{13}C-NMR)**	88.7

Results of elemental analyses are presented in Table 2 and prove the purity of the products.

TABLE 2: ELEMENTAL ANALYSES OF POTASSIUM *O*-3,3-DIMETHYLBUTAN-2-YL DITHIOCARBONATE (1) AND POTASSIUM *O*-2,2-DIMETHYLPENTAN-3-YL DITHIOCARBONATE (2)

	Potassium *O*-3,3-dimethylbutan-2-yl dithiocarbonate (1)		Potassium *O*-2,2-dimethylpentan-3-yl dithiocarbonate (2)	
	calculated	found	calculated	found
C (%)	38.85	38.75	41.70	41.70
S (%)	29.63	29.74	27.83	26.38
H (%)	6.05	6.10	6.56	6.59

Fourier transform infrared spectroscopy was used to investigate the chemical structure of synthesised potassium dithiocarbonates. The assignment of the FTIR results is based on literature data, and is summarised in Table 3. [6], [30], [34], [35], [36]

TABLE 3: SELECTED FEATURES AND CORRESPONDING INTERPRETATION OF THE VIBRATIONAL SPECTRA OF POTASSIUM *O*-3,3-DIMETHYLBUTAN-2-YL DITHIOCARBONATE (1) AND POTASSIUM *O*-2,2-DIMETHYLPENTAN-3-YL DITHIOCARBONATE (2)

1 (cm^{-1})	2 (cm^{-1})	assignment
2963	**2964**	CH_3 out-of-plane stretching
2870	**2872**	CH_3 in-plane stretching
1474	**1479**	CH_3 out-of-plane deformation
1456	**1457**	CH_3 out-of-plane deformation
1393	**1393**	CH_3 in-plane deformation
1377	**1382**	CH_3 in-plane deformation
1363	**1365**	CH wagging
1223	**1231**	COC out-of-plane stretching
1208	**1205**	COC out-of-plane stretching
1133	**1140**	CH_3 rocking, (S)CO stretching
1101	**1109**	CCC out-of-plane stretching
1085	**1070**	CCC out-of-plane stretching
1066	**1042**	CS_2 out-of-plane stretching
1030	**1021**	CS_2 out-of-plane stretching

METAL DITHIOCARBONATES

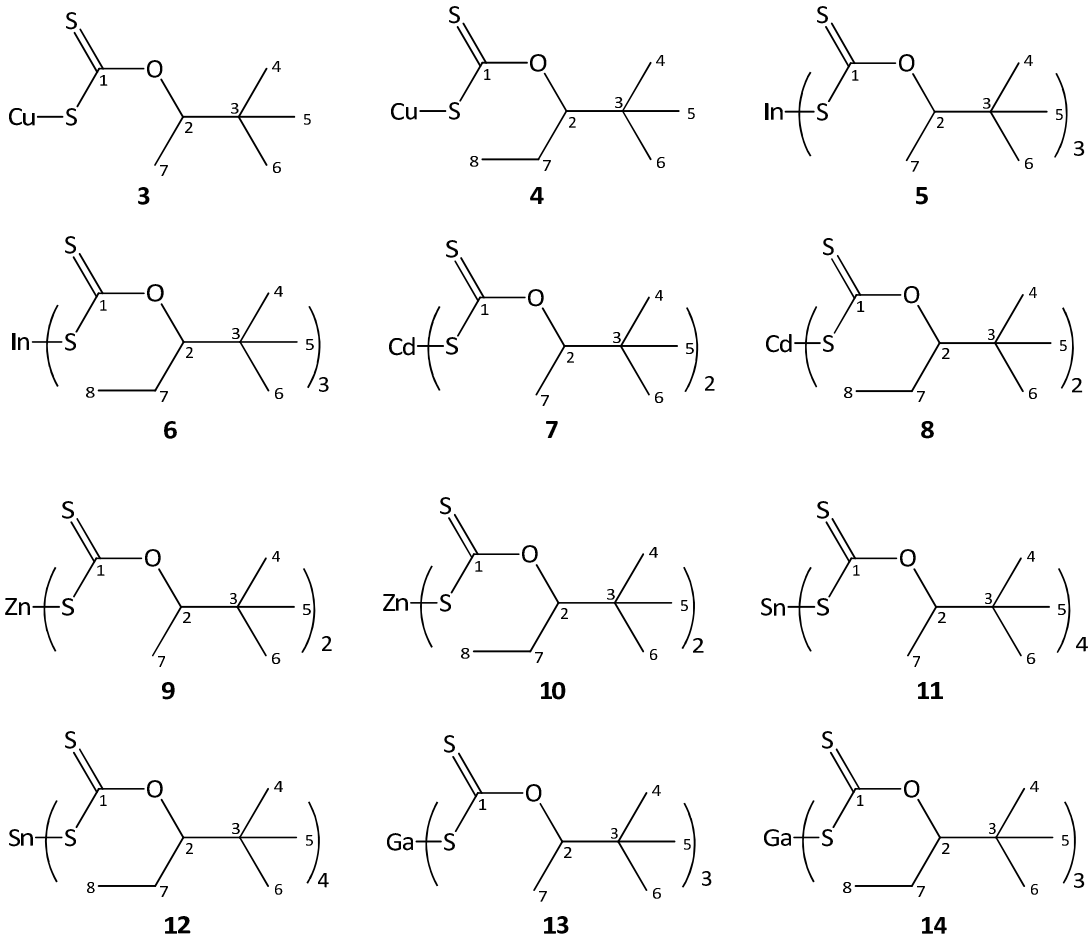

FIGURE 7: OVERVIEW OF THE SYNTHESISED METAL DITHIOCARBONATES : COPPER *O*-3,3-DIMETHYLBUTAN-2-YL DITHIOCARBONATE (3), COPPER *O*-2,2-DIMETHYLPENTAN-3-YL DITHIOCARBONATE (4), INDIUM *O*-3,3-DIMETHYLBUTAN-2-YL DITHIOCARBONATE (5), INDIUM *O*-2,2-DIMETHYLPENTAN-3-YL DITHIOCARBONATE (6), CADMIUM *O*-3,3-DIMETHYLBUTAN-2-YL DITHIOCARBONATE (7), CADMIUM *O*-2,2-DIMETHYLPENTAN-3-YL DITHIOCARBONATE (8), ZINC *O*-3,3-DIMETHYLBUTAN-2-YL DITHIOCARBONATE (9), ZINC *O*-2,2-DIMETHYLPENTAN-3-YL DITHIOCARBONATE (10), TIN *O*-3,3-DIMETHYLBUTAN-2-YL DITHIOCARBONATE (11), TIN *O*-2,2-DIMETHYLPENTAN-3-YL DITHIOCARBONATE (12) GALLIUM *O*-3,3-DIMETHYLBUTAN-2-YL DITHIOCARBONATE (13) AND GALLIUM *O*-2,2-DIMETHYLPENTAN-3-YL DITHIOCARBONATE (14)

In the literature many similar approaches for metal dithiocarbonate syntheses are known. Most differences are given in the used solvents. [23], [24], [25], [26], [27], [28] All herein described metal dithiocarbonate syntheses followed a slightly modified procedure than that reported by *Davide Barecca et al.* and *C. G. Sceney et al.*. [30], [37] For syntheses the corresponding potassium dithiocarbonate was dissolved in deionised water and was added dropwise to aqueous solutions of metal chlorides. All products were recrystallised from chloroform through adding methanol and were

dried in vacuum. Tin *O*-2,2-dimethylpentan-3-yl dithiocarbonate (**12**) turned out to be a liquid. Due to that, it was not possible to purify the product by recrystallisation.

NMR spectroscopy evidenced good purities of the products and the typical high chemical shifts for metal dithiocarbonates as described above are present in all spectra. Elemental analysis supports the conclusion of high purity of the products (see Table 4 - Table 9). Though NMR spectroscopy revealed the good purity of gallium *O*-2,2-dimethylpentan-3-yl dithiocarbonate (**14**), the results of the elemental analysis do not match with the calculated values, probably due to some degradation processes within the sample.

TABLE 4: ELEMENTAL ANALYSES OF COPPER *O*-3,3-DIMETHYLBUTAN-2-YL DITHIOCARBONATE (3) AND COPPER *O*-2,2-DIMETHYLPENTAN-3-YL DITHIOCARBONATE (4)

	copper *O*-3,3-dimethylbutan-2-yl dithiocarbonate (3)		**copper *O*-2,2-dimethylpentan-3-yl dithiocarbonate (4)**	
	calculated	found	calculated	found
C (%)	34.91	34.31	37.70	37.71
S (%)	26.43	27.09	25.16	25.62
H (%)	5.44	5.37	5.93	5.89

TABLE 5: ELEMENTAL ANALYSES OF INDIUM *O*-3,3-DIMETHYLBUTAN-2-YL DITHIOCARBONATE (5) AND INDIUM *O*-2,2-DIMETHYLPENTAN-3-YL DITHIOCARBONATE (6)

	indium *O*-3,3-dimethylbutan-2-yl dithiocarbonate (5)		**indium *O*-2,2-dimethylpentan-3-yl dithiocarbonate (6)**	
	calculated	found	calculated	found
C (%)	39.00	38.87	41.85	41.88
S (%)	29.75	30.25	27.93	28.39
H (%)	6.08	6.01	6.58	6.60

TABLE 6: ELEMENTAL ANALYSES OF CADMIUM *O*-3,3-DIMETHYLBUTAN-2-YL DITHIOCARBONATE (7) AND CADMIUM *O*-2,2-DIMETHYLPENTAN-3-YL DITHIOCARBONATE (8)

	cadmium *O*-3,3-dimethylbutan-2-yl dithiocarbonate (7)		cadmium *O*-2,2-dimethylpentan-3-yl dithiocarbonate (8)	
	calculated	found	calculated	found
C (%)	36.00	34.76	38.82	38.84
S (%)	27.46	26.76	25.91	25.91
H (%)	5.61	5.28	6.11	6.11

TABLE 7: ELEMENTAL ANALYSES OF ZINC *O*-3,3-DIMETHYLBUTAN-2-YL DITHIOCARBONATE (9) AND ZINC *O*-2,2-DIMETHYLPENTAN-3-YL DITHIOCARBONATE (10)

	zinc *O*-3,3-dimethylbutan-2-yl dithiocarbonate (9)		zinc *O*-2,2-dimethylpentan-3-yl dithiocarbonate (10)	
	calculated	found	calculated	found
C (%)	40.04	39.88	42.89	42.45
S (%)	30.54	31.03	28.63	28.57
H (%)	6.24	6.23	6.75	6.79

TABLE 8: ELEMENTAL ANALYSES OF TIN *O*-3,3-DIMETHYLBUTAN-2-YL DITHIOCARBONATE (11) AND TIN *O*-2,2-DIMETHYLPENTAN-3-YL DITHIOCARBONATE (12)

	tin *O*-3,3-dimethylbutan-2-yl dithiocarbonate (11)		tin *O*-2,2-dimethylpentan-3-yl dithiocarbonate (12)	
	calculated	found	calculated	found
C (%)	33.27	32.20	43.48	40.04
S (%)	31.72	30.95	29.02	26.02
H (%)	5.19	4.97	6.84	6.10

TABLE 9: ELEMENTAL ANALYSES OF GALLIUM *O*-3,3-DIMETHYLBUTAN-2-YL DITHIOCARBONATE (13) AND GALLIUM *O*-2,2-DIMETHYLPENTAN-3-YL DITHIOCARBONATE (14)

	gallium *O*-3,3-dimethylbutan-2-yl dithiocarbonate (13)		gallium *O*-2,2-dimethylpentan-3-yl dithiocarbonate (14)	
	calculated	found	calculated	found
C (%)	41.92	41.52	44.78	32.76
S (%)	31.98	31.88	29.89	19.11
H (%)	6.53	6.21	7.05	5.71

Fourier transform infrared spectroscopy showed similar spectra to those described above in Table 3. Hardly any differences can be found in the spectra of products. Major differences occur only in the range of 1300 – 1200 cm^{-1}. The absorption peaks in this range shift slightly depending on the deployed metal atom (see Figure 8 and Figure 9). The absorption peaks of the potassium dithiocarbonates are marked with dashed lines for a better visibility, and to point out the considerable effect of the deployed metal atoms.

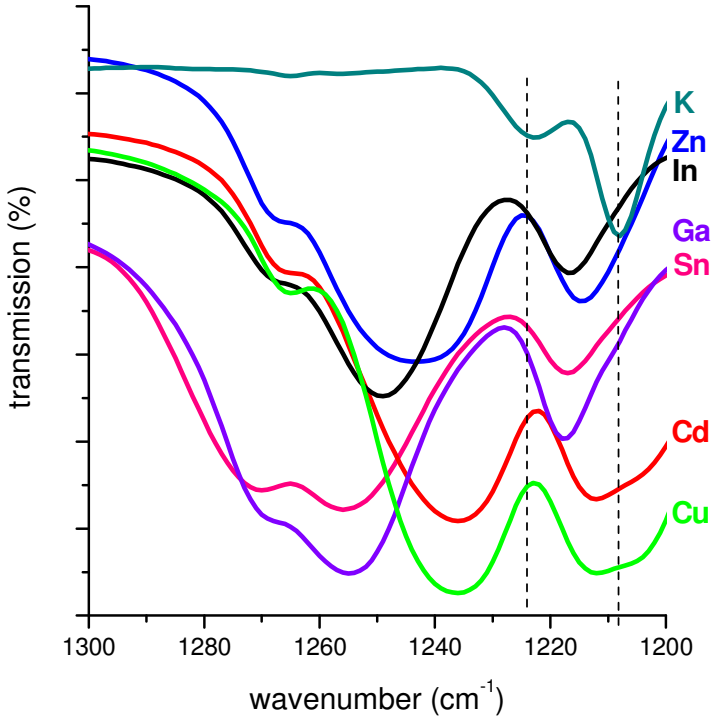

FIGURE 8: INFRARED SPECTRA OF THE SYNTHESISED METAL *O*-3,3-DIMETHYLBUTAN-2-YL DITHIOCARBONATES (1, 3, 5, 7, 9, 11, 13) IN THE RANGE OF 1300 – 1200 CM^{-1}

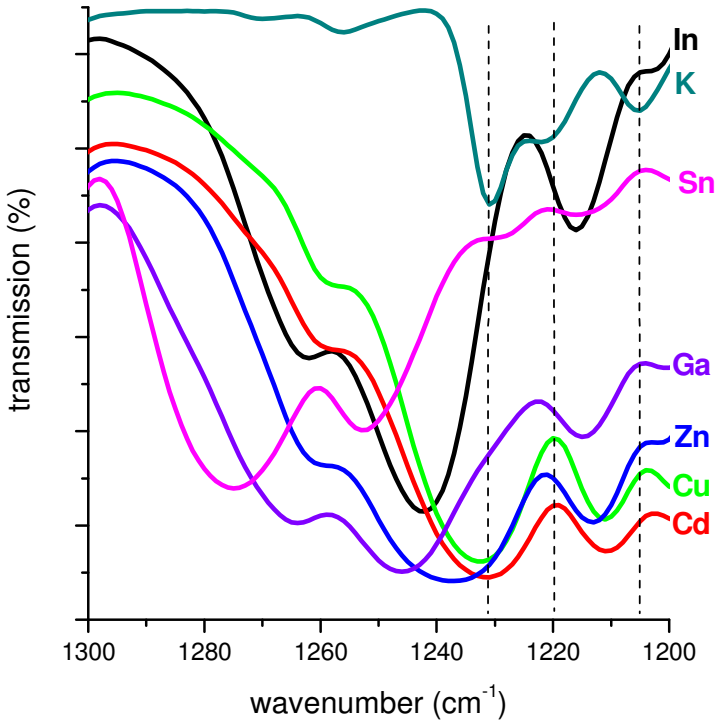

FIGURE 9: INFRARED SPECTRA OF THE SYNTHESISED METAL *O*-2,2-DIMETHYLPENTAN-3-YL DITHIOCARBONATES (2, 4, 6, 8, 10, 12, 14) IN THE RANGE OF 1300 – 1200 CM^{-1}

Metal dithiocarbonates are known to have low decomposition temperatures, usually lower than those reported for the more widely exploited metal dithiocarbamates and to have a clean decomposition pathway enabled by the Chugaev rearrangement. [27], [29], [31] The thermal behaviour of all herein described metal dithiocarbonates was investigated. All products, except for gallium *O*-3,3-dimethylbutan-2-yl dithiocarbonate (**13**) show single-step decomposition in thermal gravimetric analysis. The decomposition temperatures were determined at a mass loss of 5 % and are summarised in Table 10. Representative for all thermal gravimetric analyses the thermal gravimetric curves of copper *O*-3,3-dimethylbutan-2-yl dithiocarbonate and copper *O*-2,2-dimethylpentan-3-yl dithiocarbonate are given in Figure 10 and Figure 11.

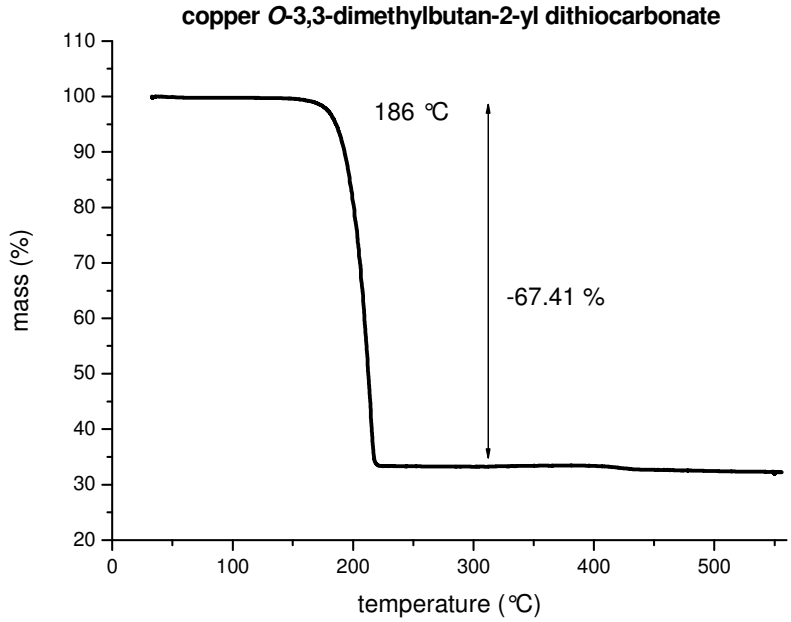

FIGURE 10 : THERMAL GRAVIMETRIC ANALYSIS OF COPPER *O*-3,3-DIMETHYLBUTAN-2-YL DITHIOCARBONATE

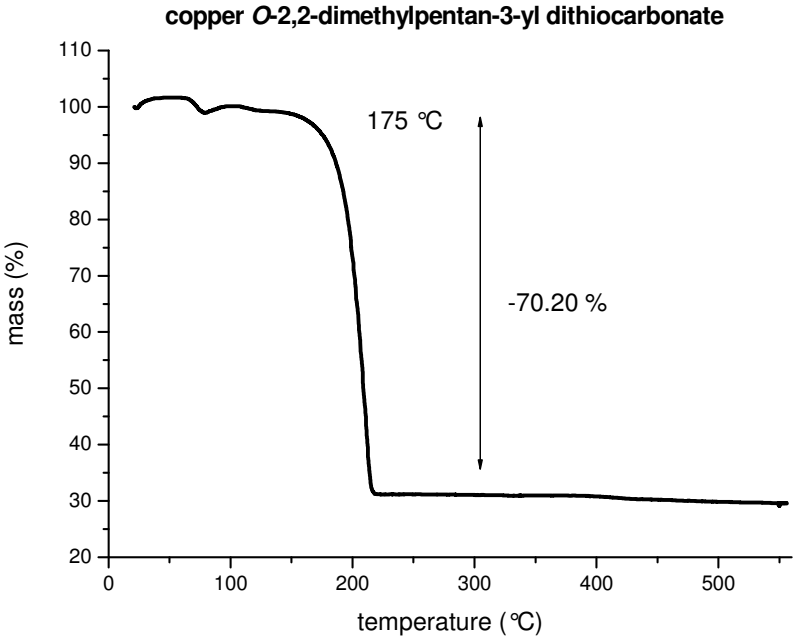

FIGURE 11: THERMAL GRAVIMETRIC ANALYSIS OF COPPER *O*-2,2-DIMETHYLPENTAN-3-YL DITHIOCARBONATE

TABLE 10: DECOMPOSITION TEMPERATURES OF THE SYNTHESISED METAL DITHIOCARBONATES

metal dithiocarbonate	T_d (°C)	metal dithiocarbonate	T_d (°C)
3 (Cu)	186	**4 (Cu)**	175
5 (In)	162	**6 (In)**	142
7 (Cd)	148	**8 (Cd)**	141
9 (Zn)	144	**10 (Zn)**	141
11 (Sn)	116	**12 (Sn)**	116
13 (Ga)	150	**14 (Ga)**	126

The gained results exhibit significant decreases of decomposition temperatures for all products with the more steric moiety. As expected the size of the moiety influences not only decomposition temperatures, but also solubility characteristics. Metal *O*-2,2 dimethylpentan-3-yl dithiocarbonates are soluble in a wide range of common solvents, e.g. chloroform, tetrahydrofuran, benzene, toluene, chlorobenzene, trichlorobenzene, xylene, pyridine and others. Metal dithiocarbonates having the less steric moiety show good solubility only in few of those solvents.

Mass spectrometric analyses were performed to determine the purity of the products. The molecular ion peak was hard to find, but the typical decomposition products of metal dithiocarbonates as expected by the Chugaev rearrangement, like carbon oxide sulphide, carbon disulphide and the corresponding alkenyl residue are present in the mass spectra. [31] Additionally typical fragmentation patterns can be found. Representatively for all synthesised metal dithiocarbonates the mass spectra of indium *O*-3,3-dimethylbutan-2-yl and indium *O*-2,2-dimethylpentan-3-yl dithiocarbonate are depicted in Figure 12 and Figure 13. In both cases the molecular ion peak at m^*z^{-1} is 646.02 and 688.06, respectively, were found with low intensities. Typical fragmentation products, like single-substituted metal atoms can be found and are pointed out in the presented figures. Furthermore the expected decomposition products of the metal dithiocarbonates are also given, including the theoretical isotope pattern, in the figures.

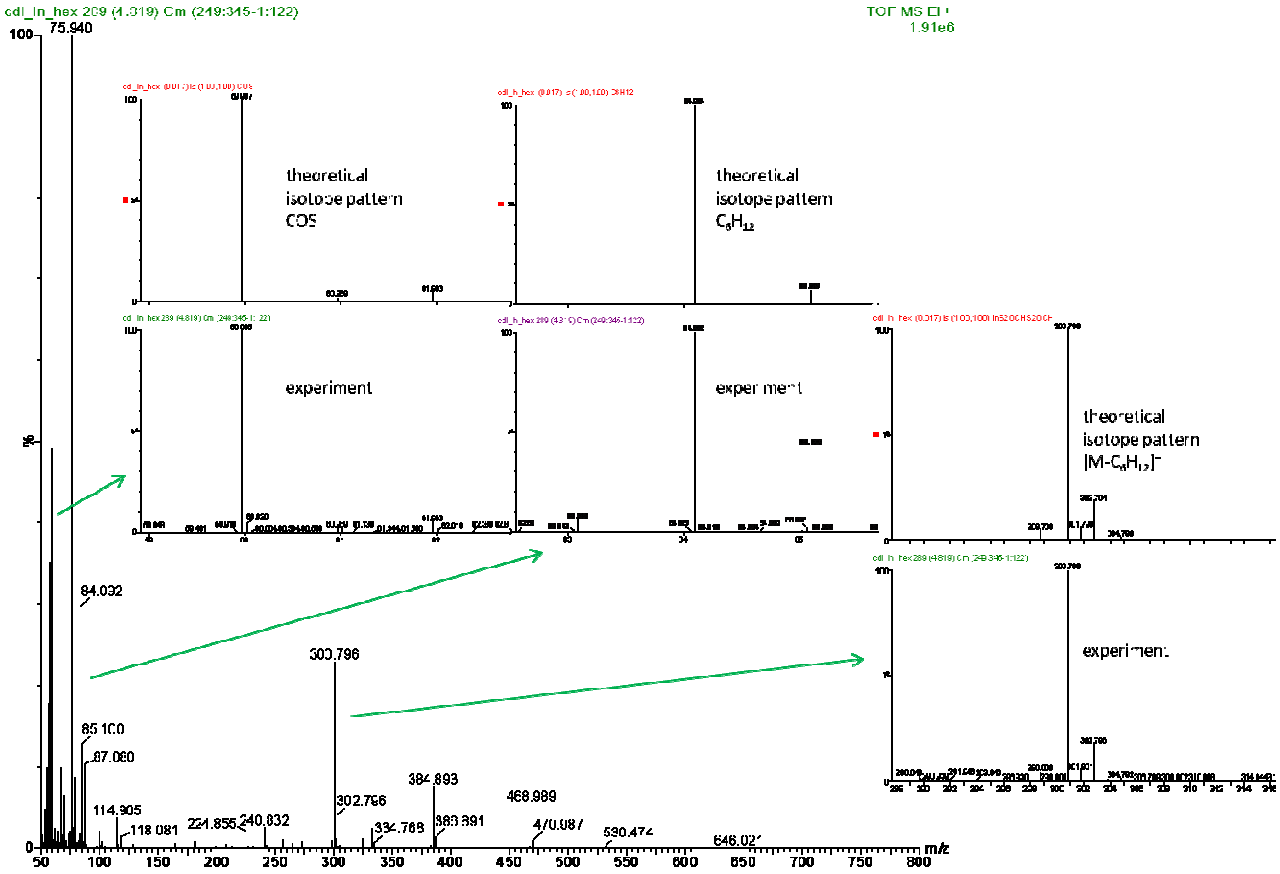

FIGURE 12: MASS SPECTRUM OF INDIUM *O*-3,3-DIMETHYLBUTAN-2-YL DITHIOCARBONATE (5)

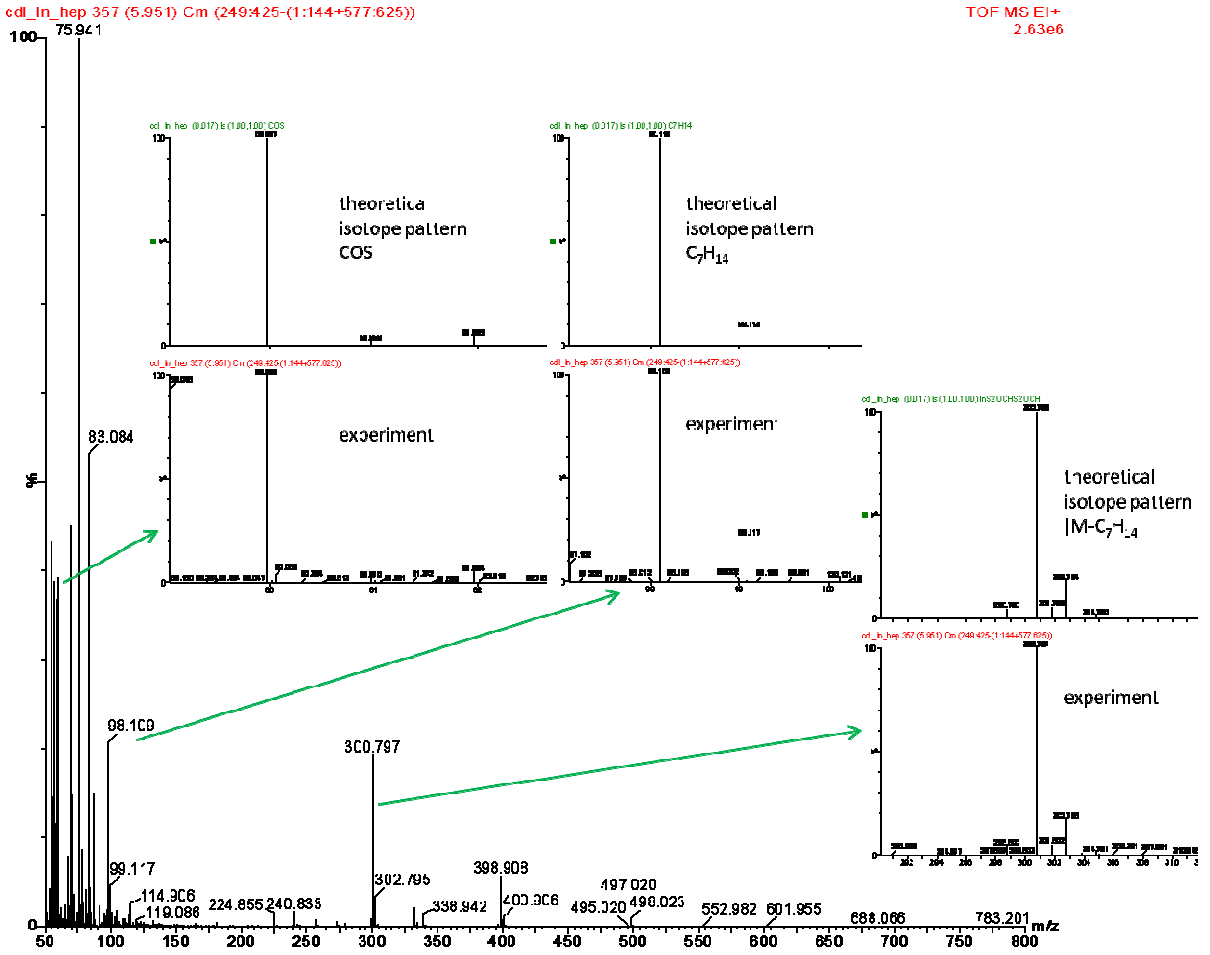

FIGURE 13: MASS SPECTRUM OF INDIUM *O*-2,2-DIMETHYLPENTAN-3-YL DITHIOCARBONATE (6)

FORMATION OF COPPER INDIUM DISULPHIDE

Copper indium disulphide is a semiconductor with very attractive properties as absorber material for thin-film photovoltaic applications due to a low direct band gap and a corresponding high absorption coefficient of approximately $10^4 – 10^5$ cm^{-1}. [1], [10] In literature different routes for semiconductor formation are given. Most common techniques are vacuum based approaches, like sputtering [38] and evaporation [39]. To reduce production costs of thin-film solar cells solution processed approaches are nowadays of strong scientific interest. Various attempts to prepare $CuInS_2$ via non-vacuum routes, like spray pyrolysis [40], [41], [42] and electro deposition [43], can be found in literature. [1]

As metal dithiocarbonates are known to decompose at moderate temperatures in a clean decomposition pathway towards metal sulphides [27], [29], [31], the concept of mixing the corresponding copper and indium dithiocarbonates to obtain the desired $CuInS_2$ was formed.

Copper and indium *O*-2,2-dimethylpentan-3-yl dithiocarbonates were mixed in different stoichiometric ratios, due to the reported problem, that indium sublimates during annealing processes and is therefore lost for $CuInS_2$ formation. [44] The xanthate mixtures were analysed by thermogravimetry. The thermal gravimetric curves are presented in Figure 14 - Figure 17. All mixtures exhibit single-step decomposition with much lower decomposition temperatures, which were determined at a mass loss of 5 %, than those for each metal dithiocarbonate (see Table 10). For example, the copper *O*-2,2-dimethylpentan-3-yl dithiocarbonate decomposes at 175 °C and the indium *O*-2,2-dimethylpentan-3-yl dithiocarbonate decomposes at 142 °C. Even the decomposition of the mixtures is finished at lower temperatures than the copper dithiocarbonate. These results confirm that the mixture reacts as a single compound, since no two-step decomposition has been observed. All mass losses are close to the theoretically estimated loss of 74.66 %. The slightly increased mass losses could be due to the high volatility of the indium compound.

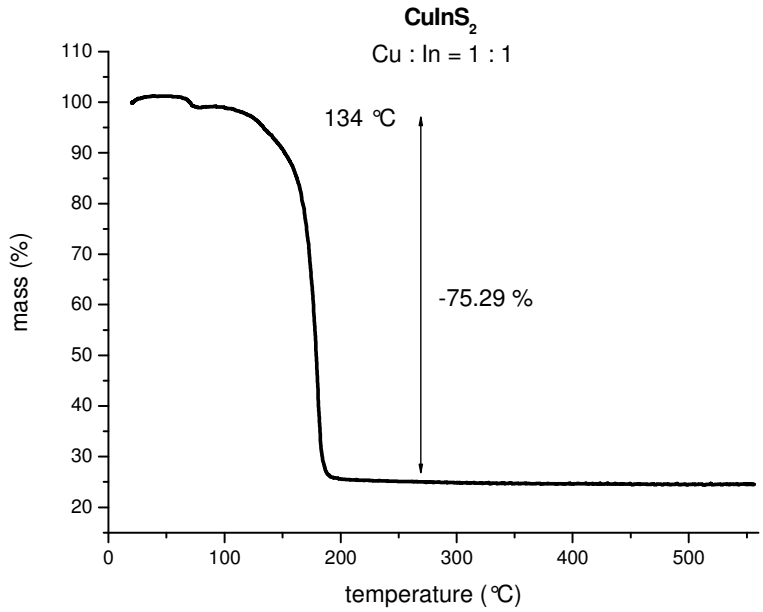

FIGURE 14: THERMAL GRAVIMETRIC CURVE OF COPPER AND INDIUM DITHIOCARBONATE MIXTURE WITH STOICHIOMETRIC RATIOS OF CU : IN = 1 : 1

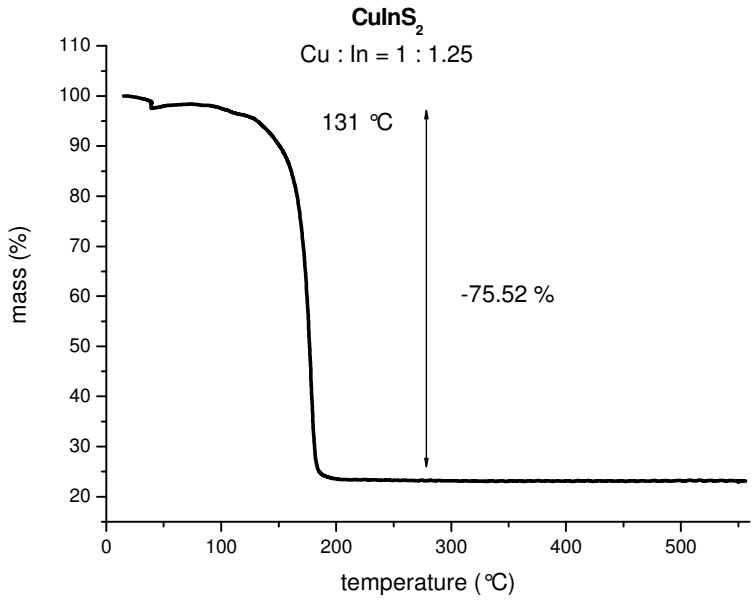

FIGURE 15: THERMAL GRAVIMETRIC CURVE OF COPPER AND INDIUM DITHIOCARBONATE MIXTURE WITH STOICHIOMETRIC RATIOS OF CU : IN = 1 : 1.25

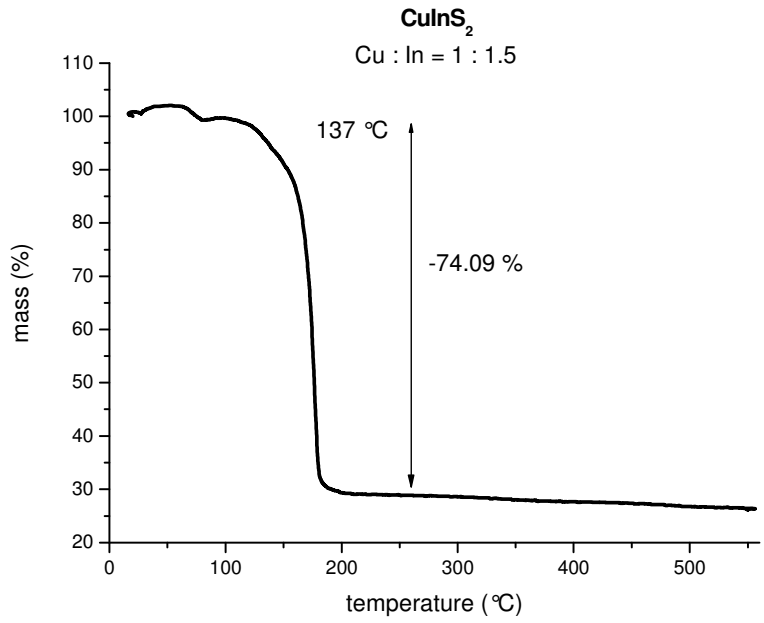

FIGURE 16: THERMAL GRAVIMETRIC CURVE OF COPPER AND INDIUM DITHIOCARBONATE MIXTURE WITH STOICHIOMETRIC RATIOS OF CU : IN = 1 : 1.5

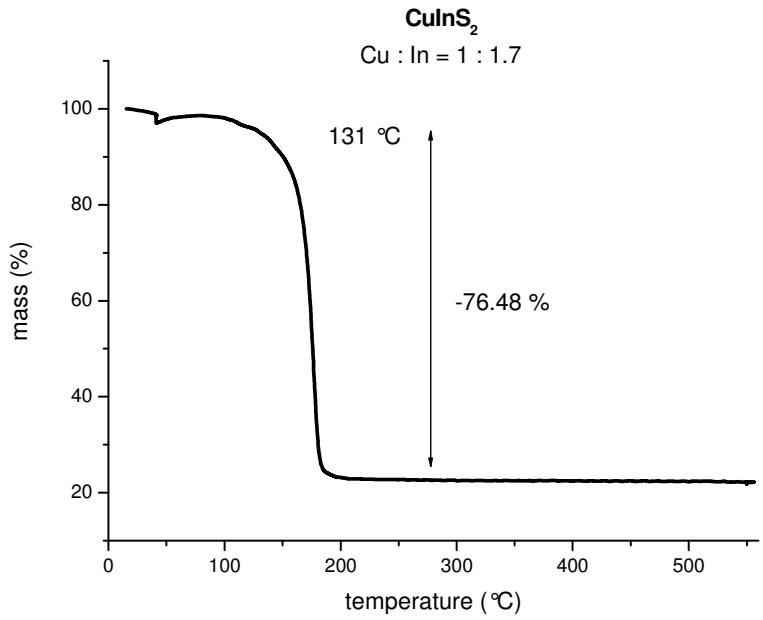

FIGURE 17: THERMAL GRAVIMETRIC CURVE OF COPPER AND INDIUM DITHIOCARBONATE MIXTURE WITH STOICHIOMETRIC RATIOS OF CU : IN = 1 : 1.7

Further experiments were arranged to support the conclusion, that copper indium disulphide could be produced by thermal treatment of copper and indium dithiocarbonate mixtures. Mixtures with the same stoichiometric ratios of the dithiocarbonates as described above were dissolved in chloroform and drop coated on glass substrates. The precursor containing substrates were baked at different temperatures (see Table 33) with a heating rate of about 7 °C*min^{-1}. The obtained $CuInS_2$ was scratched off the glass substrates and characterised with X-ray powder diffraction and energy dispersive X-ray transmission electron microscopy.

Powder diffraction profiles (see Figure 18 - Figure 21) exhibit that all deposited films show the typical chalcopyrite crystalline structure with preferred (112) orientation. [45] For all samples the major characteristic diffraction X-ray reflexes (112), (220) and (312) for the chalcopyrite type structures were observed. With increasing annealing temperature more characteristic peaks, which match with the reference, appeared in the diffraction profiles. The presence of the cubic spinel structure of $CuIn_5S_8$ [46], [47] and the zinc blende structure of Cu-In-S ternary phases [48] cannot be fully ruled out.

Scherrer's equation was used to estimate the crystallite grain size and the obtained results are presented in Table 11. According to the analysis, smaller full-width at half maximum (FWHM) of the peaks indicates larger crystallite grain size. [41] For Scherrer's analysis the grain sizes of the (112), (220) and (312) reflexes were calculated and averaged. Increasing annealing temperatures lead to larger crystallite grain sizes. An increasing indium amount decreases in fact the crystallite grain sizes.

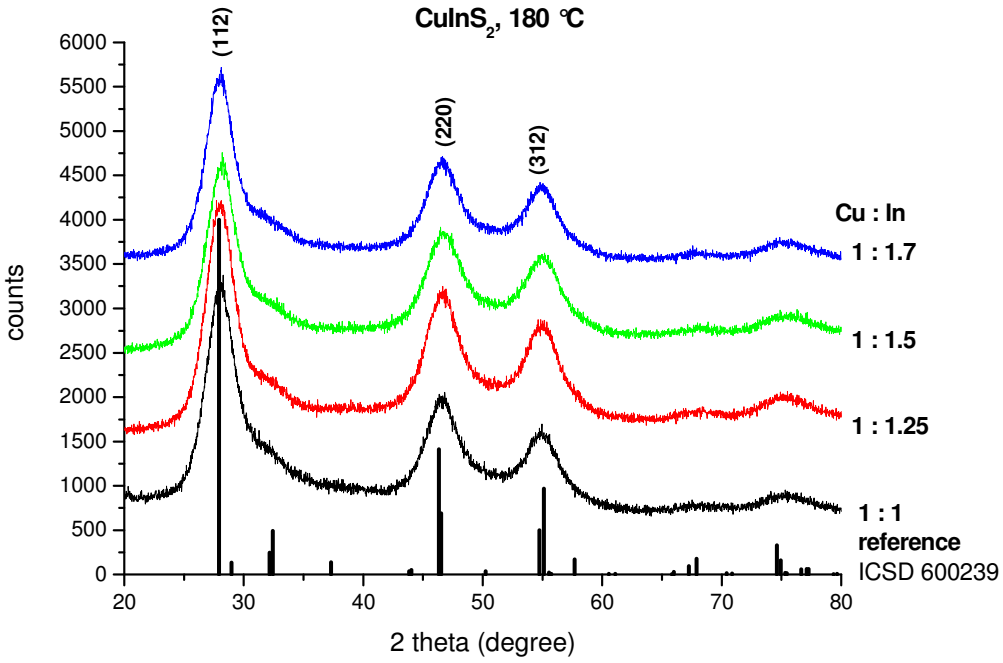

FIGURE 18: XRD-PROFILES OF $CuInS_2$ SAMPLES TREATED AT 180 °C

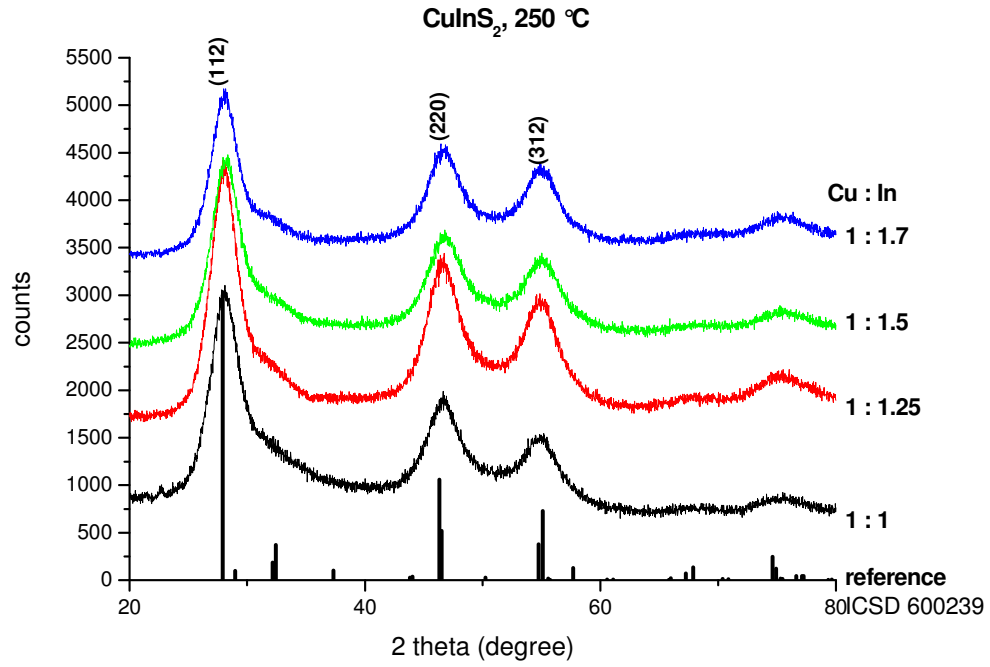

FIGURE 19: XRD-PROFILES OF $CuInS_2$ SAMPLES TREATED AT 250 °C

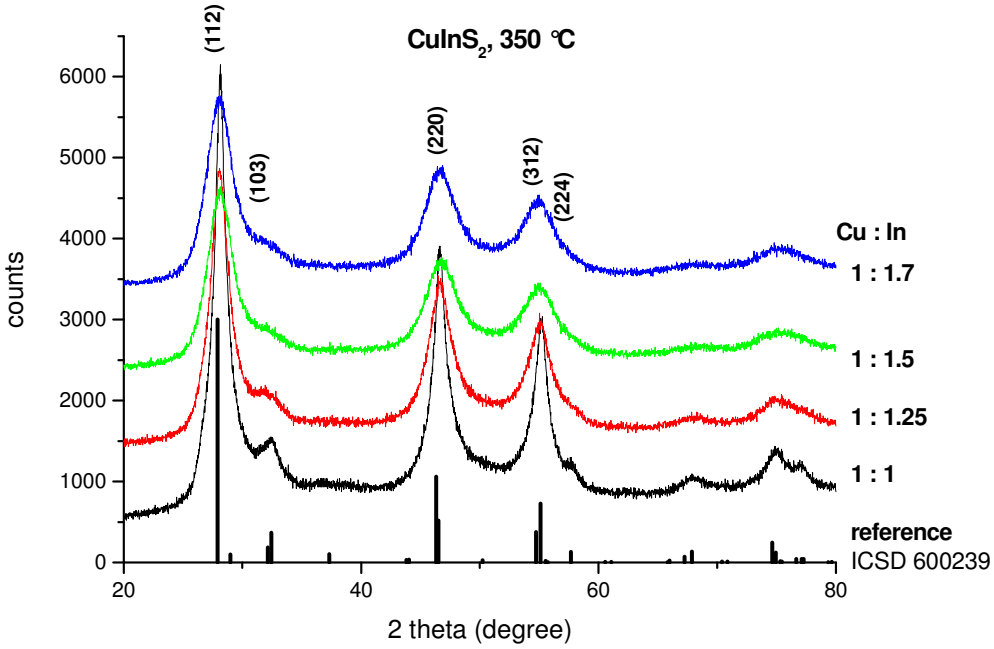

FIGURE 20: XRD-PROFILES OF $CuInS_2$ SAMPLES TREATED AT 350 °C

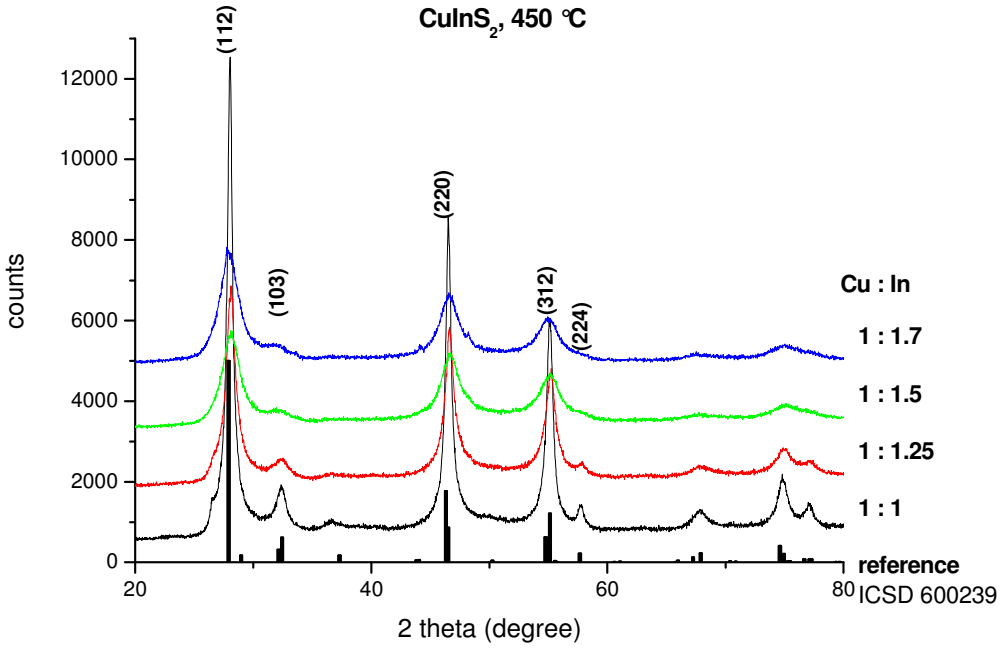

FIGURE 21: XRD-PROFILES OF $CuInS_2$ SAMPLES TREATED AT 450 °C

TABLE 11: CRYSTALLITE GRAIN SIZES FOR $CuInS_2$ SAMPLES TREATED AT DIFFERENT TEMPERATURES, ACCORDING TO SCHERRER'S ANALYSIS

	$d_{180°C}$ (nm)	$d_{250°C}$ (nm)	$d_{350°C}$ (nm)	$d_{450°C}$ (nm)
CIS (1:1)	4.09	3.39	9.24	15.40
CIS (1:1.25)	3.39	3.55	5.82	10.63
CIS (1:1.5)	3.19	3.40	3.88	5.56
CIS (1:1.7)	3.55	3.76	3.86	5.31

Scanning transmission electron microscopy with an energy dispersive X-ray detector was used to determine the chemical composition of the $CuInS_2$ samples annealed at 450 °C. At least 5 points were investigated of each sample. The atom percentages were calculated using the copper Kα, indium Lβ and sulphur Kα peaks using the Cliff - Lorimer approximation. [49] The obtained atom percentages were used to determine the sample composition referring to the calculated copper amount. The averaged atom percentages of the measured points for each sample are listed in Table 12.

TEM-EDX analyses showed that with increasing amounts of indium, different Cu-In-S ternary phases occur within the samples. The samples prepared with stoichiometric ratios of copper to indium of 1 : 1.5 and 1 : 1.7 contain additionally to the desired $CuInS_2$ phase also the probably zinc blende phases $CuIn_2S_{3.5}$ and $CuIn_3S_5$ and the probably cubic spinel phase of $CuIn_5S_8$. [46], [48] The samples with stoichiometric ratios of copper to indium of 1 : 1 and 1 : 1.25 give only $CuInS_2$.

Representative for all particles, which have been analysed, the scanning transmission electron microscopic picture of one investigated particle is given in Figure 22. The points of measurement for energy dispersive X-ray analyses are tagged with a white "X". An EDX spectrum of these points is also depicted in Figure 23 to give an example for all analyses of the $CuInS_2$ particles.

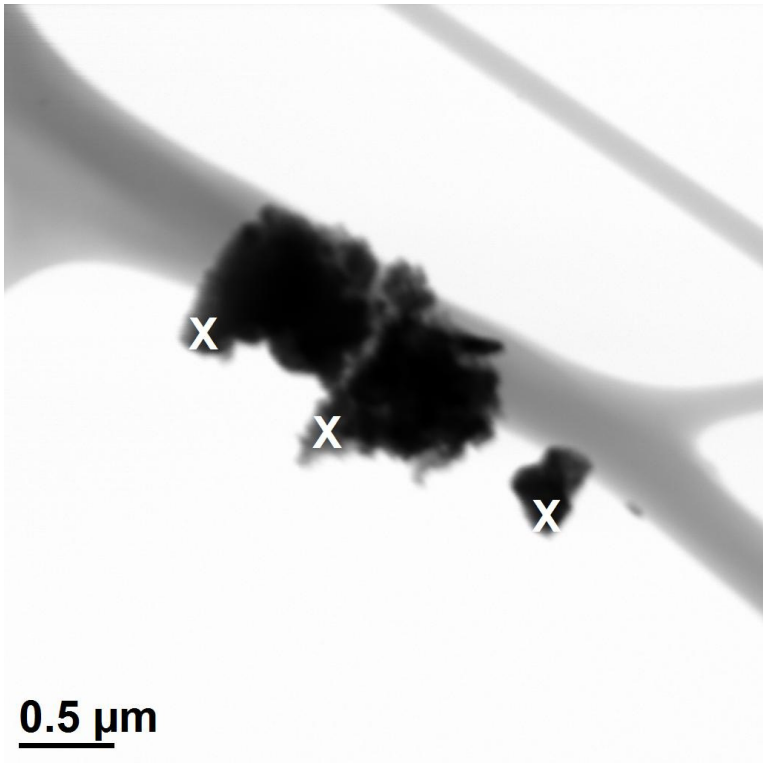

FIGURE 22: SCANNING TRANSMISSION ELECTRON MICROSCOPIC PICTURE OF A COPPER INDIUM DISULPHIDE PARTICLE

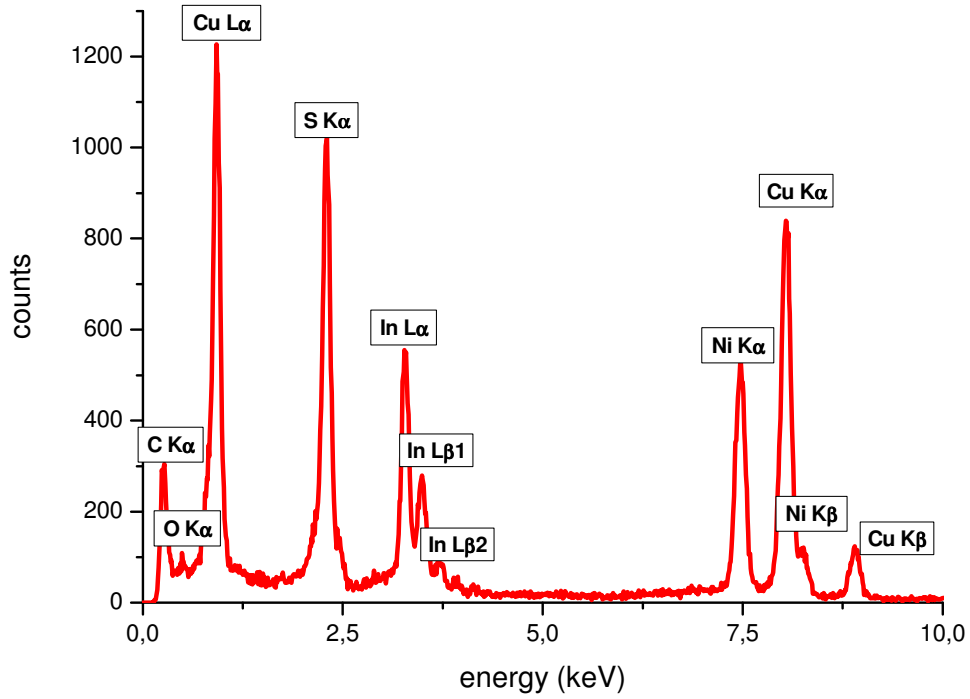

FIGURE 23: ENERGY DISPERSIVE X-RAY SPECTRUM OF A COPPER INDIUM DISULPHIDE PARTICLE

Due to the used nickel grids for sample preparation, the Cu Lα peak could not be employed for the atom percentage calculation, because of the overlapping with the Ni Lα peak.

The influence of the stoichiometric amount of indium within the samples is clearly visible in the calculated and averaged atom percentages in Table 12.

TABLE 12: AVERAGED ATOM PERCENTAGES OF THE COPPER INDIUM DISULPHIDE SAMPLES

	% copper (theoretical)	% indium (theoretical)	% sulphur (theoretical)
CIS (1 : 1)	28.98 (25.00)	21.93 (25.00)	49.10 (50.00)
CIS (1 : 1.25)	20.26 (25.00)	26.11 (25.00)	53.63 (50.00)
CIS (1 : 1.5)	11.93 (25.00)	30.52 (25.00)	57.39 (50.00)
CIS (1 : 1.7)	13.71 (25.00)	31.94 (25.00)	54.35 (50.00)

The optical properties of the synthesised $CuInS_2$ films were analysed by transmittance and reflectance measurements. The gained absorption profiles are presented in Figure 24 - Figure 27. The absorption coefficient α was calculated on the basis of the following equation.

$$\alpha = \frac{1}{d}\ln\left(\frac{1-r}{t}\right)$$

d is the thickness of the film, r the reflectance and t the transmittance of the film. The thicknesses of samples were obtained by surface profiling measurements and are summarised in Table 13.

TABLE 13: FILM THICKNESSES OF THE $CuInS_2$ SAMPLES TREATED AT DIFFERENT TEMPERATURES

	$d_{180°C}$ (nm)	$d_{250°C}$ (nm)	$d_{350°C}$ (nm)	$d_{450°C}$ (nm)
Cu : In = 1 : 1	60	55	50	65
Cu : In = 1 : 1.25	80	45	60	30
Cu : In = 1 : 1.5	65	70	70	50
Cu : In = 1 : 1.7	80	50	65	35

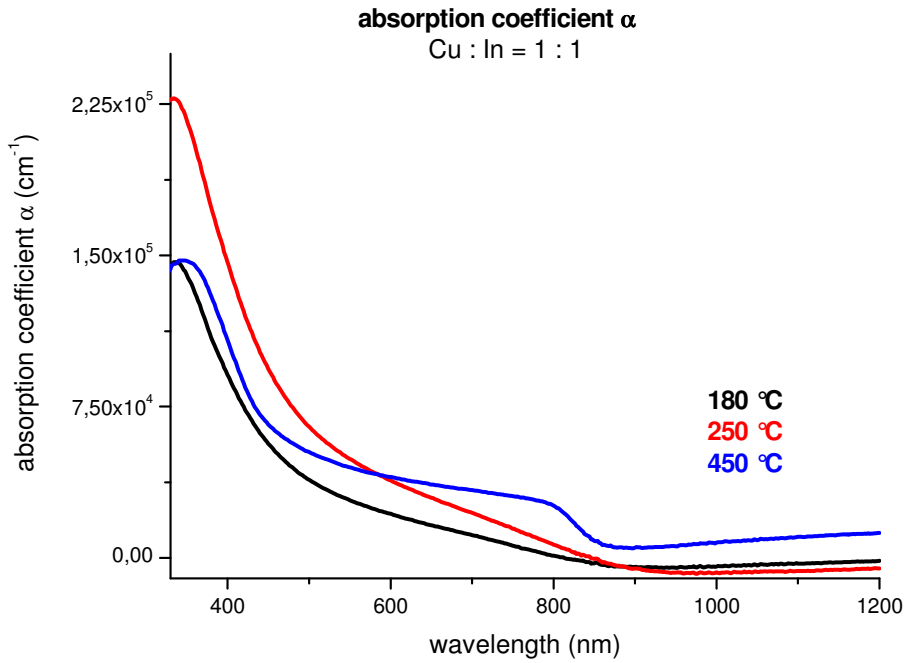

FIGURE 24: OPTICAL ABSORPTION COEFFICIENT OF $CuInS_2$ WITH A COPPER TO INDIUM RATIO OF 1 : 1

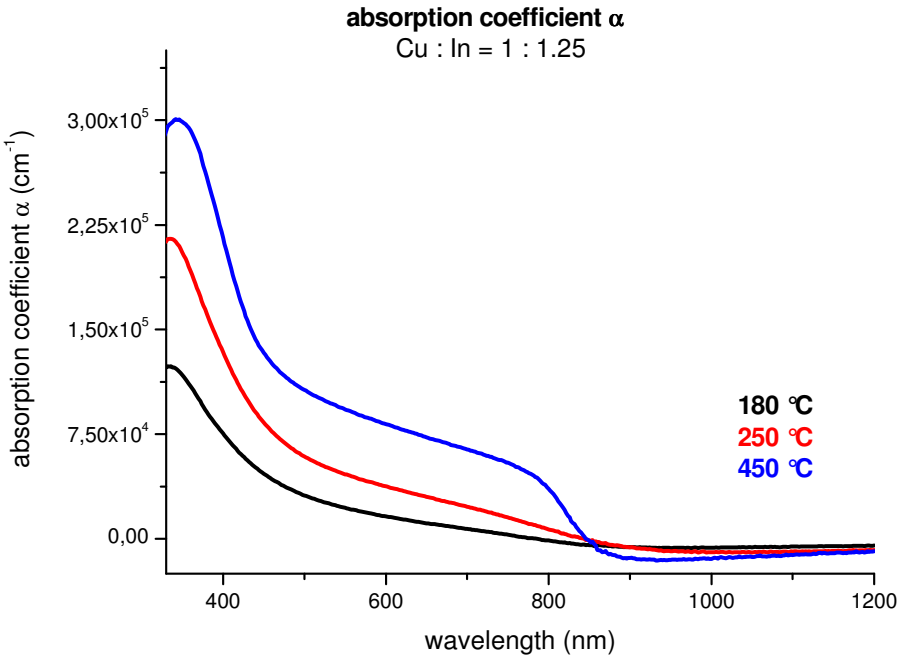

FIGURE 25: OPTICAL ABSORPTION COEFFICIENT OF $CuInS_2$ WITH A COPPER TO INDIUM RATIO OF 1 : 1.25

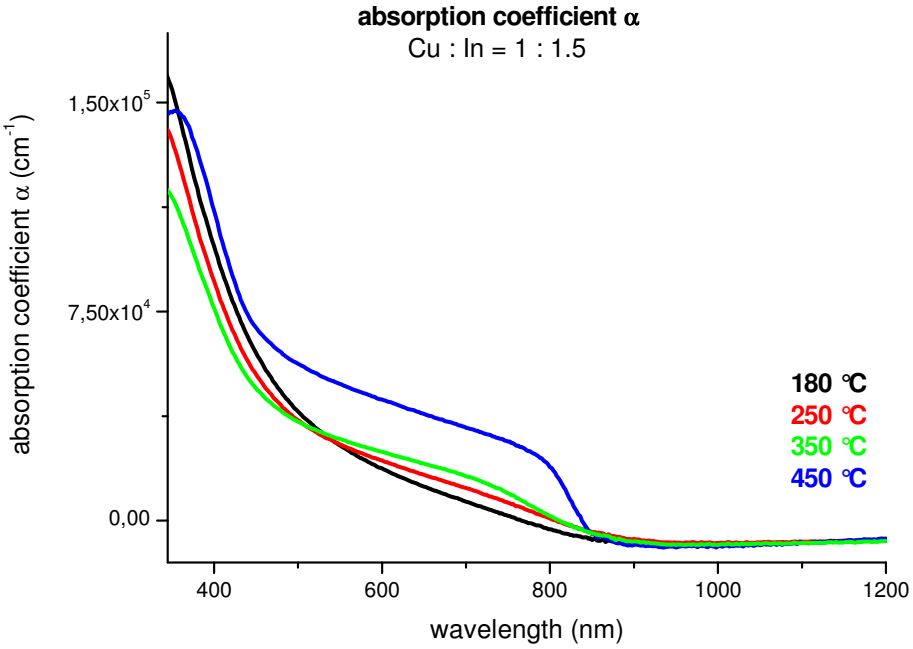

FIGURE 26: OPTICAL ABSORPTION COEFFICIENT OF $CuInS_2$ WITH A COPPER TO INDIUM RATIO OF 1 : 1.5

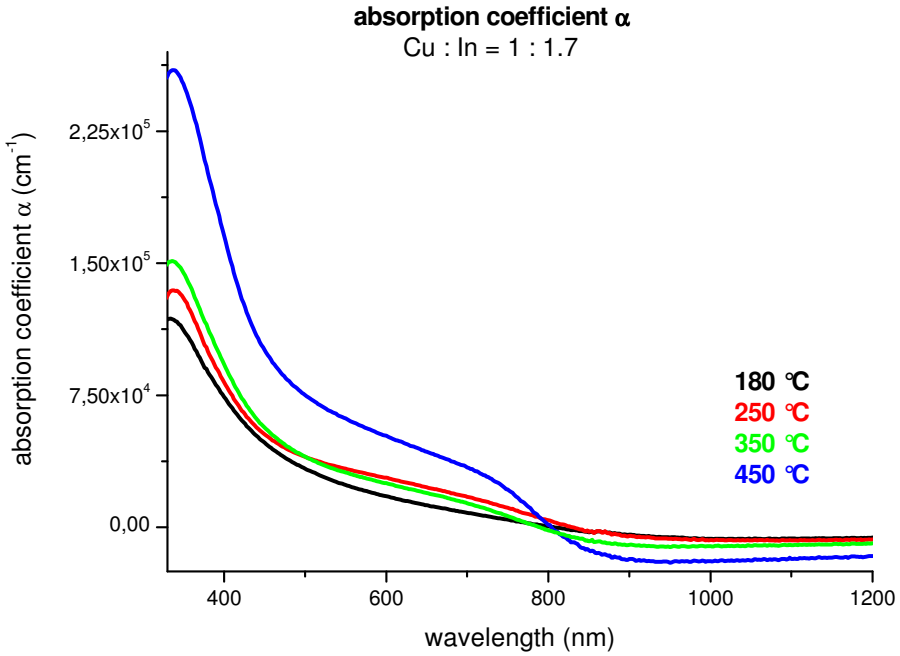

FIGURE 27: OPTICAL ABSORPTION COEFFICIENT OF $CuInS_2$ WITH A COPPER TO INDIUM RATIO OF 1 : 1.7

In agreement with the literature all samples exhibit a high optical absorption coefficient larger than 10^4 cm^{-1}. [1], [10]

The optical band gap E_g can be obtained by following equation. A is constant, $h\nu$ the photon energy, and n an exponent, which indicates a direct band gap, because it was found to be 1/2. [39], [50]

$$\alpha = \frac{A(h\nu - E_g)^n}{h\nu}$$

Therefore the band gap values were determined from $(\alpha h\nu)^2$ versus $h\nu$ plots by linear extrapolation of the functions as shown in the Figure 28 - Figure 31. [51]

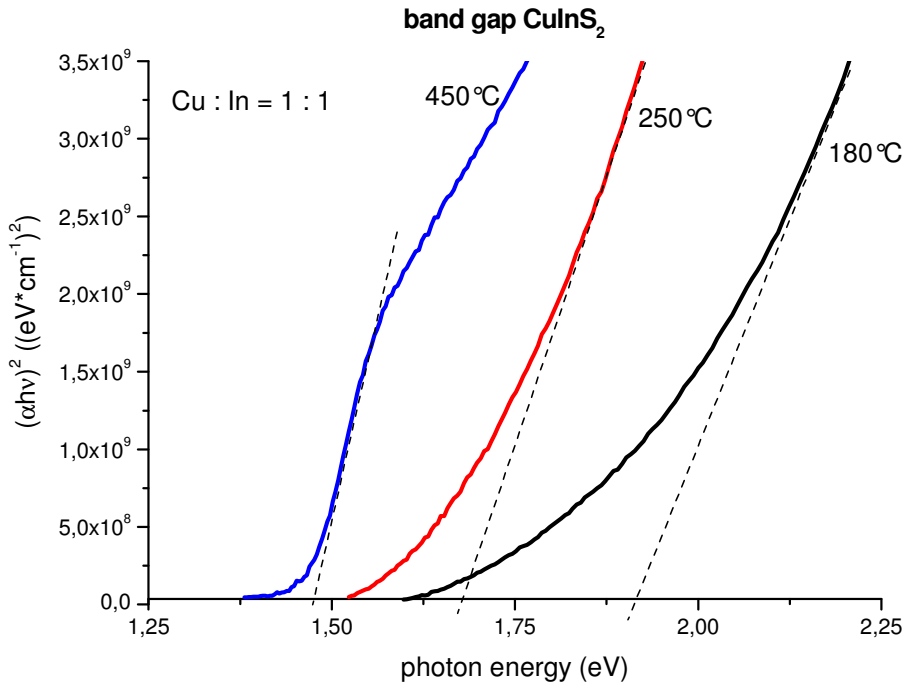

FIGURE 28: OPTICAL BAND GAPS OF $CuInS_2$ WITH A COPPER TO INDIUM RATIO OF 1 : 1 TREATED AT DIFFERENT TEMPERATURES

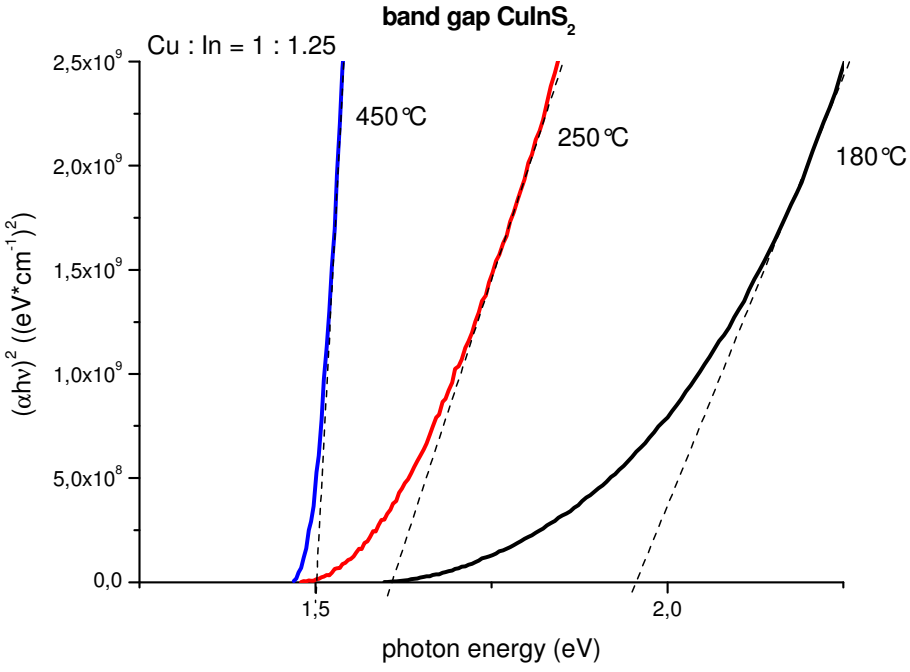

FIGURE 29: OPTICAL BAND GAPS OF $CuInS_2$ WITH A COPPER TO INDIUM RATIO OF 1 : 1.25 TREATED AT DIFFERENT TEMPERATURES

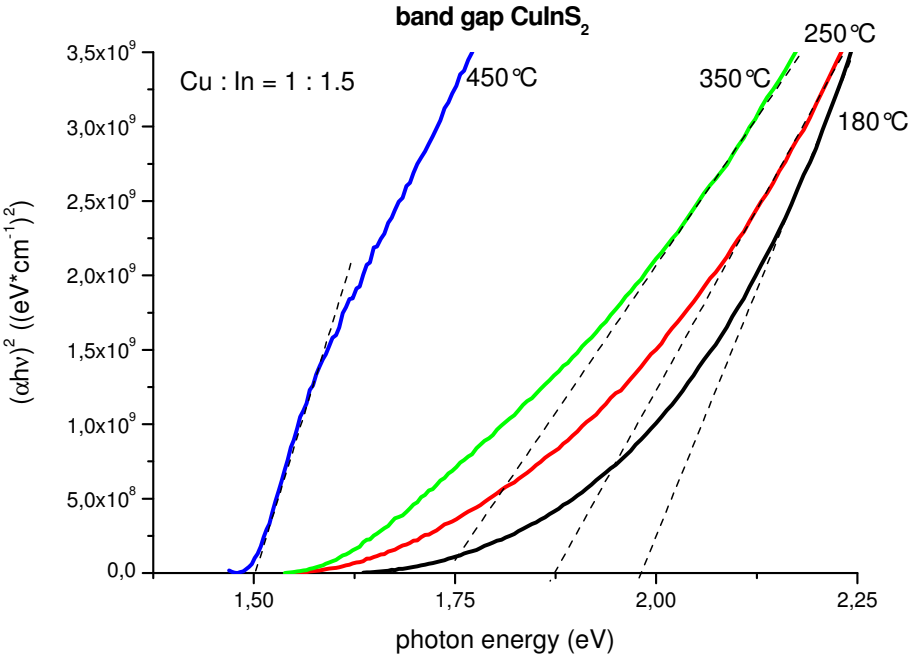

FIGURE 30: OPTICAL BAND GAPS OF $CuInS_2$ WITH A COPPER TO INDIUM RATIO OF 1 : 1.5 TREATED AT DIFFERENT TEMPERATURES

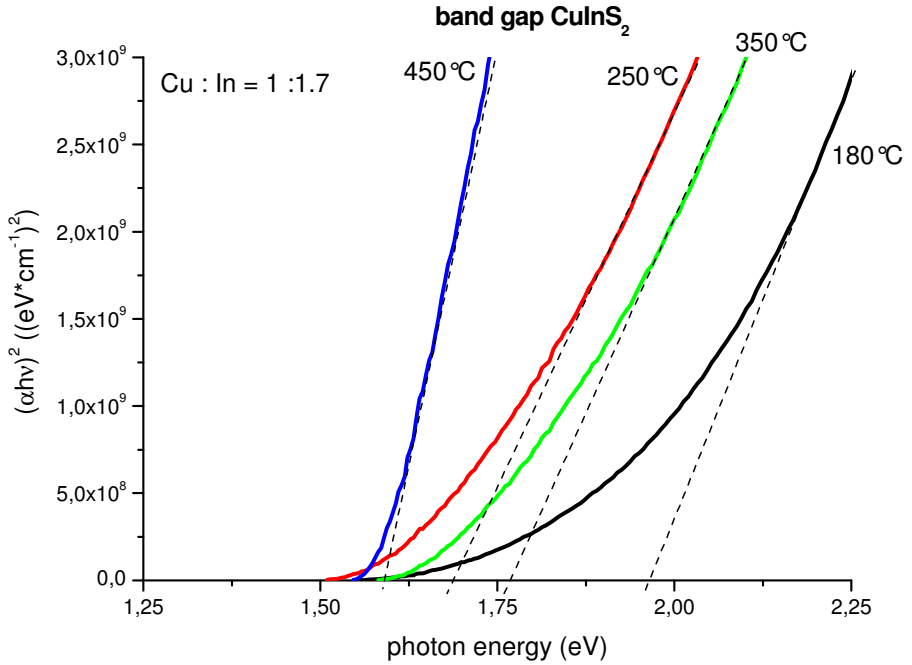

FIGURE 31: OPTICAL BAND GAPS OF $CuInS_2$ WITH A COPPER TO INDIUM RATIO OF 1 : 1.7 TREATED AT DIFFERENT TEMPERATURES

The obtained band gap values for the synthesised $CuInS_2$ samples annealed at 450 °C vary in a range from 1.46 – 1.56 eV, which is also observed in reports in the literature. [1], [13], [39], [41] Optical

band gaps of $CuInS_2$ films synthesised at lower temperature and especially samples prepared at 180 °C exhibit a significant blue shift towards higher eV values.

On the one hand this could be due to quantum dot confinement effect, as the crystallite size increases with higher temperatures and vice versa. [52] On the other hand these blue shifts could be caused by impurities and discrepancies in the chemical composition of samples, as described above. The inaccuracy of the measurement set up should be considered, due to the fact that some samples have very close absorption profiles, which have impact on the band gap estimation.

Due to the promising results of the reflectance and transmittance measurements, the synthesised copper, indium and cadmium *O*-2,2-dimethylpentan-3-yl dithiocarbonates were retained to produce inorganic solar cells. First attempts were arranged in a basic bilayer assembly on indium tin oxide as transparent conductive electrode. The first layer was the copper indium disulphide as p-semiconductor and the second was cadmium sulphide as n-semiconductor to gain the p-n heterojunction. [53] Aluminium was deposited by an evaporation process and was used as back contact.

Dithiocarbonate mixtures with a stoichiometric ratio of the copper to indium of 1 : 1.25 were dissolved in chloroform and doctor bladed on ITO substrates. The precursor containing substrates were baked for 15 minutes at 350 °C in vacuum with a heating rate of about 25 °C*min^{-1}. Then a solution of cadmium dithiocarbonate was doctor bladed on the synthesised $CuInS_2$ film and annealed at 200 °C for 15 minutes in vacuum.

The current density - voltage curve is presented in Figure 32. First attempts of solar cell fabrication with synthesised copper indium disulphide gained satisfying results. Further improvements should be obtained by optimisation of all parameters of the solar cell set up.

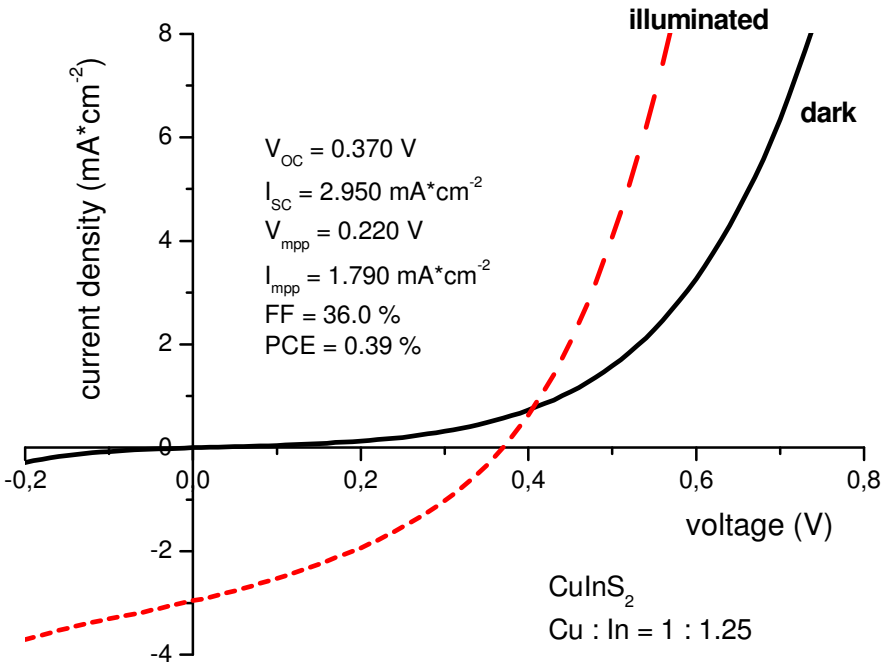

FIGURE 32: CURRENT DENSITY – VOLTAGE CHARACTERISTICS OF A FABRICATED CDS/CUINS$_2$ SOLAR CELL

FORMATION OF COPPER ZINC TIN SULPHIDE

Copper zinc tin sulphide is a semiconductor with very attractive properties as absorber material for thin-film photovoltaic applications due to a low direct band gap and a corresponding high absorption coefficient of approximately 10^4 – 10^5 cm^{-1}. In addition it is a promising candidate to replace semiconductors based on gallium and indium as solar absorber material, due to the fact that it only consists of abundant and cheap elements. [10], [11], [51], [54], [55]

In literature different routes for semiconductor deposition are given. Most common techniques are vacuum based approaches, like sputtering [56], [57], [58] and evaporation [59]. To reduce production costs of thin-film solar cells solution processed approaches are of strong scientific interest. Chemical methods to prepare non-vacuum Cu_2ZnSnS_4 like spray pyrolysis [54], [60], [61], electrochemically deposition [62] and ink based approaches [15] can be found in literature. [10]

Due to good results for preparation of $CuInS_2$ by decomposition of previously mixed metal dithiocarbonates, the concept of this preparation method was adopted to synthesise Cu_2ZnSnS_4 as semiconductor material for photovoltaic applications.

Copper, zinc and tin *O*-3,3-dimethylbutan-2-yl dithiocarbonates were mixed in different stoichiometric ratios. These mixtures were analysed by thermogravimetry. The thermal gravimetric profiles are presented in Figure 33 - Figure 35. All mixtures exhibit single-step decomposition with much lower decomposition temperatures, which were determined at a mass loss of 5 %, than those for each metal dithiocarbonate (see Table 10). For example the copper *O*-3,3-dimethylbutan-2-yl dithiocarbonate decomposes at 186 °C, the zinc *O*-3,3-dimethylbutan-2-yl dithiocarbonate decomposes at 144 °C and the tin *O*-3,3-dimethylbutan-2-yl dithiocarbonate decomposes at 116 °C. Even the decomposition of the mixtures is finished clearly at a much lower temperature compared to the copper dithiocarbonate. These results confirm that the mixture reacts as a single compound, since no three-step decomposition has been observed. All mass losses are close to the theoretically estimated loss of 74.35 %. The decreased mass losses could be due to carbon residues.

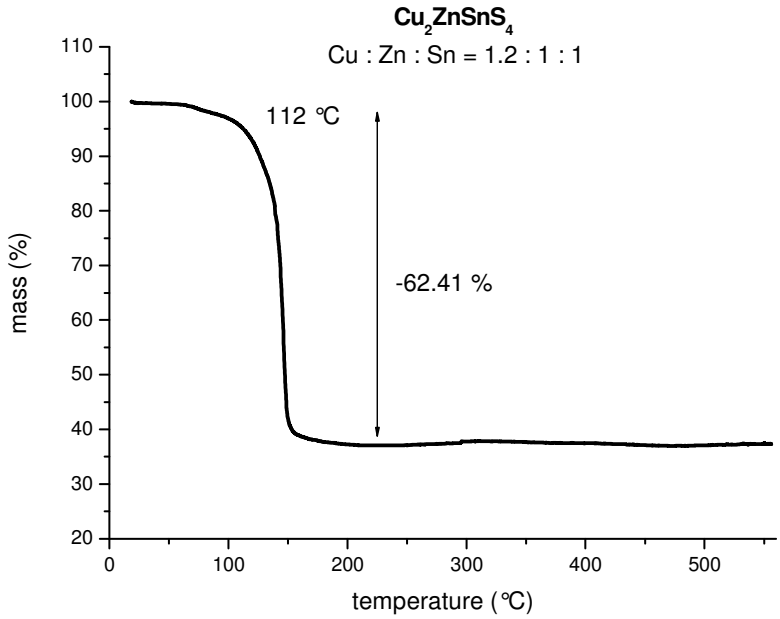

FIGURE 33: THERMAL GRAVIMETRIC CURVE OF COPPER, ZINC AND TIN DITHIOCARBONATE MIXTURE WITH STOICHIOMETRIC RATIOS OF CU : ZN : SN = 1.2 : 1 : 1

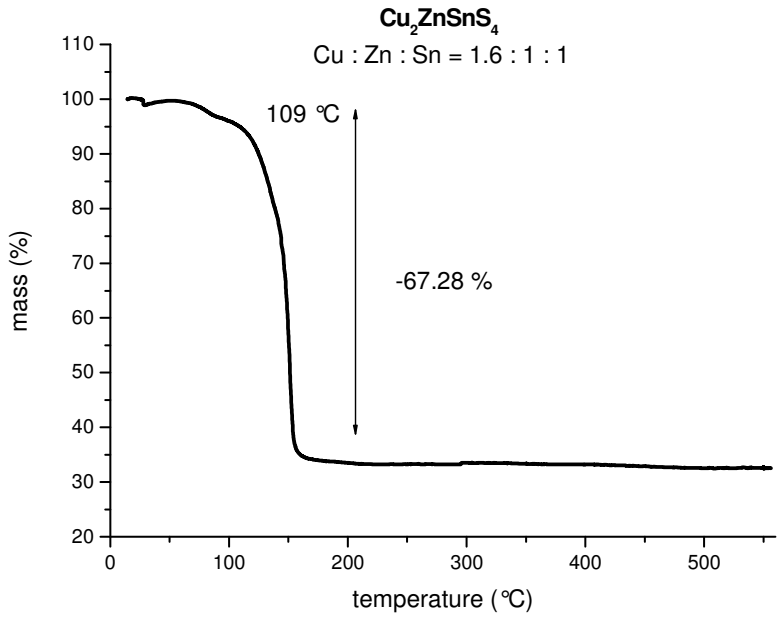

FIGURE 34: THERMAL GRAVIMETRIC CURVE OF COPPER, ZINC AND TIN DITHIOCARBONATE MIXTURE WITH STOICHIOMETRIC RATIOS OF CU : ZN : SN = 1.6 : 1 : 1

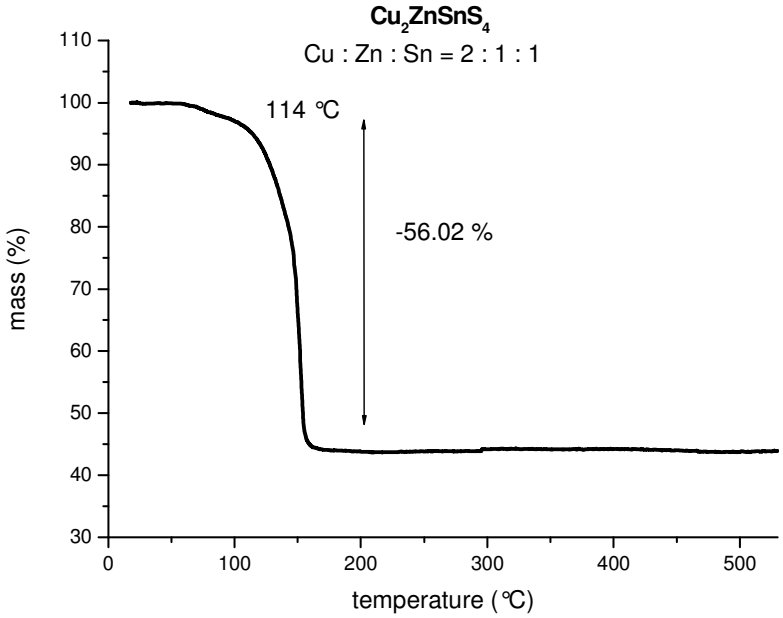

FIGURE 35: THERMAL GRAVIMETRIC CURVE OF COPPER, ZINC AND TIN DITHIOCARBONATE MIXTURE WITH STOICHIOMETRIC RATIOS OF CU : ZN : SN = 2 : 1 : 1

Further experiments were arranged to support the conclusion, that copper zinc tin sulphide could be produced by thermal treatment of copper, zinc and tin dithiocarbonate mixtures. Mixtures with the same stoichiometric ratios of the dithiocarbonates as described above were dissolved in chloroform and drop coated on glass substrates. The precursor containing substrates were baked at different temperatures (see Table 33) with a heating rate of about 7 °C*min^{-1}. The obtained Cu_2ZnSnS_4 was scratched off the glass substrates and characterised with X-ray powder diffraction and energy dispersive X-ray transmission electron microscopy.

Powder diffraction profiles (Figure 36 - Figure 39) exhibit that all deposited films show the typical kesterite crystalline structure with preferred (112) orientation. [14], [63] For all samples the major characteristic diffraction X-ray reflexes (112), (220) and (312) for the kesterite type structure were observed. With increasing annealing temperature more characteristic peaks, which match with the reference, appeared in the diffraction profiles. The Cu_2ZnSnS_4 sample with a copper to zinc to tin ratio of 1.2 : 1 : 1 treated at 450 °C matches perfectly with the Powder Diffraction File PDF26-0575 of the International Centre for Diffraction Data (see Figure 40). However, due to the fact that Cu and Zn have similar scattering factors, it is not possible to exclude the presence of stannite as possible modification, since it has a similar structure to that of kesterite. [51], [64], [65] As zinc sulphide and copper tin sulphide (Cu_2SnS_3) have a very similar crystal structure to copper zinc tin sulphide, it is not possible to exclude their presence in the synthesised phases. [51]

In several powder diffraction profiles of the Cu_2ZnSnS_4 samples an unknown peak occurs at 2θ = 46.36 ° and is marked with an asterisk.

Scherrer's equation was used to estimate the crystallite grain size and its results are summarised in Table 14. According to the analysis, smaller full-width at half maximum (FWHM) of the peaks indicates larger crystallite grain size. [41] For Scherrer's analysis the grain sizes of the (112), (220) and (312) reflexes were calculated and averaged. Increasing annealing temperatures lead to larger crystallite grain sizes.

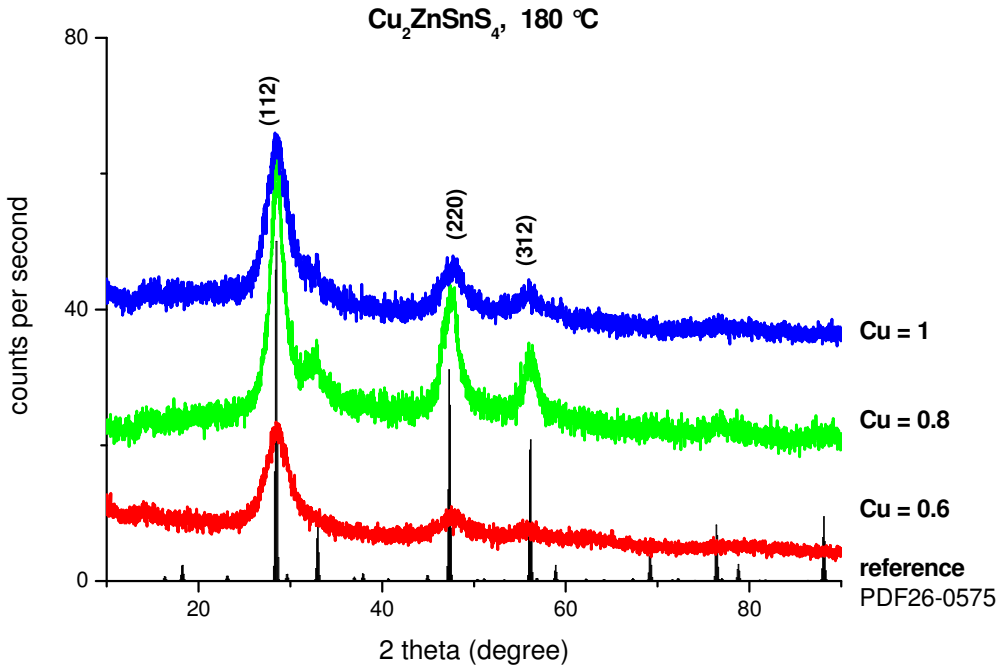

FIGURE 36: XRD-PROFILES OF Cu_2ZnSnS_4 SAMPLES TREATED AT 180 °C

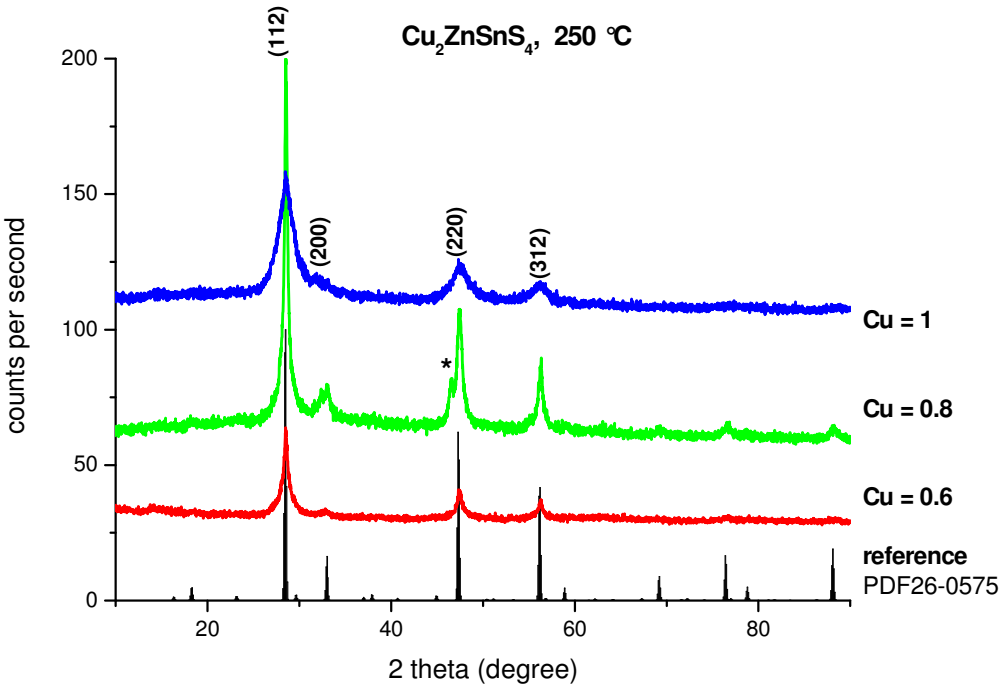

FIGURE 37: XRD-PROFILES OF Cu_2ZnSnS_4 SAMPLES TREATED AT 250 °C

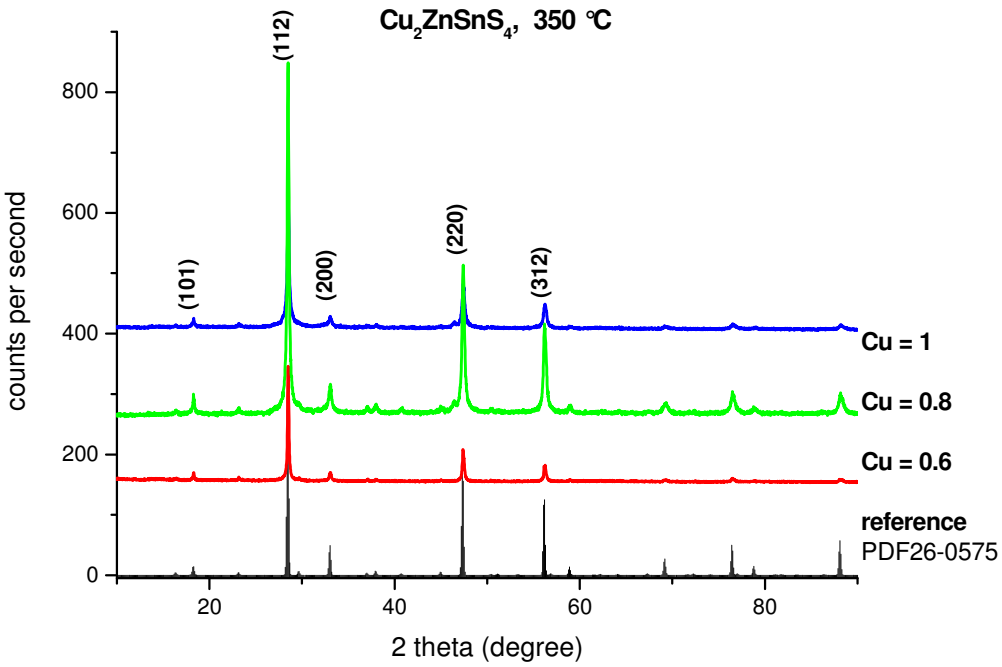

FIGURE 38: XRD-PROFILES OF Cu_2ZnSnS_4 SAMPLES TREATED AT 350 °C

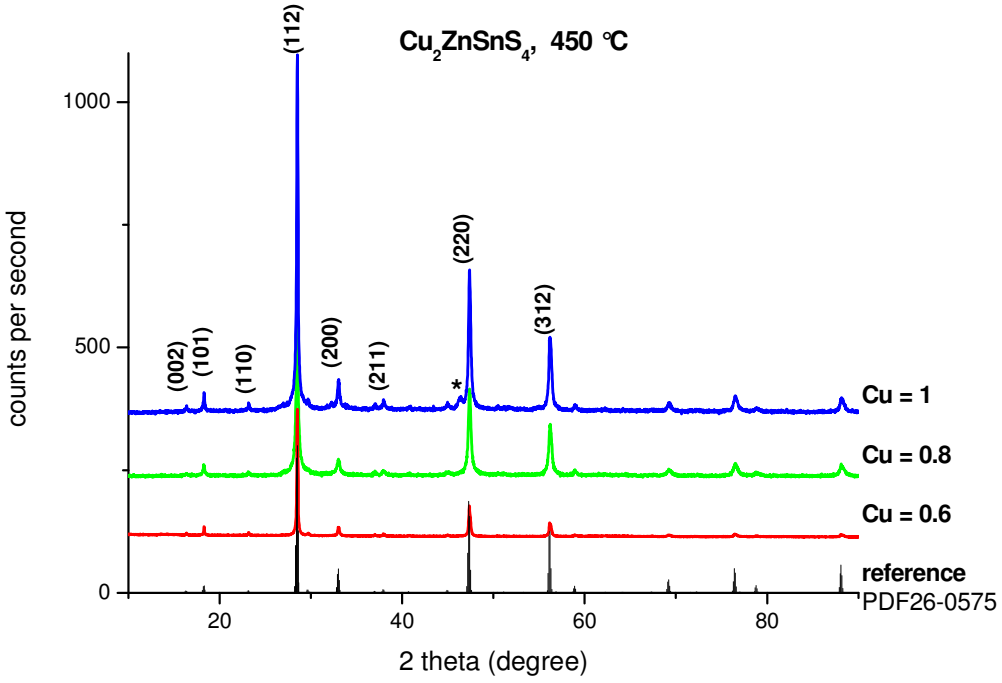

FIGURE 39: XRD-PROFILES OF Cu_2ZnSnS_4 SAMPLES TREATED AT 450 °C

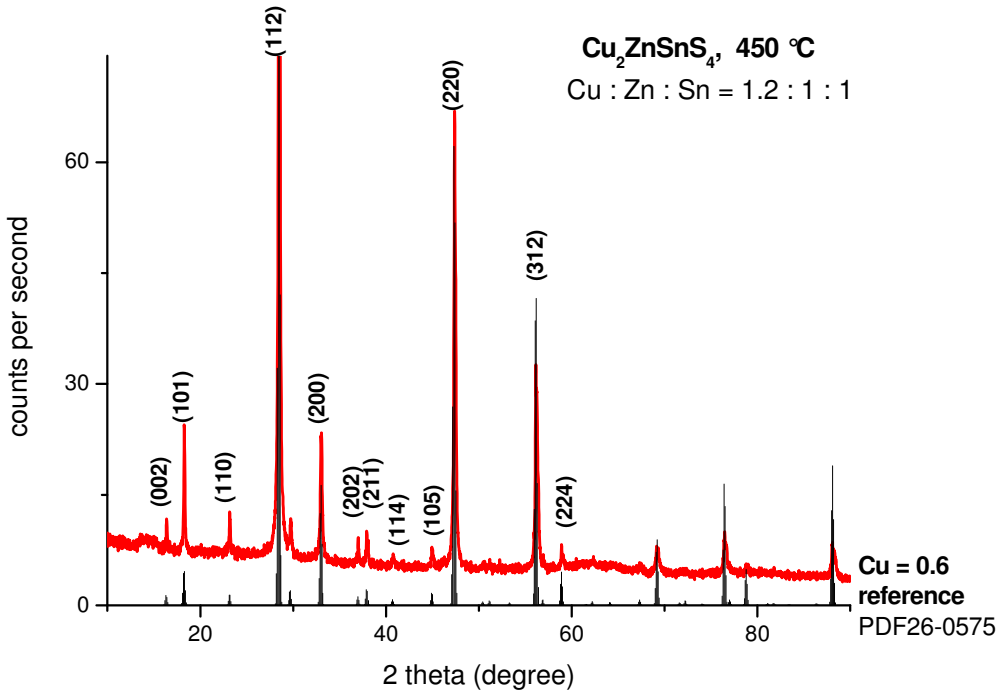

FIGURE 40: XRD-PROFILE OF A Cu_2ZnSnS_4 SAMPLE WITH A STOICHIOMETRIC RATIO OF CU : ZN : SN = 1.2 : 1 : 1 TREATED AT 450 °C

TABLE 14: CRYSTALLITE GRAIN SIZES FOR Cu_2ZnSnS_4 SAMPLES TREATED AT DIFFERENT TEMPERATURES, ACCORDING TO SCHERRER'S ANALYSIS

	$d_{180°C}$ (nm)	$d_{250°C}$ (nm)	$d_{350°C}$ (nm)	$d_{450°C}$ (nm)
CZTS (1.2:1:1)	3.38	15.22	43.03	45.76
CZTS (1.6:1:1)	6.06	18.88	32.78	31.99
CZTS (2:1:1)	4.94	7.28	33.39	37.40

Scanning transmission electron microscopy with an energy dispersive X-ray detector was used to determine the chemical composition of the Cu_2ZnSnS_4 samples. At least 8 points were investigated of each sample. The atom percentages were calculated using the copper Kα, zinc Kα, tin Lα and sulphur Kα peaks using the Cliff - Lorimer approximation. [49] The obtained atom percentages were used to determine the sample composition referring to the calculated copper amount. The averaged atom percentages of the measured points for each sample are listed in Table 15.

TEM-EDX analyses showed that with increasing temperature, the samples developed stoichiometries closer to the theoretical of Cu_2ZnSnS_4. The samples prepared at lower temperatures additionally contained CuS and Cu_2ZnS_2. Best results were obtained with a stoichiometric ratio of copper to zinc to tin of 1.2 : 1 : 1. All samples possessing this stoichiometry did not contain any other phases than Cu_2ZnSnS_4.

Representative for all particles, which have been analysed, the scanning transmission electron microscopic picture of one investigated particle is given in Figure 41. The points of measurement for energy dispersive X-ray analyses are tagged with a white "X". An EDX spectrum of one of these points is also depicted in Figure 42 to give an example for all analyses of the Cu_2ZnSnS_4 particles.

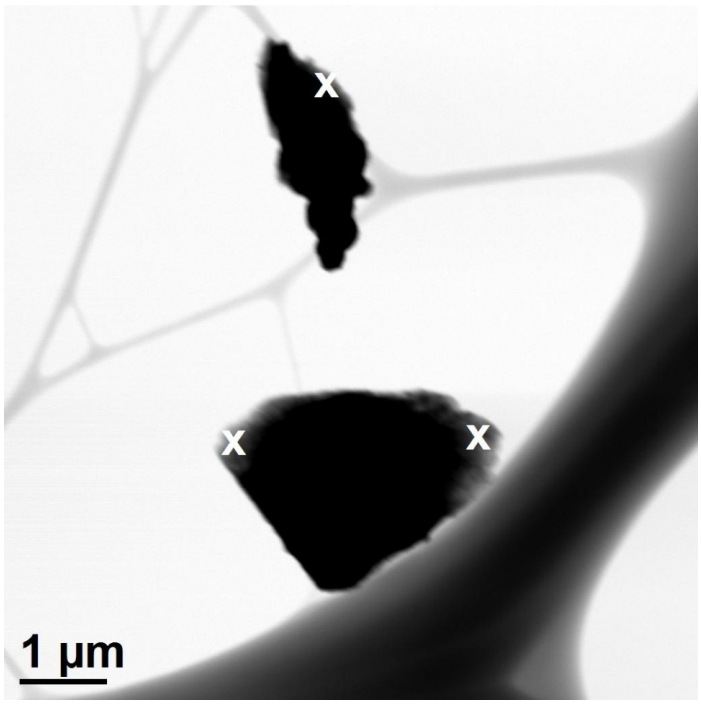

FIGURE 41: SCANNING TRANSMISSION ELECTRON MICROSCOPIC PICTURE OF A COPPER ZINC TIN SULPHIDE PARTICLE

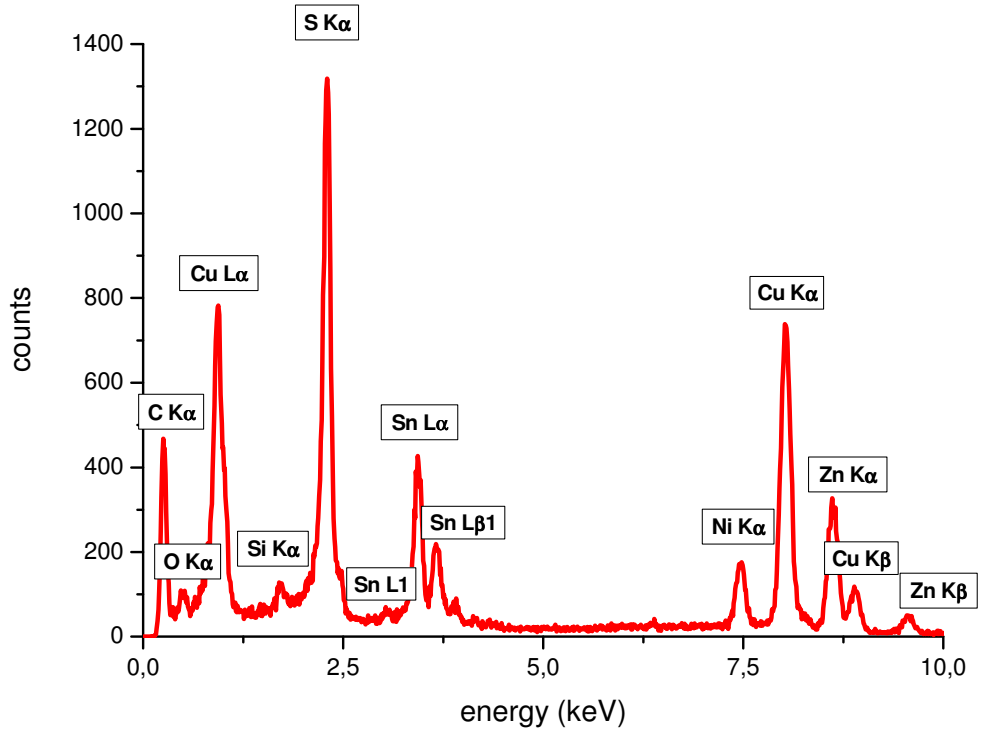

FIGURE 42: ENERGY DISPERSIVE X-RAY SPECTRUM OF A COPPER ZINC TIN SULPHIDE PARTICLE

Due to the used nickel grids for sample preparation, the Cu Lα peak could not be employed for the atom percentage calculation, because of the overlapping with the Ni Lα peak. The appearance of silicon in the EDX spectrum could be due to some residues of silicon grease within the samples.

TABLE 15: AVERAGED ATOM PERCENTAGES OF THE COPPER ZINC TIN SULPHIDE SAMPLES

	% sulphur (theoretical)	% copper (theoretical)	% zinc (theoretical)	% tin (theoretical)
CZTS (1.2 : 1 : 1) 180°C	45.59 (50.00)	30.20 (25.00)	13.08 (12.50)	11.13 (12.50)
CZTS (1.2 : 1 : 1) 250 °C	46.75 (50.00)	29.80 (25.00)	11.94 (12.50)	11.51 (12.50)
CZTS (1.2 : 1 : 1) 350°C	50.38 (50.00)	26.63 (25.00)	11.41 (12.50)	11.58 (12.50)
CZTS (1.2 : 1 : 1) 450°C	49.28 (50.00)	27.54 (25.00)	11.65 (12.50)	11.53 (12.50)

CZTS (1.6 : 1 : 1) 180°C	47.83 (50.00)	38.97 (25.00)	8.63 (12.50)	4.57 (12.50)
CZTS (1.6 : 1 : 1) 250 °C	47.33 (50.00)	35.38 (25.00)	11.54 (12.50)	5.75 (12.50)
CZTS (1.6 : 1 : 1) 350°C	48.74 (50.00)	30.19 (25.00)	10.57 (12.50)	10.49 (12.50)
CZTS (1.6 : 1 : 1) 450°C	49.07 (50.00)	25.20 (25.00)	12.00 (12.50)	13.73 (12.50)
CZTS (2 : 1 : 1) 180°C	48.68 (50.00)	35.74 (25.00)	10.37 (12.50)	5.96 (12.50)
CZTS (2 : 1 : 1) 250°C	50.83 (50.00)	37.11 (25.00)	7.79 (12.50)	6.69 (12.50)
CZTS (2 : 1 : 1) 350°C	47.97 (50.00)	34.73 (25.00)	8.66 (12.50)	11.12 (12.50)
CZTS (2 : 1 : 1) 450°C	44.52 (50.00)	32.34 (25.00)	13.91 (12.50)	8.78 (12.50)

The optical properties of the synthesised Cu_2ZnSnS_4 films were analysed by transmittance and reflectance measurements. The obtained absorption spectra are presented in Figure 43 - Figure 45. The absorption coefficient α was calculated on the basis of following equation.

$$\alpha = \frac{1}{d}\ln\left(\frac{1-r}{t}\right)$$

d is the thickness of the film, r the reflectance and t the transmittance of the film. The thicknesses of samples were obtained by surface profiling measurements (see Table 16).

TABLE 16: FILM THICKNESSES OF THE CU_2ZNSNS_4 SAMPLES TREATED AT DIFFERENT TEMPERATURES

	$d_{180°C}$ (nm)	$d_{250°C}$ (nm)	$d_{350°C}$ (nm)	$d_{450°C}$ (nm)
CZTS (1.2:1:1)	35	35	35	35
CZTS (1.6:1:1)	35	35	35	35
CZTS (2:1:1)	35	55	55	30

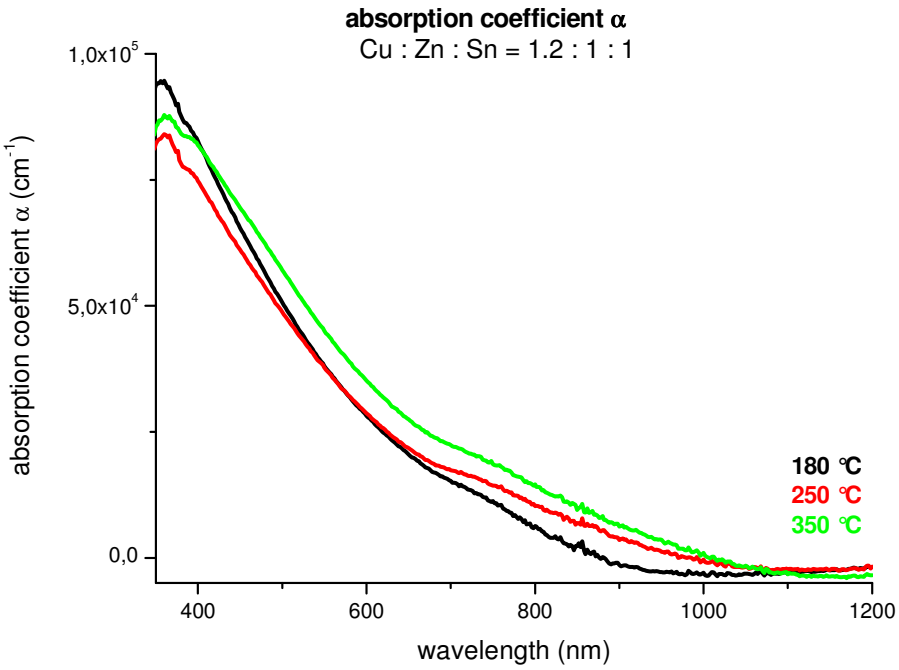

FIGURE 43: OPTICAL ABSORPTION COEFFICIENT OF Cu_2ZnSnS_4 WITH A COPPER TO ZINC TO TIN RATIO OF 1.2 : 1 : 1

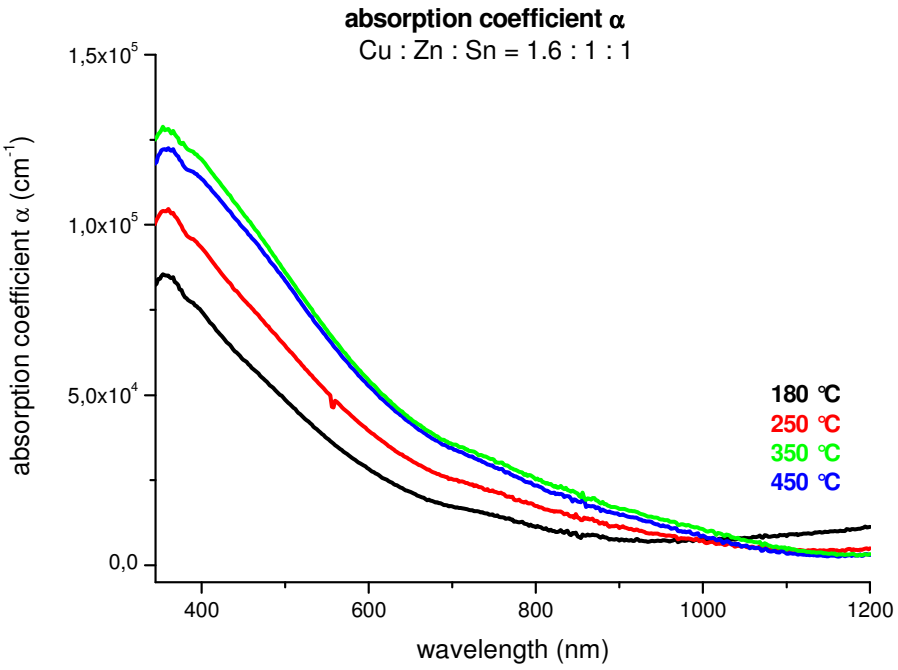

FIGURE 44: OPTICAL ABSORPTION COEFFICIENT OF Cu_2ZnSnS_4 WITH A COPPER TO ZINC TO TIN RATIO OF 1.6 : 1 : 1

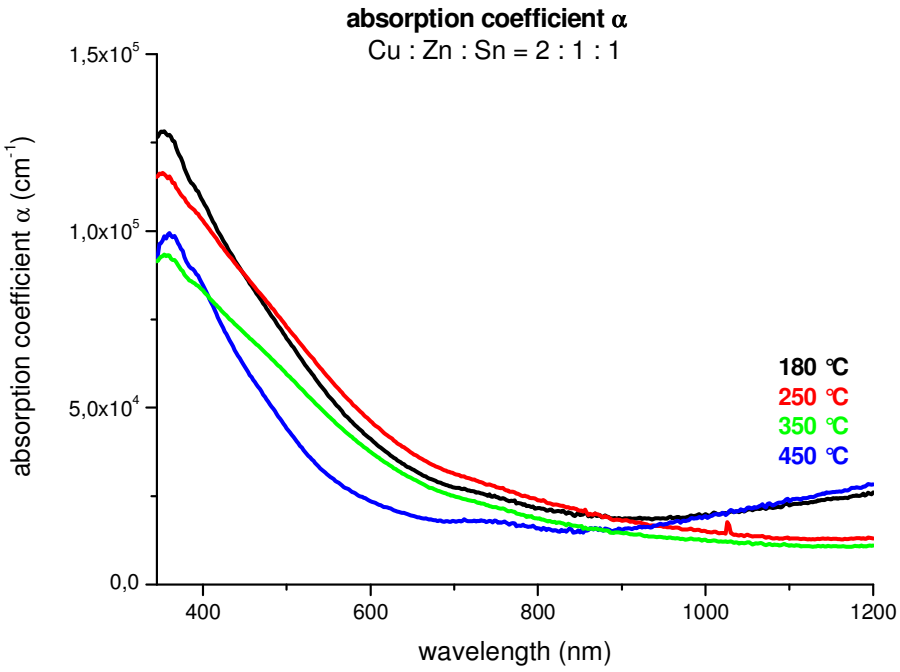

FIGURE 45: OPTICAL ABSORPTION COEFFICIENT OF Cu_2ZnSnS_4 WITH A COPPER TO ZINC TO TIN RATIO OF 2 : 1 : 1

The optical band gap E_g can be obtained by following equation. A is constant, $h\nu$ the photon energy, and n an exponent, which indicates a direct band gap, because it was found to be 1/2. [51], [54]

$$\alpha = \frac{A(h\nu - E_g)^n}{h\nu}$$

Therefore the band gap values were determined from $(\alpha h\nu)^2$ versus $h\nu$ plots by linear extrapolation of the functions as shown in the figures Figure 46 - Figure 48. [51]

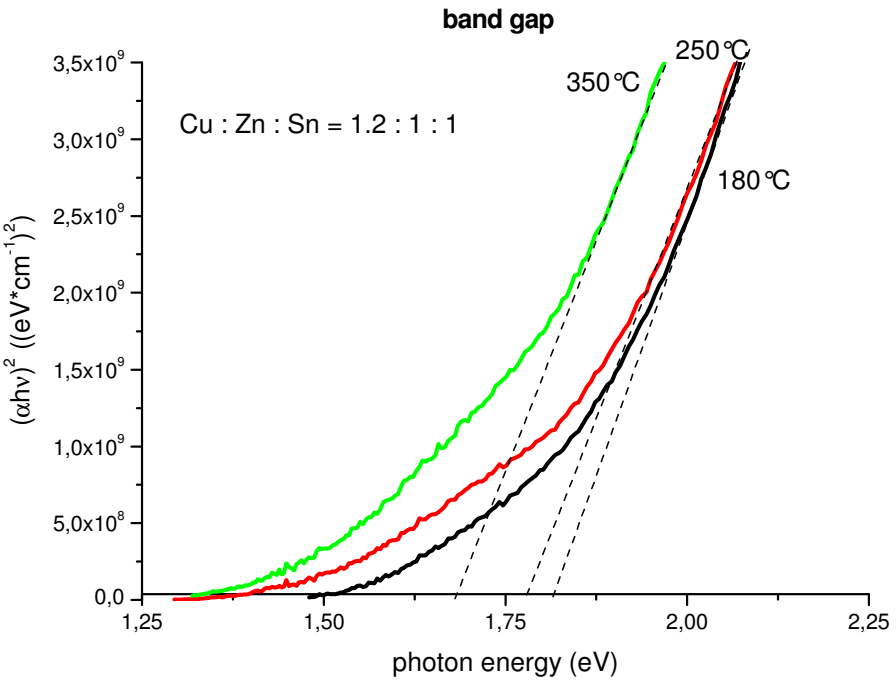

FIGURE 46: OPTICAL BAND GAPS OF Cu_2ZnSnS_4 WITH A COPPER TO ZINC TO TIN RATIO OF 1.2 : 1 : 1 TREATED AT DIFFERENT TEMPERATURES

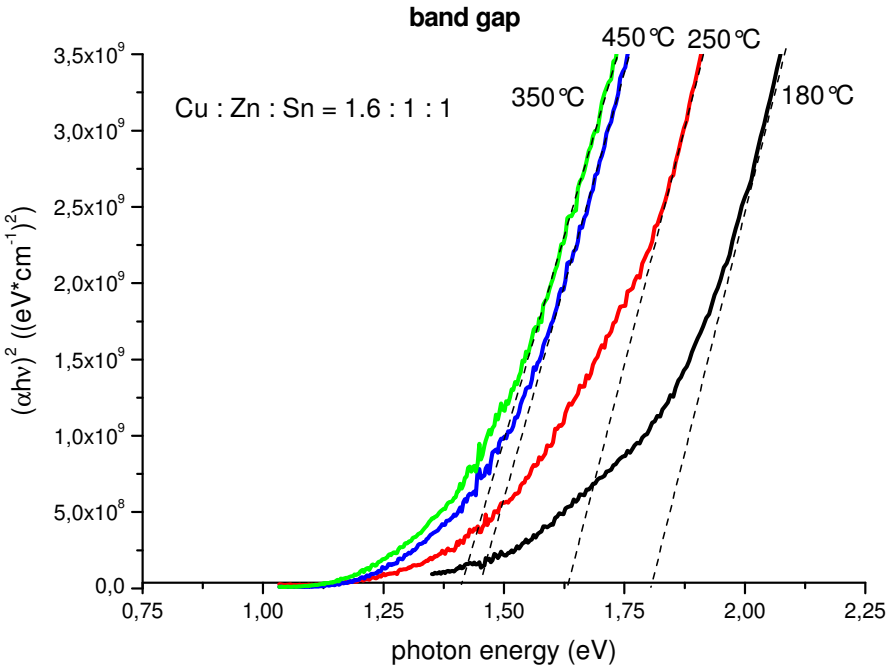

FIGURE 47: OPTICAL BAND GAPS OF Cu_2ZnSnS_4 WITH A COPPER TO ZINC TO TIN RATIO OF 1.6 : 1 : 1 TREATED AT DIFFERENT TEMPERATURES

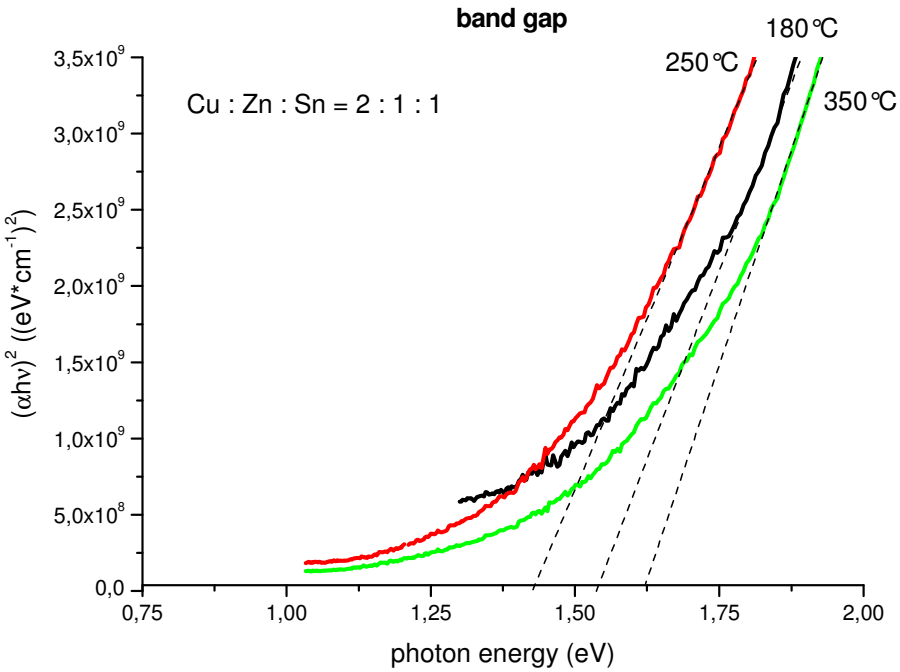

FIGURE 48: OPTICAL BAND GAPS OF Cu_2ZnSnS_4 WITH A COPPER TO ZINC TO TIN RATIO OF 2 : 1 : 1 TREATED AT DIFFERENT TEMPERATURES

The obtained band gap values for the synthesised Cu_2ZnSnS_4 samples vary in a range from 1.43 – 1.8 eV, which is in agreement with reports in the literature. [10], [11], [51], [54], [55] Optical band gaps of Cu_2ZnSnS_4 films synthesised with different stoichiometric ratios exhibit significant discrepancies.

On the one hand this could be due to high roughness inhomogeneities of the synthesised films, which have been observed by surface profiling measurements. On the other hand these differences could be caused by impurities and discrepancies in the compositional order of the samples and the inaccuracy of the measurement set up.

Due to the results of the reflectance and transmittance measurements, the synthesised copper, zinc, tin and cadmium *O*-3,2-dimethylbutan-2-yl dithiocarbonates were retained to produce inorganic solar cells. First attempts were arranged in a basic bilayer assembly on indium tin oxide as transparent conductive electrode. The first layer was the copper zinc tin sulphide as p-semiconductor and the second was cadmium sulphide as n-semiconductor to gain the p-n heterojunction. Aluminium was deposited by an evaporation process and was used as back contact.

Dithiocarbonate mixtures with a stoichiometric ratio of the copper to zinc to tin of 1.2 : 1 : 1 were dissolved in chloroform and doctor bladed on ITO substrates. The precursor containing substrates were baked for 15 minutes at 350 °C in vacuum with a heating rate of about 25 °C*min^{-1}. Then a solution of cadmium dithiocarbonate was doctor bladed on the synthesised Cu_2ZnSnS_4 film and annealed at 200 °C for 15 minutes in vacuum.

The current density – voltage curve is presented below in Figure 49. Due to the previously described fact of high inhomogeneities in the film roughness of the synthesised copper zinc tin sulphide, the gained results of solar cell fabrication are rather dissatisfying. Further improvements should be obtained by optimisation of all parameters of the solar cell set up.

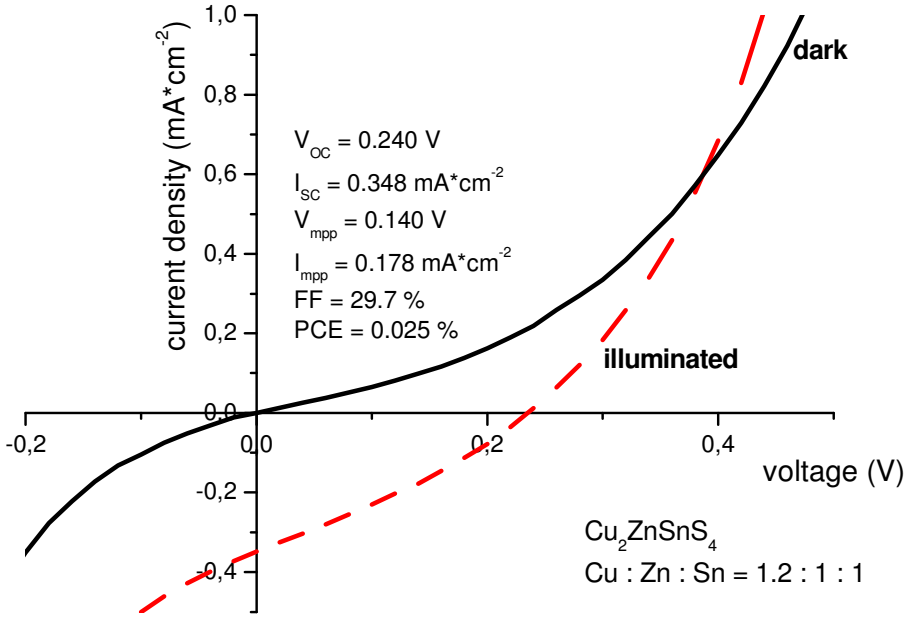

FIGURE 49: CURRENT DENSITY – VOLTAGE CHARACTERISTICS OF A FABRICATED CDS/Cu_2ZnSnS_4 SOLAR CELL

EXPERIMENTAL WORK

MATERIALS AND METHODS

All chemicals, solvents and materials were used as purchased and are summarised in Table 17.

TABLE 17: USED CHEMICALS AND MATERIALS AND THEIR SOURCE OF SUPPLY

chemicals / materials	purity / properties	source of supply
acetone	puriss.	Sigma-Aldrich
2-propanol	puriss.	Sigma-Aldrich
tetrahydrofuran	anhydrous, ≥ 99.9 %	Sigma-Aldrich
methanol	puriss.	Sigma-Aldrich
chlorofrom	puriss. p.a.	Sigma-Aldrich
carbon disulphide	≥ 99.9 %	Sigma-Aldrich
hydrochloric acid	min. 37 %, puriss. p.a.	Sigma-Aldrich
copper(II) chloride	99.99+ % metal basis	Sigma-Aldrich
indium (III) chloride	98 %	Sigma-Aldrich
zinc (II) chloride	puriss. p.a.	Sigma-Aldrich
tin (IV) chloride pentahydrate	lumps, 98 %	Sigma-Aldrich
potassium *tert*-butoxide	purum, ≥ 97 %	Sigma-Aldrich
cadmium chloride	≥ 99.99 %	Sigma-Aldrich
gallium chloride	anhydrous, ≥ 99.99 %	Sigma-Aldrich
3,3-dimethyl-2-butanol	98 %	Sigma-Aldrich
2,2-dimethyl-3-pentanol	97 %	Sigma-Aldrich
zinc	dust <10 µm	Sigma-Aldrich
ITO covered glass substrates	24 x 75 x 1.1 mm, R_S = 15-25 Ω	Delta Technologies
aluminum	wire, 1.0 mm diam., 99.99 %	Sigma-Aldrich
diethyl ether	puriss., stabilised	Sigma-Aldrich
microscope slides	26 x 75 x 1.1 mm	VWR

NUCLEAR MAGNETIC RESONANCE SPECTROSCOPY

NMR spectra were recorded on a Bruker Ultrashield 300. ^{1}H- and ^{13}C-NMR spectra were obtained in $(CD_3)_2CO$ and $CDCl_3$ solutions at 300 MHz for ^{1}H and 75 MHz for ^{13}C. Chemical shifts are reported in δ units, parts per million (ppm) relative to the multiplet of $(CD_3)_2CO$ at 2.050 ppm and relative to the singlet of $CDCl_3$ at 7.240 ppm for ^{1}H-NMR spectra. For ^{13}C-NMR spectra the chemical shifts are referenced relative to the multiplet of $(CD_3)_2CO$ at 29.920 ppm and relative to the triplet of $CDCl_3$ at 77.230 ppm.

FOURIER TRANSFORM INFRARED SPECTROSCOPY

FTIR-spectra were measured on a Perkin Elmar Spectrum One, and all spectra were collected in transmission mode and are reported in cm^{-1}. All measurements were performed on silicon wafer substrates.

ELEMENTAL ANALYSIS

Elemental analyses were carried out on a Universal CHNS Elemental Analyzer Vario El III.

THERMAL GRAVIMETRIC ANALYSIS

Thermal gravimetric measurements were performed on a Netzsch Jupiter STA 449C with a Netzsch Aëolos QMS 403C quadrupole mass spectrometer for gas analysis. All measurements were carried out in helium atmosphere and a heating rate of 10 °C*min^{-1}. The decomposition temperature T_d was determined at a mass loss of 5 %.

MASS SPECTROMETRY

Mass spectra were recorded on a Waters GCT Premier with an orthogonal acceleration time-of-flight mass analyser. Samples were analysed by direct insertion with electron impact ionisation (70eV) by applying a heating ramp.

X-RAY DIFFRACTION MEASUREMENTS

X-ray diffraction profiles of the Cu_2ZnSnS_4 samples were measured with a Siemens D-5005 powder diffractometer with θ,θ geometry, Cu Kα radiation, graphite monochromator and a scintillation counter. Step width was set to 0.02 °, counting times were set to 20 seconds per step and the measured range was 20 - 90 ° in 2θ.

X-ray diffraction profiles of the $CuInS_2$ samples were measured with a Philips Expert Panalytical-diffractometer with θ,2θ geometry, Cu Kα radiation, graphite monochromator and a scintillation counter. Step width was set to 0.02 °, counting times were set to 20 seconds per step and the measured range was 20 - 90 ° in 2θ.

For XRD analysis, Cu_2ZnSnS_4 and $CuInS_2$ precursor solutions were drop coated onto glass substrates at ambient conditions, followed by different heat treatment. Finally, the Cu_2ZnSnS_4 and $CuInS_2$ layers were scraped off the glass substrate to obtain their powders.

ENERGY DISPERSIVE X-RAY ANALYSIS

EDX spectra were recorded in scanning transmission electron microscopy (STEM) mode using a Philips CM20/STEM operated at 200 kV with a LaB_6 cathode equipped with a Noran HPGe-detector.

Cu_2ZnSnS_4 and $CuInS_2$ precursor solutions were drop coated onto glass substrates at ambient conditions, followed by different heat treatment. Finally, the Cu_2ZnSnS_4 and $CuInS_2$ layers were scratched off the glass substrate to obtain their powders. The resulting particles were suspended in ethanol and a drop of the suspension was placed on a nickel grid supported holey carbon film and the solvent was evaporated.

TRANSMITTANCE AND REFLECTANCE MEASUREMENTS

Transmittance and reflectance spectra were measured with a Perkin Elmer Lambda 900 spectrometer including a PELA 1000 external integrating sphere diffuse reflectance accessory.

Cu_2ZnSnS_4 and $CuInS_2$ precursor solutions were doctor bladed on glass substrates and baked at different temperatures. The surface morphology was studied with a Veeco Dektak 150 surface profiler.

POTASSIUM *O*-3,3-DIMETHYLBUTAN-2-YL DITHIOCARBONATE (1) [32]

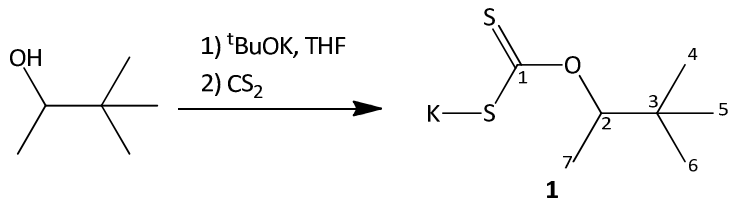

1

TABLE 18: CHEMICALS AND MASSES FOR THE REACTION

	3,3-dimethyl-2-butanol	^{t}BuOK	CS_2	THF
MW (g*mol^{-1})	116.22	112.22	76.14	74.12
mass (g)	15.00	14.98	11.28	
density (g*ml^{-1})	0.82		1.27	0.71
volume (ml)	18.30		8.9	253.50
molar amount (mmol)	146.80	133.45	148.13	
equivalents	1.10	1.00	1.11	

The reaction was performed under argon atmosphere and all used chemicals are listed in Table 18. Potassium *tert*-butoxide was dissolved in THF. The solution was cooled down to 0 °C, than 3,3-dimethyl-2-butanol was added slowly. After stirring for several minutes, carbon disulphide was added dropwise, and the solution was stirred for about 5 hours. The reaction mixture was diluted with diethyl ether to give the crude product. The obtained solid was dried in vacuum and dissolved in acetone to separate the insoluble side products. The acetone solution was concentrated and diluted with diethyl ether to give the white-yellowish product. The xanthate was dried in vacuum. (76.2 % yield)

^{1}H-NMR (300 MHz, $(CD_3)_2CO$, in ppm): 5.43 - 5.36 (dd, 1H at C_2), 1.11 – 1.09 (d, 3H at C_7), 0.91 (s, 9H at C_4, C_5, C_6)

^{13}C-NMR (75 MHz, $(CD_3)_2CO$, in ppm): 14.77 (C_5), 26.46 (C_4, C_6), 35.32 (C_7), 84.36 (C_2), 233.65 (C_1)

IR (on Si, in cm^{-1}): 2963, 2870, 1474, 1456, 1393, 1377, 1363, 1223, 1208, 1133, 1101, 1085, 1066, 1030, 985

Elemental analysis: calculated: %C = 38.85, %S = 29.63, %H = 6.05

found: %C = 38.75, %S = 29.74, %H = 6.10

Thermal gravimetric analysis: T_d = 230 °C, mass loss = 62.57 % (calc. 74.52 %)

POTASSIUM *O*-2,2-DIMETHYLPENTAN-3-YL DITHIOCARBONATE (2) [32]

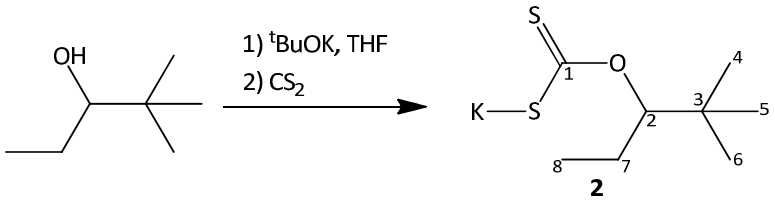

2

TABLE 19: CHEMICALS AND MASSES FOR THE REACTION

	2,2-dimethyl- 3-pentanol	^{t}BuOK	CS_2	THF
MW (g*mol^{-1})	116.22	112.22	76.14	74.12
mass (g)	15.00	13.17	9.92	
density (g*ml^{-1})	0.82		1.27	0.71
volume (ml)	18.29		7.81	222.93
molar amount (mmol)	129.07	117.33	130.24	
equivalents	1.10	1.00	1.11	

The reaction was performed under argon atmosphere and all used chemicals are listed in Table 19. Potassium *tert*-butoxide was dissolved in THF. The solution was cooled down to 0 °C, than 2,2-dimethyl- 3-pentanol was added slowly. After stirring for several minutes, carbon disulphide was added dropwise, and the solution was stirred for about 5 hours. The reaction mixture was diluted with diethyl ether to give the crude product. The obtained solid was dried in vacuum and dissolved in acetone to separate the insoluble side products. The acetone solution was concentrated and diluted with diethyl ether to give the white-yellowish product. The xanthate was dried in vacuum. (68.3 % yield)

^{1}H-NMR (300 MHz, $(CD_3)_2CO$, in ppm): 5.64 - 5.59 (dd, 1H at C_2), 1.68 – 1.46 (m, 2H at C_7), 0.93 – 0.89 (t, 12H at C_4, C_5, C_6, C_8)

^{13}C-NMR (75 MHz, $(CD_3)_2CO$, in ppm): 11.63 (C_5), 24.11 (C_4, C_6), 26.77 (C_7), 36.19 (C_8), 88.68 (C_2), 235.40 (C_1)

IR (on Si, in cm^{-1}): 2964, 2872, 1479, 1457, 1393, 1382, 1365, 1231, 1205, 1140, 1109, 1070, 1042, 1021, 951

Elemental analysis: calculated: %C = 41.70, %S = 27.83, %H = 6.56
found: %C = 41.70, %S = 26.38, %H = 6.59

Thermal gravimetric analysis: T_d = 206 °C, mass loss = 62.19 % (calc. 76.07 %)

COPPER (I) *O*-3,3-DIMETHYLBUTAN-2-YL DITHIOCARBONATE (3)

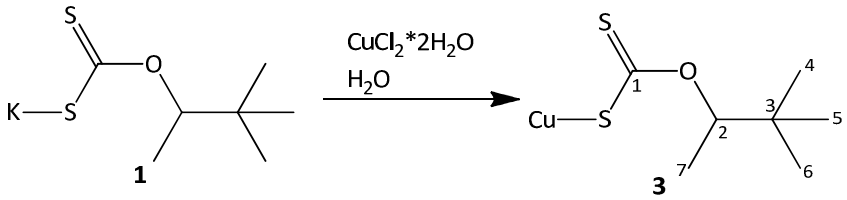

TABLE 20: CHEMICALS AND MASSES FOR THE REACTION

	$CuCl_2*H_2O$	potassium xanthate	H_2O
MW (g*mol^{-1})	170.48	216.41	18.02
mass (g)	4.30	12.00	221.80
molar amount (mmol)	25.20	55.45	
equivalents	1.00	2.20	

The used chemicals are listed in Table 20. Copper (II) chloride dihydrate was dissolved in about 50 ml deionised water. **1** was dissolved in the remaining amount of deionised water. The potassium xanthate solution was added dropwise to the copper dichloride solution under vigorous stirring. A sticky brown residue appeared immediately. The reaction was allowed to stir for about 5 hours, then the water was decanted and the residue was dried in vacuum. The residue was dissolved in chloroform and added to methanol to obtain a yellow powder, which was dried under vacuum.

Afterwards this powder was dispersed in n-pentane, stirred for an hour, filtered and dried in vacuum to obtain the corresponding pure yellow copper xanthate. (65.9 % yield)

^{1}H-NMR (300 MHz, $CDCl_3$, in ppm): 5.16 - 5.09 (q, 1H at C_2), 1.29 – 1.27 (d, 3H at C_7), 0.95 (s, 9H at C_4, C_5, C_6)

^{13}C-NMR (75 MHz, $CDCl_3$, in ppm): 14.16 (C_5), 25.89 (C_4, C_6), 35.42 (C_7), 93.66 (C_2), 228.70 (C_1)

IR (on Si, in cm^{-1}): 2964, 2872, 1479, 1398, 1378, 1366, 1338, 1236, 1212, 1113, 1075, 1049, 1018

Elemental analysis: calculated: %C = 34.91, %S = 26.43, %H = 5.44
found: %C = 34.31, %S = 27.09, %H = 5.37

Thermal gravimetric analysis: T_d = 186 °C, mass loss = 67.41 % (calc. 62.49 %)

COPPER (I) *O*-2,2-DIMETHYLPENTAN-3-YL DITHIOCARBONATE (4)

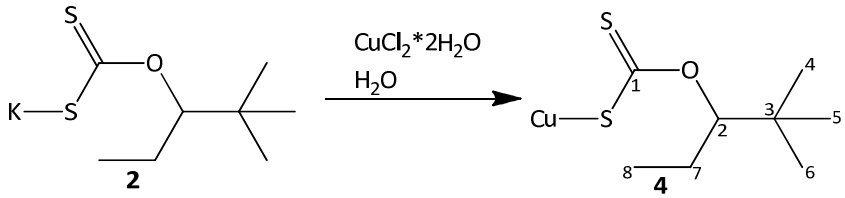

TABLE 21: CHEMICALS AND MASSES FOR THE REACTION

	$CuCl_2*H_2O$	potassium xanthate	H_2O
MW ($g*mol^{-1}$)	170.48	230.44	18.02
mass (g)	4.04	12.00	210.00
molar amount (mmol)	23.67	52.07	
equivalents	1.00	2.20	

The used chemicals are listed in Table 21. Copper (II) chloride dihydrate was dissolved in about 50 ml deionised water. **2** was dissolved in the remaining amount of deionised water. The potassium xanthate solution was added dropwise to the copper dichloride solution under vigorous stirring. A sticky brown residue appeared immediately. The reaction was allowed to stir for about 5 hours, then the water was decanted and the residue was dried in vacuum. The residue was dissolved in

chloroform and added to methanol to obtain a yellow powder, which was dried under vacuum. Afterwards this powder was dispersed in n-pentane, stirred for an hour, filtered and dried in vacuum to obtain the corresponding pure yellow copper xanthate. (87.8 % yield)

^{1}H-NMR (300 MHz, $CDCl_3$, in ppm): 5.27 - 5.17 (m, 1H at C_2), 1.75 – 1.66 (m, 2H at C_7), 0.94 – 0.89 (m, 12H at C_4, C_5, C_6, C_8)

^{13}C-NMR (75 MHz, $CDCl_3$, in ppm): 11.27 (C_5), 23.51 (C_4, C_6), 26.21 (C_8), 36.23 (C_7), 98.93 (C_2), 230.37 (C_1)

IR (on Si, in cm^{-1}): 2969, 2875, 1478, 1463, 1397, 1367, 1340, 1233, 1211, 1127, 1081, 1051, 1023, 950

Elemental analysis: calculated: %C = 37.70, %S = 25.15, %H = 5.93
found: %C = 37.71, %S = 25.62, %H = 5.89

Thermal gravimetric analysis: T_d = 175 °C, mass loss = 70.20 % (calc. 64.44 %)

INDIUM (III) *O*-3,3-DIMETHYLBUTAN-2-YL DITHIOCARBONATE (5)

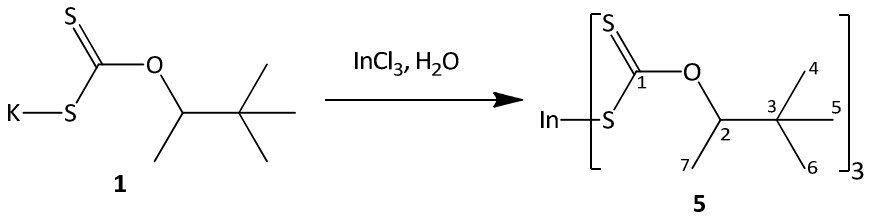

1 **5**

TABLE 22: CHEMICALS AND MASSES FOR THE REACTION

	$InCl_3$	potassium xanthate	H_2O
MW (g*mol^{-1})	221.18	216.41	18.02
mass (g)	4.79	15.00	650.00
molar amount (mmol)	21.66	69.31	
equivalents	1.00	3.20	

The used chemicals are listed in Table 22. Indium (III) chloride was dissolved in about 300 ml deionised water. **1** was dissolved in the remaining amount of deionised water. The potassium

xanthate solution was added dropwise to the indium chloride solution under stirring. The reaction was allowed to stir for about 2.5 hours, the white precipitate was filtered off and dried in vacuum. The precipitate was dissolved in chloroform and added to methanol to obtain a white powder, which was dried in vacuum. (81.2 % yield)

^{1}H-NMR (300 MHz, $CDCl_3$, in ppm): 4.76 – 4.70 (q, 1H at C_2), 1.34 – 1.32 (d, 3H at C_7), 0.98 (s, 9H at C_4, C_5, C_6)

^{13}C-NMR (75 MHz, $CDCl_3$, in ppm): 14.44 (C_5), 25.81 (C_4, C_6), 35.50 (C_7), 97.18 (C_2), 229.51 (C_1)

IR (on Si, in cm^{-1}): 2967, 2873, 1478, 1379, 1344, 1249, 1217, 1115, 1075, 1056, 1026

Elemental analysis: calculated: %C = 39.00, %S = 30.25, %H = 6.08
found: %C = 39.87, %S = 29.75, %H = 6.01

Thermal gravimetric analysis: T_d = 162 °C, mass loss = 74.44 % (calc. 49.62 %)

INDIUM (III) *O*-2,2-DIMETHYLPENTAN-3-YL DITHIOCARBONATE (6)

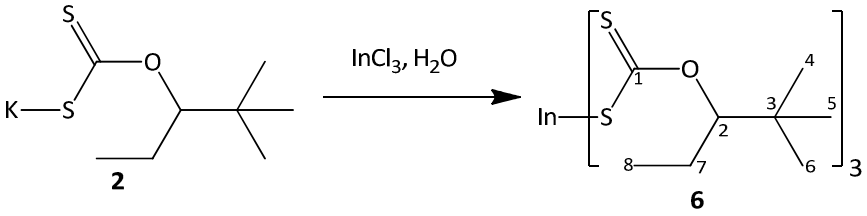

TABLE 23: CHEMICALS AND MASSES FOR THE REACTION

	$InCl_3$	potassium xanthate	H_2O
MW (g*mol^{-1})	221.18	230.44	18.02
mass (g)	4.50	15.00	650.00
molar amount (mmol)	20.34	65.09	
equivalents	1.00	3.20	

The used chemicals are listed in Table 23. Indium (III) chloride was dissolved in about 300 ml deionised water. **2** was dissolved in the remaining amount of deionised water. The potassium xanthate solution was added dropwise to the indium chloride solution under stirring. The reaction

was allowed to stir for about 2.5 hours, the white precipitate was filtered off and dried in vacuum. The precipitate was dissolved in chloroform and added to methanol to obtain a white powder, which was dried in vacuum. (85.2 % yield)

^{1}H-NMR (300 MHz, $CDCl_3$, in ppm): 4.77 – 4.70 (m, 1H at C_2), 1.78 – 1.69 (m, 2H at C_7), 1.02 - 0.97 (m, 12H at C_4, C_5, C_6, C_8)

^{13}C-NMR (75 MHz, $CDCl_3$, in ppm): 11.17 (C_5), 23.54 (C_4, C_6), 26.12 (C_8), 36.23 (C_7), 103.31 (C_2), 231.03 (C_1)

IR (on Si, in cm^{-1}): 2970, 2877, 1479, 1461, 1369, 1346, 1242, 1216, 1131, 1082, 1057, 1038, 1019, 951

Elemental analysis: calculated: %C = 41.85, %S = 27.93, %H = 6.58
found: %C = 41.88, %S = 28.39, %H = 6.60

Thermal gravimetric analysis: T_d = 142 °C, mass loss = 76.78 % (calc. 52.65 %)

CADMIUM (II) *O*-3,3-DIMETHYLBUTAN-2-YL DITHIOCARBONATE (7)

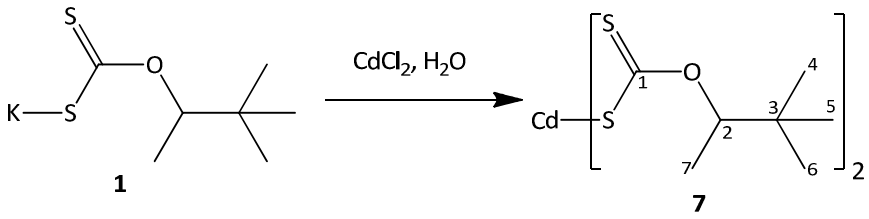

TABLE 24: CHEMICALS AND MASSES FOR THE REACTION

	$CdCl_2$	potassium xanthate	H_2O
MW (g*mol^{-1})	183.32	216.41	18.02
mass (g)	1.93	5.00	160.00
molar amount (mmol)	10.50	23.10	
equivalents	1.00	2.20	

The used chemicals are listed in Table 24. Cadmium (II) chloride was dissolved in about 80 ml deionised water. **1** was dissolved in the remaining amount of deionised water. The potassium

xanthate solution was added dropwise to the cadmium chloride solution under stirring. The reaction was allowed to stir for about 2.5 hours, the white precipitate was filtered off and dried in vacuum. The precipitate was dissolved in chloroform and added to methanol to obtain a white powder, which was dried in vacuum. (76.1 % yield)

^{1}H-NMR (300 MHz, $CDCl_3$, in ppm): 4.98 – 4.92 (q, 1H at C_2), 1.31 – 1.29 (m, 2H at C_7), 0.96 (s, 9H at C_4, C_5, C_6)

^{13}C-NMR (75 MHz, $CDCl_3$, in ppm): 14.53 (C_5), 25.99 (C_4, C_6), 36.35 (C_7), 95.47 (C_2), 229.48 (C_1)

IR (on Si, in cm^{-1}): 2966, 2872, 1478, 1397, 1379, 1367, 1343, 1236, 1212, 1115, 1076, 1057, 1025, 984

Elemental analysis: calculated: %C = 36.00, %S = 27.46, %H = 5.61
found: %C = 34.76, %S = 26.76, %H = 5.28

Thermal gravimetric analysis: T_d = 121 °C, mass loss = 68.32 % (calc. 68.84 %)

CADMIUM (II) *O*-2,2-DIMETHYLPENTAN-3-YL DITHIOCARBONATE (8)

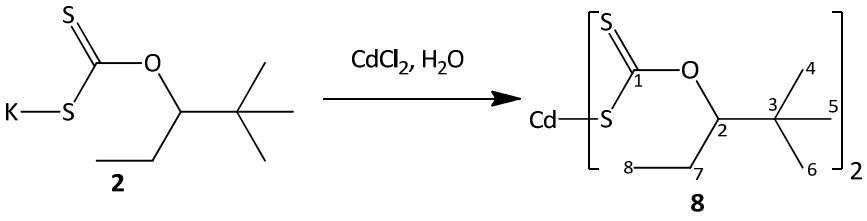

TABLE 25: CHEMICALS AND MASSES FOR THE REACTION

	$CdCl_2$	potassium xanthate	H_2O
MW (g*mol^{-1})	183.32	230.44	18.02
mass (g)	1.81	5.00	150.00
molar amount (mmol)	9.86	21.70	
equivalents	1.00	2.20	

The used chemicals are listed in Table 25. Cadmium (II) chloride was dissolved in about 75 ml deionised water. **2** was dissolved in the remaining amount of deionised water. The potassium

xanthate solution was added dropwise to the cadmium chloride solution under stirring. The reaction was allowed to stir for about 2.5 hours, the white precipitate was filtered off and dried in vacuum. The precipitate was dissolved in chloroform and added to methanol to obtain a white powder, which was dried in vacuum. (77.8 % yield)

^{1}H-NMR (300 MHz, $CDCl_3$, in ppm): 5.00 – 4.95 (m, 1H at C_2), 1.80 – 1.66 (m, 2H at C_7), 0.99 – 0.95 (m, 12H at C_4, C_5, C_6, C_8)

^{13}C-NMR (75 MHz, $CDCl_3$, in ppm): 11.35 (C_5), 23.57 (C_4, C_6), 26.33 (C_8), 36.11 (C_7), 101.21 (C_2), 230.80 (C_1)

IR (on Si, in cm^{-1}): 2968, 2876, 1478, 1398, 1383, 1368, 1344, 1231, 1211, 1130, 1082, 1057, 1034, 951

Elemental analysis: calculated: %C = 38.82, %S = 25.91, %H = 6.11
found: %C = 38.84, %S = 25.91, %H = 6.11

Thermal gravimetric analysis: T_d = 141 °C, mass loss = 69.52 % (calc. 70.61 %)

ZINC (II) *O*-3,3-DIMETHYLBUTAN-2-YL DITHIOCARBONATE (9)

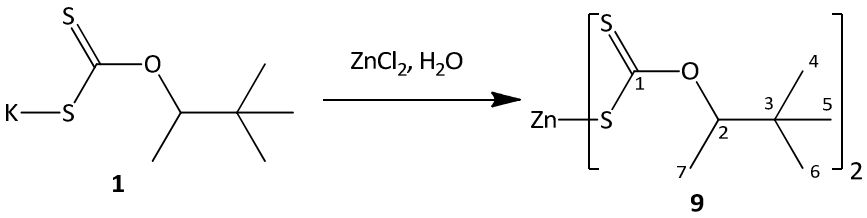

1 **9**

TABLE 26: CHEMICALS AND MASSES FOR THE REACTION

	$ZnCl_2$	potassium xanthate	H_2O
MW (g*mol^{-1})	136.30	216.41	18.02
mass (g)	2.86	10.00	170.00
molar amount (mmol)	21.00	46.21	
equivalents	1.00	2.20	

The used chemicals are listed in Table 26. Zinc (II) chloride was dissolved in about 85 ml deionised water. **1** was dissolved in the remaining amount of deionised water. The potassium xanthate solution was added dropwise to the zinc chloride solution under stirring. The reaction was allowed to stir for about 2.5 hours, the white precipitate was filtered off and dried in vacuum. The precipitate was dissolved in chloroform and added to methanol to obtain a white powder, which was dried in vacuum. (69.8 % yield)

^{1}H-NMR (300 MHz, $CDCl_3$, in ppm): 4.94 – 4.92 (q, 1H at C_2), 1.33 – 1.31 (d, 3H at C_7), 0.98 (s, 9H at C_4, C_5, C_6)

^{13}C-NMR (75 MHz, $CDCl_3$, in ppm): 14.55 (C_5), 25.85 (C_4, C_6), 35.30(C_7), 95.00 (C_2), 229.78 (C_1)

IR (on Si, in cm^{-1}): 2987, 2873, 1479, 1398, 1379, 1367, 1345, 1243, 1215, 1115, 1079, 1059, 1029, 985

Elemental analysis: calculated: %C = 40.04, %S = 30.54, %H = 6.24
found: %C = 39.88, %S = 31.03, %H = 6.23

Thermal gravimetric analysis: T_d = 144 °C, mass loss = 76.85 % (calc. 78.25 %)

ZINC (II) *O*-2,2-DIMETHYLPENTAN-3-YL DITHIOCARBONATE (10)

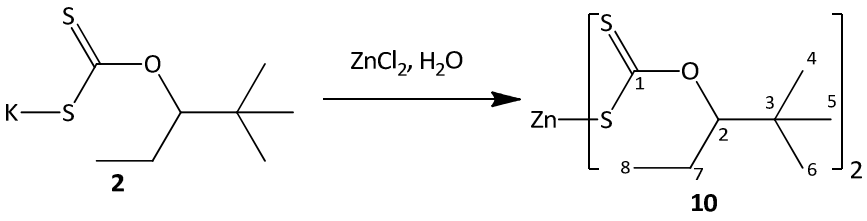

TABLE 27: CHEMICALS AND MASSES FOR THE REACTION

	$ZnCl_2$	potassium xanthate	H_2O
MW (g*mol^{-1})	136.30	230.44	18.02
mass (g)	2.69	10.00	160.00
molar amount (mmol)	19.72	43.39	
equivalents	1.00	2.20	

The used chemicals are listed in Table 27. Zinc (II) chloride was dissolved in about 80 ml deionised water. **2** was dissolved in the remaining amount of deionised water. The potassium xanthate solution was added dropwise to the zinc chloride solution under stirring. The reaction was allowed to stir for about 2.5 hours, the white precipitate was filtered off and dried in vacuum. The precipitate was dissolved in chloroform and added to methanol to obtain a white powder, which was dried in vacuum. (70.8 % yield)

^{1}H-NMR (300 MHz, $CDCl_3$, in ppm): 4.94 – 4.86 (m, 1H at C_2), 1.80 – 1.70 (m, 2H at C_7), 1.02 - 0.99 (m, 12H at C_4, C_5, C_6, C_8)

^{13}C-NMR (75 MHz, $CDCl_3$, in ppm): 11.15 (C_5), 23.39 (C_4, C_6), 26.13 (C_8), 36.10 (C_7), 101.21 (C_2), 231.22 (C_1)

IR (on Si, in cm^{-1}): 2970, 2877, 1479, 1398, 1383, 1369, 1351, 1275, 1253, 1216, 1197, 1129, 1081, 1052, 1028, 951

Elemental analysis: calculated: %C = 42.89, %S = 28.63, %H = 6.75
found: %C = 42.45, %S = 28.57, %H = 6.79

Thermal gravimetric analysis: T_d = 141 °C, mass loss = 77.01 % (calc. 79.53 %)

TIN (IV) *O*-3,3-DIMETHYLBUTAN-2-YL DITHIOCARBONATE (11)

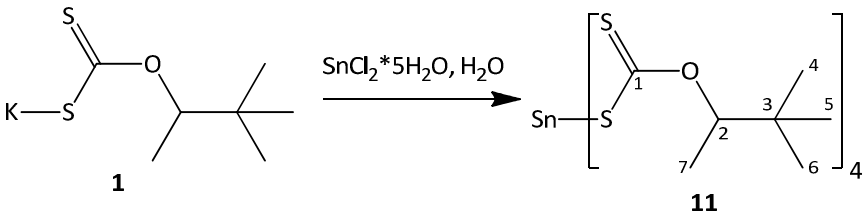

1 **11**

TABLE 28: CHEMICALS AND MASSES FOR THE REACTION

	$SnCl_2*5H_2O$	potassium xanthate	H_2O
MW ($g*mol^{-1}$)	350.53	216.41	18.02
mass (g)	9.72	9.00	200.00
molar amount (mmol)	27.73	41.59	
equivalents	1.00	1.50	

The used chemicals are listed in Table 28. Tin (IV) chloride pentahydrate was dissolved in about 85 ml deionised water. **1** was dissolved in the remaining amount of deionised water. The potassium xanthate solution was added dropwise to the tin chloride solution under stirring. The reaction was allowed to stir for about 5 hours, the yellow precipitate was educed with chloroform and added to methanol to obtain a yellow powder, which was dried in vacuum. (24.8 % yield)

^{1}H-NMR (300 MHz, $CDCl_3$, in ppm): 4.64 – 4.58 (q, 1H at C_2), 1.35 – 1.33 (d, 3H at C_7), 0.97 (s, 9H at C_4, C_5, C_6)

^{13}C-NMR (75 MHz, $CDCl_3$, in ppm): 14.49 (C_5), 25.78 (C_4, C_6), 35.68 (C_7), 98.44 (C_2), 227.66 (C_1)

IR (on Si, in cm^{-1}): 2967, 2873, 1478, 1447, 1399, 1379, 1367, 1348, 1256, 1217, 1115, 1075, 1052, 1022, 984

Elemental analysis: calculated: %C = 33.27, %S = 31.72, %H = 5.19
found: %C = 32.20, %S = 30.95, %H = 4.97

Thermal gravimetric analysis: T_d = 116 °C, mass loss = 65.27 % (calc. 66.78 %)

TIN (IV) *O*-2,2-DIMETHYLPENTAN-3-YL DITHIOCARBONATE (12)

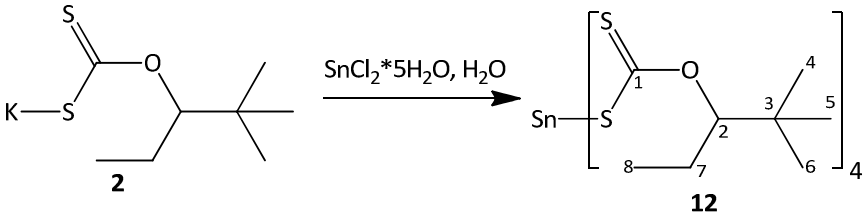

TABLE 29: CHEMICALS AND MASSES FOR THE REACTION

	$SnCl_2*5H_2O$	potassium xanthate	H_2O
MW ($g*mol^{-1}$)	350.53	230.44	18.02
mass (g)	2.82	9.00	200.00
molar amount (mmol)	8.04	39.05	
equivalents	1.00	4.86	

The used chemicals are listed in Table 29. Tin (IV) chloride pentahydrate was dissolved in about 85 ml deionised water. **2** was dissolved in the remaining amount of deionised water. The potassium xanthate solution was added dropwise to the tin chloride solution under stirring. The reaction was allowed to stir for about 5 hours, the reaction solution was educed with chloroform. The obtained chloroform solution was evaporated under reduced pressure to give an orange oily residue (25.7 % yield)

^{1}H-NMR (300 MHz, $CDCl_3$, in ppm): 4.92 – 4.82 (m, 1H at C_2), 1.82 – 1.70 (m, 2H at C_7), 1.03 - 0.92 (m, 9H at C_4, C_5, C_6, C_8)

^{13}C-NMR (75 MHz, $CDCl_3$, in ppm): 11.16 (C_5), 23.53 (C_4, C_6), 26.15 (C_8), 36.29 (C_7), 102.73 (C_2), 229.05 (C_1)

IR (on Si, in cm^{-1}): 2970, 2878, 1478, 1399, 1383, 1368, 1345, 1237, 1215, 1131, 1082, 1060, 1038, 951

Elemental analysis: calculated: %C = 43.48 %S = 29.02, %H = 6.84
found: %C = 40.04, %S = 26.02, %H = 6.10

Thermal gravimetric analysis: T_d = 116 °C, mass loss = 75.39 % (calc. 68.53 %)

GALLIUM (III) *O*-3,3-DIMETHYLBUTAN-2-YL DITHIOCARBONATE (13)

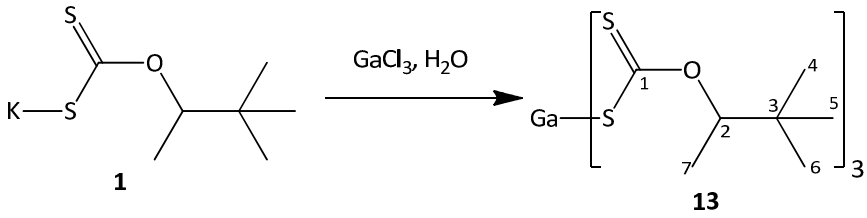

1 **13**

TABLE 30: CHEMICALS AND MASSES FOR THE REACTION

	$GaCl_3$	potassium xanthate	H_2O
MW ($g*mol^{-1}$)	176.08	216.41	18.02
mass (g)	1.14	4.50	150.00
molar amount (mmol)	6.50	20.79	
equivalents	1.00	3.20	

The used chemicals are listed in Table 30. Gallium (III) chloride was dissolved in about 750 ml deionised water. **1** was dissolved in the remaining amount of deionised water. The potassium xanthate solution was added dropwise to the gallium chloride solution under stirring. The reaction was allowed to stir for about 2.5 hours, the white precipitate was filtered off and dried in vacuum. The precipitate was dissolved in chloroform and added to methanol to obtain a white powder, which was dried in vacuum. (48.2 % yield)

^{1}H-NMR (300 MHz, $CDCl_3$, in ppm): 4.86 – 4.80 (q, 1H at C_2), 1.32 – 1.30 (d, 3H at C_7), 0.97 (s, 9H at C_4, C_5, C_6)

^{13}C-NMR (75 MHz, $CDCl_3$, in pmm): 14.45 (C_5), 25.84 (C_4, C_6), 35.40 (C_7), 97.11 (C_2), 226.37 (C_1)

IR (on Si, in cm^{-1}): 2965, 2873, 1479, 1397, 1379, 1367, 1347, 1255, 1218, 1114, 1076, 1061, 1052, 1023, 1003, 986

Elemental analysis: calculated: %C = 41.92, %S = 31.98, %H = 6.53
found: %C = 41.52, %S = 31.88, %H = 6.21

Thermal gravimetric analysis: T_d = 150 °C, mass loss = 81.30 % (calc. 60.83 %)

GALLIUM (III) *O*-2,2-DIMETHYLPENTAN-3-YL DITHIOCARBONATE (14)

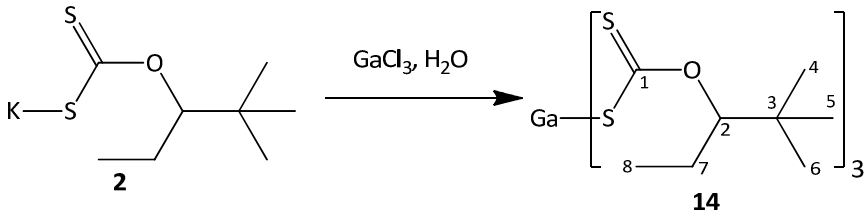

TABLE 31: CHEMICALS AND MASSES FOR THE REACTION

	$GaCl_3$	potassium xanthate	H_2O
MW ($g*mol^{-1}$)	176.08	230.44	18.02
mass (g)	1.07	4.50	150.00
molar amount (mmol)	6.10	19.53	
equivalents	1.00	3.20	

The used chemicals are listed in Table 31. Gallium (III) chloride was dissolved in about 70 ml deionised water. **2** was dissolved in the remaining amount of deionised water. The potassium xanthate solution was added dropwise to the gallium chloride solution under stirring. The reaction was allowed to stir for about 2.5 hours, the white precipitate was filtered off and dried in vacuum. The precipitate was recrystallised from dichloromethane to obtain a white powder. (85.2 % yield)

^{1}H-NMR (300 MHz, $CDCl_3$, in ppm): 4.79 – 4.75 (m, 1H at C_2), 1.77 – 1.70 (m, 2H at C_7), 1.00 - 0.94 (m, 12H at C_4, C_5, C_6, C_8)

^{13}C-NMR (75 MHz, $CDCl_3$, in ppm): 11.18 (C_5), 23.48 (C_4, C_6), 26.14 (C_8), 36.14 (C_7), 101.38 (C_2), 228.63 (C_1)

IR (on Si, in cm^{-1}): 2970, 2877, 1479, 1458, 1398, 1383, 1368, 1348, 1246, 1215, 1130, 1082, 1060, 1041, 951

Elemental analysis: calculated: %C = 41.85, %S = 27.93, %H = 6.58
found: %C = 32.76, %S = 19.11, %H = 5.71

Thermal gravimetric analysis: T_d = 126 °C, mass loss = 63.12 % (calc. 63.39 %)

PREPARATION OF $CuInS_2$ SAMPLES FOR X-RAY DIFFRACTION MEASUREMENTS AND TRANSMISSION ELECTRON MICROSCOPIC ANALYSIS

Precursor solutions with different stoichiometric ratios of copper and indium were prepared. The $CuInS_2$ precursor solution consisted of **4** and **6** dissolved in 2 ml chloroform (see Table 32). The solutions were drop coated on glass substrates, followed by different annealing programs in vacuum as described in Table 33. The $CuInS_2$ layers were scratched off the glass substrates to obtain the $CuInS_2$ powders.

TABLE 32: CHEMICALS AND MASSES

	4 MW = 254.9 g*mol^{-1}	**6** MW = 688.7 g*mol^{-1}
Cu : In = 1 : 1	75.70 mg (0.15 mol*l^{-1})	204.54 mg (0.15 mol*l^{-1})
Cu : In = 1 : 1.25	67.69 mg (0.13 mol*l^{-1})	228.61 mg (0.17 mol*l^{-1})
Cu : In = 1 : 1.5	61.21 mg (0.12 mol*l^{-1})	248.06 mg (0.18 mol*l^{-1})
Cu : In = 1 : 1.7	56.85 mg (0.11 mol*l^{-1})	261.14 mg (0.19 mol*l^{-1})

TABLE 33: ANNEALING PROGRAMS

program	T_1 (°C)	t_1 (min)	T_2 (°C)	t_2 (min)
1	rt	7	180	15
2	rt	10	250	15
3	rt	15	350	15
4	rt	18	450	15

PREPARATION OF Cu_2ZnSnS_4 SAMPLES FOR X-RAY DIFFRACTION MEASUREMENTS AND TRANSMISSION ELECTRON MICROSCOPIC ANALYSIS

Precursor solutions with different stoichiometric ratios of copper, zinc and tin were prepared. The Cu_2ZnSnS_4 precursor solution consisted of **3**, **9** and **11** dissolved in 2 ml chloroform (see Table 34). The solutions were drop coated on glass substrates, followed by different annealing programs in vacuum as described in Table 33. The Cu_2ZnSnS_4 layers were scratched off the glass substrates to obtain the Cu_2ZnSnS_4 powders.

TABLE 34: CHEMICALS AND MASSES

	3	**9**	**11**
	MW = 240.9 g*mol^{-1}	**MW = 420.0 g*mol^{-1}**	**MW = 505.4 g*mol^{-1}**
Cu : Zn : Sn = 1.2 : 1 : 1	26.8 mg	38.9 mg	46.8 mg
Cu : Zn : Sn = 1.6 : 1 : 1	33.5 mg	36.5 mg	44.0 mg
Cu : Zn : Sn = 2 : 1 : 1	39.5 mg	34.4 mg	41.4 mg

PREPARATION OF $CuInS_2$ SAMPLES FOR TRANSMITTANCE AND REFLECTANCE MEASUREMENTS

Precursor solutions with different stoichiometric ratios of copper and indium were prepared as described in Table 32. The $CuInS_2$ precursor solution consisted of **4** and **6** dissolved in 2 ml chloroform. The solutions were doctor bladed on glass substrates, followed by different annealing programs in vacuum given in Table 33.

PREPARATION OF Cu_2ZnSnS_4 SAMPLES FOR TRANSMITTANCE AND REFLECTANCE MEASUREMENTS

Precursor solutions with different stoichiometric ratios of copper, zinc and tin were prepared as described in Table 34. The Cu_2ZnSnS_4 precursor solution consisted of **3**, **9** and **11** dissolved in 2 ml chloroform. The solutions were doctor bladed on glass substrates, followed by different annealing programs in vacuum given in Table 33.

PREPARATION OF $CuInS_2$ SAMPLES FOR THERMAL GRAVIMETRIC ANALYSIS

Precursor solutions with different stoichiometric ratios of copper and indium were prepared as described in Table 32. The $CuInS_2$ precursor solution consisted of **4** and **6** dissolved in 2 ml chloroform. The solutions were evaporated and the residues were used for thermal gravimetric analyses.

PREPARATION OF Cu_2ZnSnS_4 SAMPLES FOR THERMAL GRAVIMETRIC ANALYSIS

Precursor solutions with different stoichiometric ratios of copper, zinc and tin were prepared as described in Table 34. The Cu_2ZnSnS_4 precursor solution consisted of **3**, **9** and **11** dissolved in 2ml chloroform. The solutions were evaporated and the residues were used for thermal gravimetric analyses.

PREPARATION OF CDS/$CuInS_2$ SOLAR CELLS

Copper and indium *O*-2,2-dimethylpentan-3-yl dithiocarbonate containing mixtures with a stoichiometric ratio of copper to indium of 1 : 1.25 were dissolved in chloroform and doctor bladed on ITO substrates. The used parameters for doctor blading are summarised in Table 35. The precursor containing substrates were baked for 15 minutes at 350 °C in vacuum (program 2). Then a solution of cadmium *O*-2,2-dimethylpentan-3-yl dithiocarbonate was doctor bladed on the prepared $CuInS_2$ film and annealed at 200 °C for 15 minutes in vacuum (program 1).

TABLE 35: PARAMETERS FOR SOLAR CELL PREPARATION

parameter	
doctor blade support temperature	40 °C
substrate temperature	120 °C
wet film thickness	100 µm
number of doctor bladed layers	2

TABLE 36: ANNEALING PROGRAMS

program	T_1.(°C)	t_1 (min)	T_2 (°C)	t_2 (min)
1	rt	7	200	15
2	rt	15	350	15

PREPARATION OF CDS/Cu_2ZnSnS_4 SOLAR CELLS

Copper, zinc and tin *O*-3,3-dimethylbutan-2-yl dithiocarbonate containing mixtures with a stoichiometric ratio of copper to zinc to tin of 1.2 : 1 : 1 were dissolved in chloroform and doctor bladed on ITO substrates. The used parameters are summarised in Table 35. The precursor containing substrates were baked for 15 minutes at 350 °C in vacuum (program 2). Then a solution of cadmium *O*-3,3-dimethylbutan-2-yl dithiocarbonate was doctor bladed on the prepared Cu_2ZnSnS_4 film and annealed at 200 °C for 15 minutes in vacuum (program 1). Annealing programs are listed in Table 36.

SUMMARY AND OUTLOOK

Within this work novel metal-xanthates, also named dithiocarbonates, for preparation of semiconducting metal sulphides as solar absorber materials have been synthesised. Metal dithiocarbonates are known to have low decomposition temperatures and a defined decomposition pathway, enabled by the Chugaev rearrangement (Figure 5), towards remainder-free metal sulphide semiconductors. [27], [29], [31]

Initially potassium dithiocarbonates were synthesised, according to a previously published procedure, by the reaction of potassium *tert*-butoxide, an alcohol and carbon disulphide. [32] Two alcohols, 3,3-dimethyl-2-butanol and 2,2-dimethyl-3-pentanol, with differing chain lengths have been employed for syntheses.

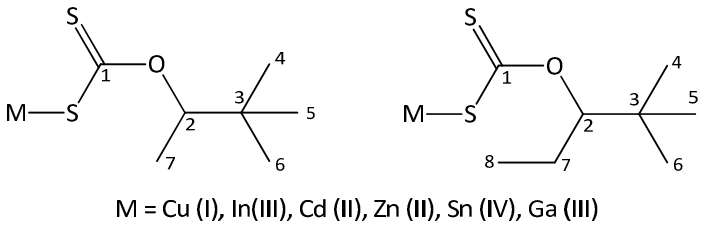

FIGURE 50: SYNTHESISED METAL DITHIOCARBONATES WITH DIFFERENT ALCOHOLIC MOIETIES

Based on the potassium dithiocarbonates metal dithiocarbonates, employing copper, indium, cadmium, zinc, tin and gallium as metal atoms, were synthesised, as shown in Figure 50 and were characterised by ^{1}H- and ^{13}C nuclear magnetic resonance spectroscopy, Fourier transform infrared spectroscopy, elemental analysis, mass spectrometry and thermal gravimetric analysis.

The typical high shifts found in ^{1}H- and ^{13}C-NMR spectra gave proof of successful reactions to metal xanthates and further FTIR-spectroscopy exhibited characteristic absorption peaks for metal dithiocarbonates. Elemental analyses encouraged the conclusion of the high purity of the synthesised products. The influence of the chain length of the alcoholic moiety was revealed in solubility tests and by thermal gravimetric analyses. The more steric moiety leads to a better solubility in most common solvents and decreases decomposition temperatures of the metal dithiocarbonates. The results of thermal gravimetric analyses point out the considerable effect of differing moieties.

In the second part, the preparation of chalcopyrite type and kesterite type semiconductors via decomposition of the previously synthesised metal xanthates was investigated.

Chalcopyrite type semiconductors like copper indium disulphide and kesterite type semiconductors like copper zinc tin sulphide are of strong scientific interest due to their beneficial properties for photovoltaic applications.

Thermal gravimetric analyses of metal dithiocarbonate mixtures were performed and the results exhibited only single-step decompositions at much lower temperatures, than those for each metal dithiocarbonate. The decomposition is finished at lower temperatures than those of the copper dithiocarbonates. These results confirm that the mixtures react as single compounds, since no multi-step decomposition has been observed. Representatively, thermal gravimetric curves for copper indium disulphide and copper zinc tin sulphide are presented below in Figure 51.

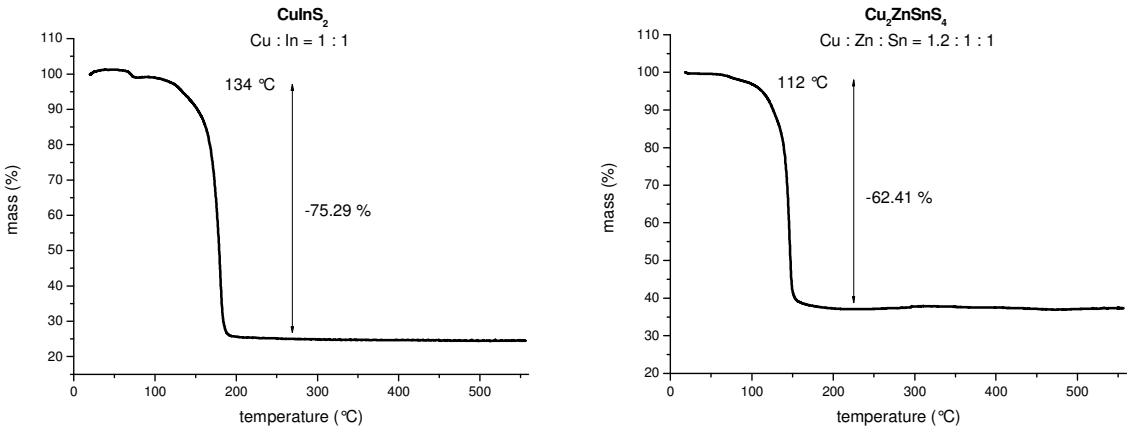

FIGURE 51: THERMAL GRAVIMETRIC CURVE OF A COPPER AND INDIUM DITHIOCARBONATE MIXTURE (LEFT) AND OF A COPPER, ZINC AND TIN DITHIOCARBONATE MIXTURE (RIGHT)

The resulting metal sulphides were studied by X-ray diffraction, energy dispersive X-ray analysis and optical transmittance and reflectance measurements.

In cases of copper indium disulphide and copper zinc tin sulphide, powder diffraction profiles exhibited that all deposited films show the typical chalcopyrite and respectively kesterite crystalline structure with preferred (112) orientation. [14], [45], [63] For all samples the major characteristic diffraction X-ray reflexes (112), (220) and (312) were observed. According to Scherrer's equation

particle grain sizes were calculated by estimation of the full-width at half maximum (FWHM) of these major peaks.

Figure 52 depicts the X-ray diffraction profile of synthesised copper zinc tin sulphide with a stoichiometric ratio of copper to zinc to tin of 1.2 : 1 : 1. This sample matches perfectly the Powder Diffraction File PDF26-0575 of the International Centre for Diffraction Data.

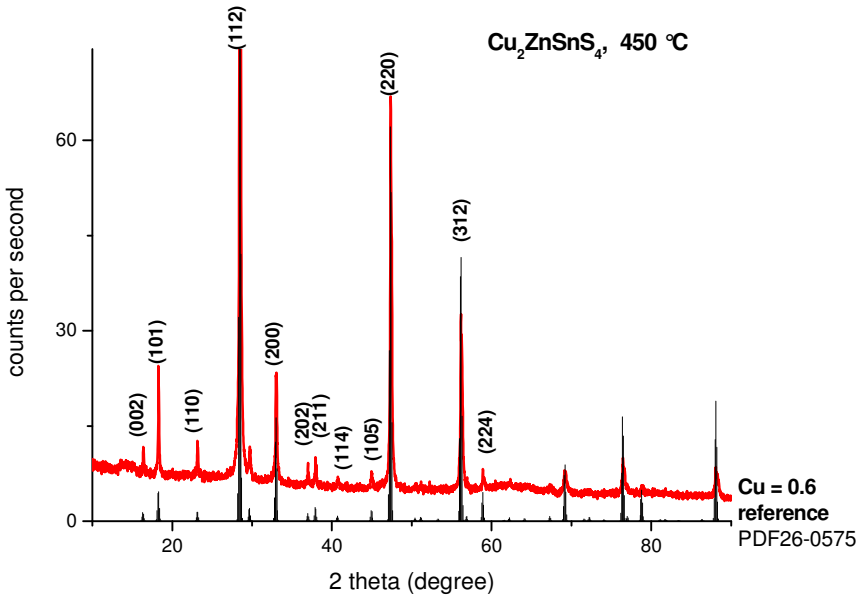

FIGURE 52: XRD-PROFILE OF A Cu_2ZnSnS_4 SAMPLE WITH A STOICHIOMETRIC RATIO OF CU : ZN : SN = 1.2 : 1 : 1 TREATED AT 450 °C

Though good results of the X-ray diffraction measurements have been obtained, the energy dispersive X-ray analysis revealed that depending on stoichiometry and annealing temperature additional phases of semiconducting metal sulphides, probably the zinc blende phases $CuIn_2S_{3.5}$ and $CuIn_3S_5$ and the cubic spinel phase of $CuIn_5S_8$ occur within copper indium disulphide samples and CuS and Cu_2ZnS_2 occur within copper zinc tin sulphide samples, respectively.

Transmittance and reflectance measurements offered high absorption coefficients of more than 10^4 cm^{-1} for copper indium disulphide and copper zinc tin sulphide, respectively. Estimated band gap values range between 1.46 – 1.56 eV for $CuInS_2$ prepared at 450 °C and 1.43 – 1.80 eV for Cu_2ZnSnS_4, respectively and are in good agreement with reports in the literature. [1], [10], [11], [13], [39], [41], [51], [54], [55]

Due to the promising properties of the synthesised semiconducting metal sulphides for photovoltaic applications, first attempts to fabricate inorganic solar cells have been carried out in a basic bilayer assembly of $CdS/CuInS_2$ and CdS/Cu_2ZnSnS_4, respectively, on indium tin oxide as transparent conductive electrode and with an aluminium back contact. Good results were achieved with the $CdS/CuInS_2$ assembled solar cells. An open circuit voltage of 370 mV and a short circuit current of 2.95 $mA*cm^{-2}$ were obtained, and yielded 0.39 % photon to current efficiency (see Figure 53). First attempts with Cu_2ZnSnS_4 were rather disappointing.

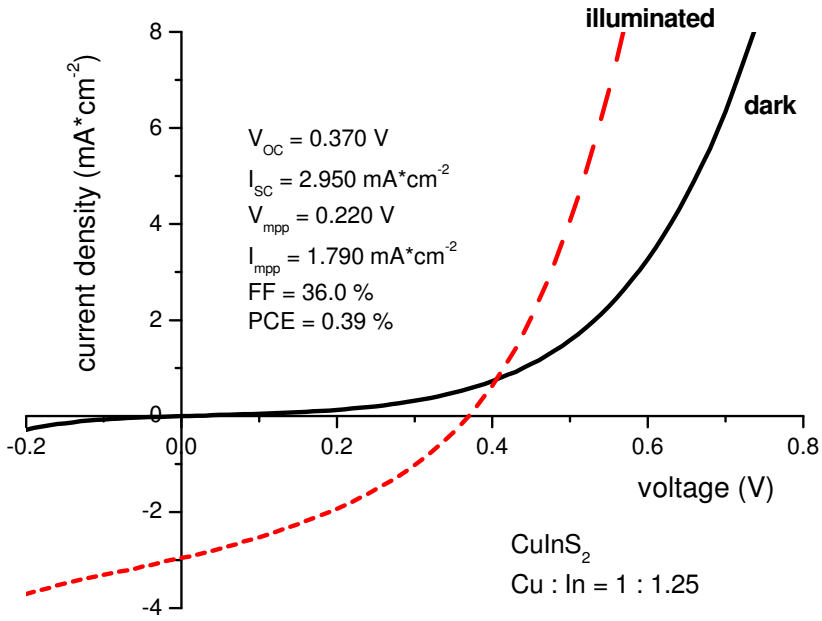

FIGURE 53: CURRENT DENSITY – VOLTAGE CHARACTERISTICS OF A FABRICATED $CdS/CuInS_2$ SOLAR CELL

Therefore further improvement of all parameters of the solar cell set up, in cases of $CuInS_2$ and Cu_2ZnSnS_4 has to be done in the coming months. To compare the gained results of solar cell fabrication, the device structure should be adapted to the most commonly used assembly, published in literature.

LITERATURE CITED

[1] T.M. Razykov, C.S. Ferekides, D. Morel, E. Stefanakos, H.S. Ullal, H.M. Upadhyaya, Solar Energy (2011).

[2] IEA, Key World Energy Statistics 2010, 2010.

[3] B. Li, L. Wang, B. Kang, P. Wang, Y. Qiu, Solar Energy Materials and Solar Cells 90 (2006) 549-573.

[4] OECD, World Energy Outlook, OECD/IEA, 2008.

[5] A.-E. Becquerel, Comptes Rendus De l□Académie Des Sciences 9 (1839) 561-567.

[6] M. Grätzel, Nature 414 (2001) 338-344.

[7] X. Wu, Solar Energy 77 (2004) 803-814.

[8] M.A. Contreras, K. Ramanathan, J. AbuShama, F. Hasoon, D.L. Young, B. Egaas, R. Noufi, Progress In Photovoltaics : Research and Applications 13 (2005) 209.

[9] I. Repins, M. Contreras, M. Romero, Y. Yan, W. Metzger, J. Li, S. Johnston, B. Egaas, C. Dehart, J. Scharf, R. Noufi, Progress In Photovoltaics: Research and Applications 16 (2008) 235–239.

[10] D.B. Mitzi, O. Gunawan, T.K. Todorov, K. Wang, S. Guha, Solar Energy Materials and Solar Cells (2011).

[11] H. Katagiri, K. Jimbo, W.S. Maw, K. Oishi, M. Yamazaki, H. Araki, A. Takeuchi, Thin Solid Films 517 (2009) 2455-2460.

[12] T.K. Todorov, K.B. Reuter, D.B. Mitzi, Advanced Materials 22 (2010) E156-E159.

[13] A. Rockett, Current Opinion In Solid State and Materials Science 14 (2010) 143-148.

[14] H. Yoo, J. Kim, Solar Energy Materials and Solar Cells 95 (2011) 239-244.

[15] T. Todorov, O. Gunawan, S.J. Chey, T.G. de Monsabert, A. Prabhakar, D.B. Mitzi, Thin Solid Films (2011).

[16] D.P. Dutta, G. Sharma, Materials Letters 60 (2006) 2395 - 2398.

[17] M. Green, P.O. Brien, Chemical Communications (Cambridge, England) (1999) 2235-2241.

[18] G. Shang, M.J. Hampden-smith, E.N. Duesler, Chemical Communications (Cambridge, England) (1996) 1733-1734.

[19] A. Keys, S.G. Bott, A.R. Barron, Chemistry Of Materials 11 (1999) 3578-3587.

[20] M.R. Lazell, P.O. Brien, D.J. Otway, J.-ho Park, M.E.M. Ga, Chemistry Of Materials 11 (1999) 3430-3432.

[21] N. Revaprasadu, M.A. Malik, J. Carstens, P.O. Brien, S. Kensington, S. Africa, Journal Of Materials Chemistry 9 (1999) 2885-2888.

[22] P.O. Brien, D.J. Otway, J.R. Walsh, Thin Solid Films 315 (1998) 57-61.

[23] K. Xu, W. Ding, Materials Letters 62 (2008) 4437-4439.

[24] D.P. Dutta, G. Sharma, S. Ghoshal, N.P. Kushwah, V.K. Jain, Journal Of Nanoscience and Nanotechnology 6 (2006) 235-240.

[25] M. Tejos, B.G. Rolón, R. del Río, G. Cabello, Materials Science In Semiconductor Processing 11 (2008) 94-99.

[26] S. Ghoshal, N.P. Kushwah, D.P. Dutta, V.K. Jain, Applied Organometallic Chemistry 19 (2005) 1257-1262.

[27] A. ur Rehman, S. Ali, G. Kociok-Köhn, K.C. Molloy, Journal Of Molecular Structure 937 (2009) 56-60.

[28] Q. Han, J. Chen, X. Yang, L. Lu, X. Wang, Journal Of Physics and Chemistry C 111 (2007) 14072-14077.

[29] H.C. Leventis, S.P. King, A. Sudlow, M.S. Hill, K.C. Molloy, S. a Haque, Nano Letters 10 (2010) 1253-8.

[30] D. Barreca, A. Gasparotto, C. Maragno, R. Seraglia, E. Tondello, A. Venzo, V. Krishnan, H. Bertagnolli, Applied Organometallic Chemistry 19 (2005) 59-67.

[31] L. Tschugaeff, Berichte Der Deutschen Chemischen Gesellschaft 32 (1899) 3332-3335.

[32] A. González-Roura, J. Casas, A. Lliberia, Lipids 37 (2002) 401-406.

[33] R. Mattes, G. Pauleickhoff, Spectrochimica Acta 30A (1974) 379-386.

[34] G. Winter, M.R. Hunt, A.G. Kruger, Australian Journal Of Chemistry 24 (1971) 53-57.

[35] L.H. Little, G.W. Poling, J. Leja, Canadian Journal Of Chemistry 39 (1961) 745-754.

[36] N.P. Colthup, L. Porter Powell, Spectrochimica Acta 43A (1987) 317-322.

[37] C.G. Sceney, J.O. Hill, R.J. Magee, Thermochimica Acta 6 (1973) 111-117.

[38] T. Unold, I. Sieber, K. Ellmer, Applied Physics Letters 88 (2006) 213502.

[39] Y. Yan, Y. Liu, L. Fang, J. Zhu, H. Zhao, D. Li, Z. Lu, S. Zhou, Transactions Of Nonferrous Metals Society Of China 18 (2008) 1083-1088.

[40] I. Oja, M. Nanu, a Katerski, M. Krunks, a Mere, J. Raudoja, a Goossens, Thin Solid Films 480-481 (2005) 82-86.

[41] D.-Y. Lee, J. Kim, Thin Solid Films 518 (2010) 6537-6541.

[42] D.-Y. Lee, S. Park, J. Kim, Current Applied Physics (2010) 1-5.

[43] D. Shivagan, P. Dale, a Samantilleke, L. Peter, Thin Solid Films 515 (2007) 5899-5903.

[44] E. Maier, T. Rath, W. Haas, O. Werzer, R. Saf, F. Hofer, D. Meissner, O. Volobujeva, S. Bereznev, E. Mellikov, Solar Energy Materials and Solar Cells (2011) 1-8.

[45] X. Hou, K. Choy, Thin Solid Films 480-481 (2005) 13-18.

[46] M. Gannouni, M. Kanzari, Journal Of Alloys and Compounds (2011).

[47] R. Nomura, Y. Seki, H. Matsuda, Thin Solid Films 209 (1992) 145-147.

[48] D. Pan, L. An, Z. Sun, W. Hou, Y. Yang, Z. Yang, Y. Lu, Journal Of the American Chemical Society 130 (2008) 5620-1.

[49] G. Cliff, G. Lorimer, Journal Of Microscopy 103 (1975) 203–207.

[50] A. Mudryi, Thin Solid Films 431-432 (2003) 197-199.

[51] A. Fischereder, T. Rath, W. Haas, H. Amenitsch, J. Albering, D. Meischler, S. Larissegger, M. Edler, R. Saf, F. Hofer, G. Trimmel, Chemistry Of Materials 22 (2010) 3399-3406.

[52] V.I. Klimov, Semiconductor and Metal Nanocrystals - Synthesis and Electronic and Optical Properties, Marcel Dekker, Inc., 2004.

[53] Y.-D. Chung, D.-H. Cho, N.-M. Park, K.-S. Lee, J. Kim, Current Applied Physics (2010) 11-13.

[54] Y.B.K. Kumar, G.S. Babu, P.U. Bhaskar, V.S.R. Ã, Solar Energy Materials and Solar Cells 93 (2009) 1230-1237.

[55] Q. Guo, G.M. Ford, W.-C. Yang, B.C. Walker, E. a Stach, H.W. Hillhouse, R. Agrawal, Journal Of the American Chemical Society (2010) 7-9.

[56] J.-S. Seol, S.-Y. Lee, J.-C. Lee, H.-D. Nam, K.-H. Kim, Solar Energy Materials and Solar Cells 75 (2003) 155-162.

[57] K. Jimbo, R. Kimura, T. Kamimura, S. Yamada, W.S. Maw, H. Araki, K. Oishi, H. Katagiri, Thin Solid Films 515 (2007) 5997–5999.

[58] T. Tanaka, T. Nagatomo, D. Kawasaki, M. Nishio, Q. Guo, A. Wakahara, A. Yoshida, H. Ogawa, Journal Of Physics and Chemistry Of Solids 66 (2005) 1978–1981.

[59] T. Tanaka, D. Kawasaki, M. Nishio, Q. Guo, H. Ogawa, Physica Status Solidi (c) 3 (2006) 2844–2847.

[60] N. Nakayama, K. Ito, Applied Surface Science 92 (1996) 171–175.

[61] N. Kamoun, H. Bouzouita, B. Rezig, Thin Solid Films 515 (2007) 5949–5952.

[62] J.J. Scragg, P.J. Dale, L.M. Peter, G. Zoppi, I. Forbes, Physica Status Solidi B 249 (2008) 1772-1778.

[63] J. Scragg, P. Dale, L. Peter, Electrochemistry Communications 10 (2008) 639-642.

[64] J. Paier, R. Asahi, A. Nagoya, G. Kresse, Physical Review B 79 (2009) 15126.

[65] C. Steinhagen, M.G. Panthani, V. Akhavan, B. Goodfellow, B. Koo, B.A. Korgel, Journal Of the American Chemical Society Communications 131 (2009) 12554–12555.

APPENDIX

LIST OF FIGURES

LIST OF TABLES